Identification and Optimization of a Ligand Efficient Benzoazepinone Bromodomain and Extra Terminal (BET) Family Acetyl-Lysine Mimetic into the Oral Candidate Quality Molecule I-BET432

Philip G. Humphreys,[†]* Niall A. Anderson,[†] Paul Bamborough,[†] Andrew Baxter,[†] Chun-wa Chung,[†] Rosa Cookson,[†] Peter D. Craggs,[†] Toryn Dalton,[†] Julie C. L. Fournier,[†] Laurie J. Gordon,[†] Matthew W. Gray,[†] Heather F. Gray,[†] Richard Gregory,[†] David J. Hirst,[†] Craig Jamieson,[‡] Katherine L. Jones,[†] Hripsimee Kessedjian,[†] Dave Lugo,[†] Grant McGonagle,[†] Vipulkumar K. Patel,[†] Christopher Patten,[†] Darren L. Poole,[†] Rab K. Prinjha,[†] Cesar Ramirez Molina,[†] Inmaculada Rioja,[†] Gail Seal,[†] Kayleigh A. J. Stafford,[†] Rishi R. Shah,[†] Daniel Tape,[†] Natalie H. Theodoulou,[†] Laura R. Tomlinson,[†] Sabri Ukuser,[†] Ian D. Wall,[†] Natalie Wellaway,[†] Gemma White[†]

[†]GSK R&D, Stevenage, Hertfordshire SG1 2NY, United Kingdom

[‡]WestCHEM, Department of Pure and Applied Chemistry, Thomas Graham Building, University of Strathclyde, 295 Cathedral Street, Glasgow, G1 1XL, United Kingdom

ABSTRACT: The bromodomain and extraterminal (BET) family of proteins are an integral part of human epigenome regulation, the dysregulation of which is implicated in multiple oncology

and inflammatory diseases. Disrupting the BET family bromodomain acetyl-lysine (KAc) histone protein-protein interaction with small molecule KAc mimetics has proven productive and multiple molecules are currently undergoing oncology clinical trials. This work describes an efficiency analysis of published GSK pan-BET bromodomain inhibitors which drove a strategic choice to focus on identification of a ligand efficient KAc mimetic with the hypothesis that lipophilic efficiency could be drastically improved during optimization. This focus drove the discovery of the highly ligand efficient and structurally distinct benzoazepinone KAc mimetic. Following crystallography to identify suitable growths vectors, the benzoazepinone core was optimised through an explore-exploit SAR approach while carefully monitoring lipophilic efficiency to deliver I-BET432 (**41**) as an oral candidate quality molecule with a 5-18 mg early predicted human efficacious dose.

KEYWORDS: Bromodomain, BET, Epigenetics, Bromodomain and Extra Terminal, Ligand Efficiency, Lipophilic Efficiency

INTRODUCTION

Small molecule disruption of the protein-protein interaction between a histone tail acetyl-lysine (KAc) and the epigenetic reader module of a bromodomain containing protein has become the subject of intensive research in both academia and industry over the past decade.[1,2] Of the 61 human bromodomains, the bromodomain and extra terminal (BET) family has been a particular focus due to the profound biology associated with its dysregulation across multiple therapeutic areas including oncology and immune inflammation.[3,4] The BET family of proteins are recruited to histones via recognition of histone tail acetylated lysines and regulate gene transcription through recruitment of transcription factors.[5,6] The BET family of bromodomain containing proteins is

made up of four proteins, the ubiquitously expressed BRD2, BRD3 and BRD4, and the testes specific BRDT. These proteins each contain dual bromodomains, the N-terminal bromodomain (BD1) and the C-terminal bromodomain (BD2). As a direct result of research interest into small molecules that disrupt the BET family bromodomain–histone KAc interaction and the fundamental biology that is impacted, as of May 2022 there are 17 molecules across 46 single agent and combination oncology clinical trials registered on clinicaltrials.gov.[7,8] The vast majority of these molecules bind all eight members of the BET bromodomain family with comparable affinity and a 2:1 ligand : protein stoichiometry, referred to as pan-BET inhibition. A notable exception to this paradigm is AZD5153 which binds bivalently to both bromodomains of each BET protein simultaneously with a 1:1 ligand : protein stoichiometry.[9,10]

The structure of the BET family bromodomains are well characterized with > 640 liganded and apo BRD4 structures available via the Protein Data Bank.[11] A bromodomain contains four antiparallel alpha helices (αZ, αA, αB, and αC) which are connected by the two loop regions, ZA and BC. This tertiary structure forms the KAc binding pocket which recognizes suitably post translationally modified histone tails.[12] The N-1 acetate group makes two canonical hydrogen bond interactions, directly to Asn140 and through water to Tyr97 (Figure 1a, BRD4 BD1 numbering). The acetate methyl group protrudes into a small pocket adjacent to a conserved water network at the base of the binding pocket. Small molecule BET inhibitors typically disrupt the interaction between KAc and the protein through mimicking the same interactions, as well as gaining additional affinity through occupying the WPF shelf, a lipophilic region accessible past gatekeeper residue Ile146 and comprised of Trp81, Pro82 and Phe83. Additionally, a narrow cleft between Trp81 and Leu92, referred to as the ZA channel, is often occupied by small molecule inhibitors further adding to the binding affinity (Figure 1b).
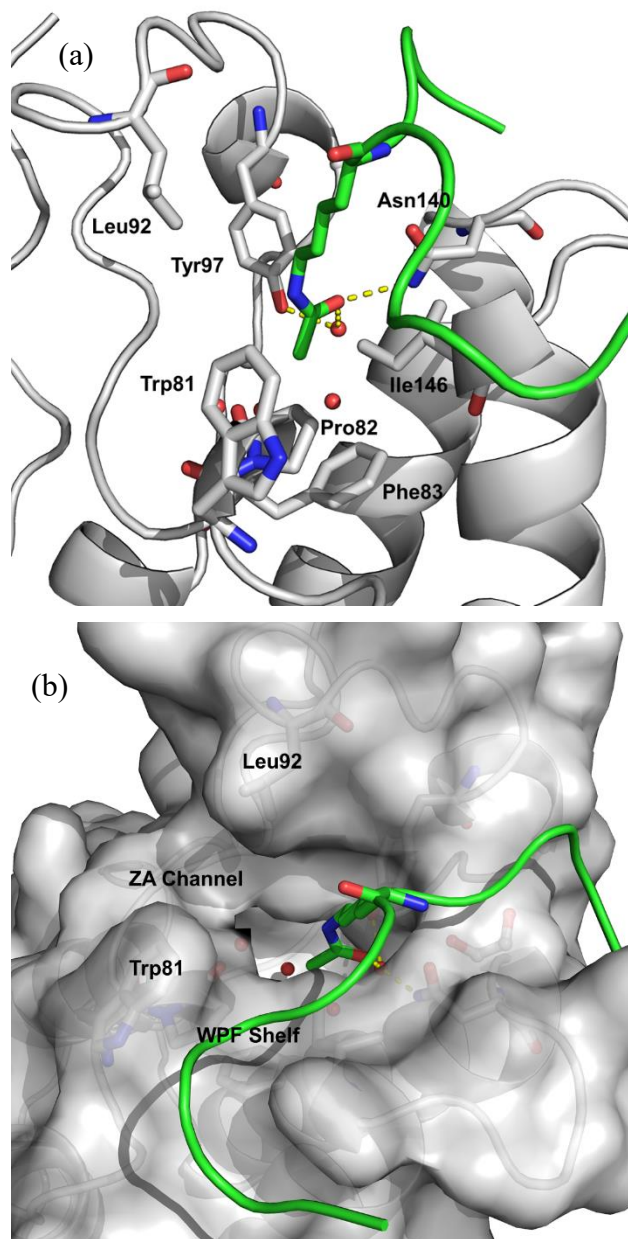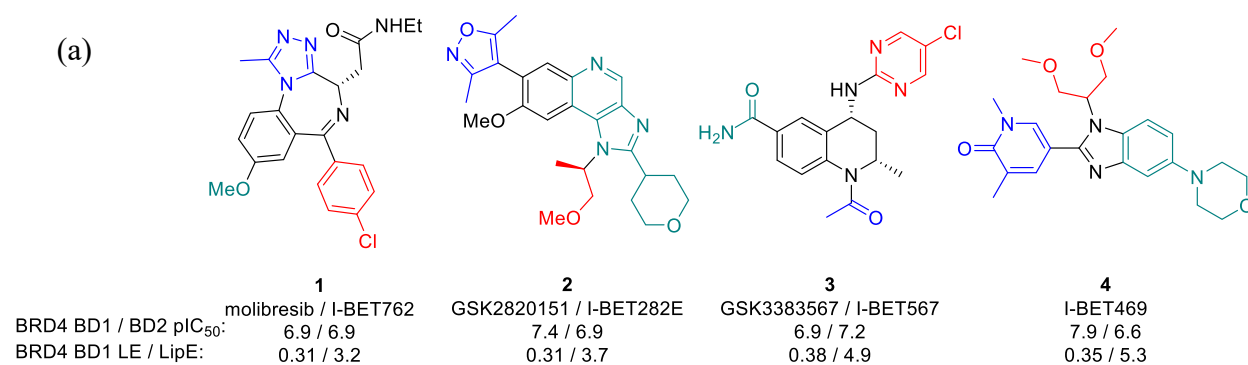
Figure 1. (a) Crystal structure of histone H4(1-12)K5/8Ac peptide (green) bound to BRD4 BD1 (grey) (pdb:3uvw). Waters are shown as red spheres and hydrogen bonds as yellow dashed lines; (b) As (a) but with the protein surface shown in grey.

The structures of several members of the GSK pan-BET inhibitor portfolio have been previously disclosed (Figure 2a).[13-16] Despite compounds **1-4** being structurally distinct, all contain motifs

which function as KAc mimetics when interacting with the eight bromodomains in the BET family. Potency at both BD1 and BD2 of BRD4 as determined by TR-FRET assay is shown as a representative of BET family potency, together with ligand efficiency [LE = (1.37 × BRD4 BD1 pIC_{50}) / heavy atom count].[17] The chromLog$D_{pH7.4}$ was also measured for each compound which enables calculation of the lipophilic efficiency (LipE, = BRD4 BD1 pIC_{50} – chromLog$D_{pH7.4}$).[18,19] Overlaying the crystallographic structures of pan-BET inhibitors **1-4** bound to BRD4 BD1 highlights how each compound occupies the WPF shelf and ZA channel from which potency and selectivity over other human bromodomains is derived (Figure 2b). Molibresib (**1**) has a benzodiazepine core with a triazole KAc mimetic, an aryl chloro group on the WPF shelf and a methoxy substituent protruding into the ZA channel.[13] GSK2820151 / I-BET282E (**2**) has an oxazole KAc mimetic together with an alkyl ether on the WPF shelf and a heteroaryl ring system in the ZA channel.[14] Tetrahydroquinoline (THQ) GSK3383567 / I-BET567 (**3**) has a simple acetate group as the KAc mimetic with a chloro pyridimidine group on the WPF shelf and a primary carboxamide in the ZA channel.[15] I-BET469 (**4**) has methyl pyridone KAc mimetic with an alkyl ether on the WPF shelf and an aryl ring in the ZA channel.[16]

(a)

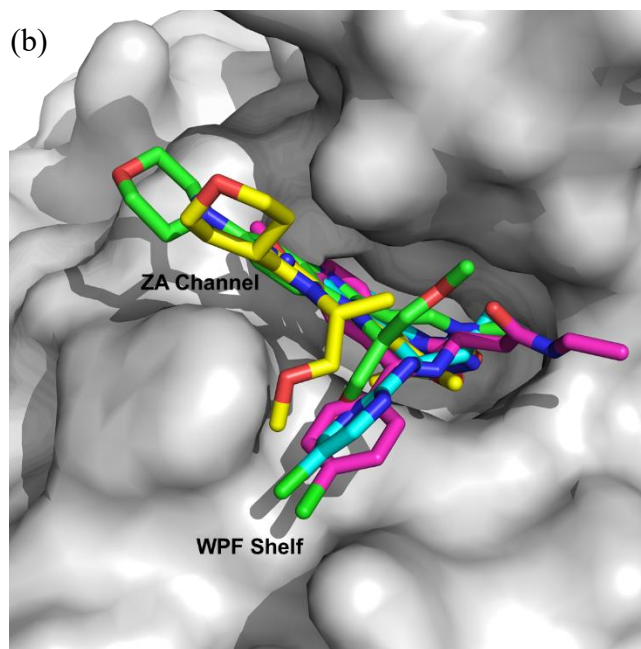|	**1** molibresib / I-BET762	**2** GSK2820151 / I-BET282E	**3** GSK3383567 / I-BET567	**4** I-BET469
BRD4 BD1 / BD2 pIC_{50}:	6.9 / 6.9	7.4 / 6.9	6.9 / 7.2	7.9 / 6.6
BRD4 BD1 LE / LipE:	0.31 / 3.2	0.31 / 3.7	0.38 / 4.9	0.35 / 5.3

(b)

Figure 2. (a) Structures of published GSK pan-BET clinical candidates and inhibitors. The KAc mimetic is colored blue, the part of the molecules interacting with the WPF shelf is colored red and the ZA channel is colored green; LE = (1.37 × BRD4 BD1 pIC_{50}) / heavy atom count; LipE = BRD4 BD1 pIC_{50} – chromLog$D_{pH7.4}$; (b) Overlays of crystal structures of **1** (magenta, pdb: 3p5o), **2** (yellow, pdb: 7o18), **3** (blue, pdb: 7qdl) and **4** (green, pdb: 6tpz) bound to BRD4 BD1 (grey surface, pdb: 6tpz).

As part of a broad ranging portfolio risk mitigation approach, GSK undertook multiple parallel research efforts to identify additional structurally distinct molecules to molibresib (**1**) and I-BET282E (**2**) to improve the probability of delivering transformational medicines to patients,[20] some of the results of which have already been disclosed.[15,16] Herein, we describe additional parallel efforts to identify a structurally distinct oral candidate quality pan-BET inhibitor. This was accomplished through a strategic focus on identifying a ligand efficient KAc mimetic fragment and subsequent crystallographically guided exploration of the WPF shelf and ZA
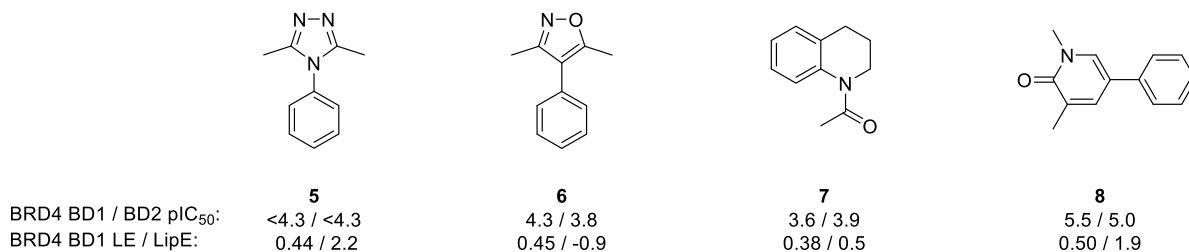
channel. Careful monitoring of LipE throughout enabled an exploitative combination of preferred groups to deliver oral candidate quality pan-BET bromodomain inhibitor I-BET432 with a 5–18 mg early predicted human dose.

RESULTS AND DISCUSSION

Target Product Profile. A structurally differentiated oral candidate quality pan-BET inhibitor was sought that met the GSK candidate quality guidelines.[21] Potency against BRD4 BD1 / BD2 $pIC_{50} > 7$ was sought with the expectation that activity would translate into pharmacologically relevant inhibition of the proinflammatory cytokine monocyte chemoattractant protein-1 (MCP-1) in lipopolysaccharide (LPS) stimulated human whole blood (hWB) (hWB MCP-1 $pIC_{50} > 6.7$). For oral exposure, passive permeability > 30 nm/s as determined by an artificial membrane permeability assay (AMP) was targeted, together with fasted state simulated intestinal fluid (FaSSIF) solubility > 100 μg/mL. From a developability perspective, we were focused on delivering a molecule with a Property Forecast Index (PFI, defined as chromLog$D_{pH7.4}$ + number of aromatic rings) < 6.[22] Perhaps most importantly, a predicted human efficacious dose < 100 mg once daily (QD) was also sought.[23]

Efficiency Analysis. As has been described elsewhere, for a given target class, drug molecules typically have higher levels of LE and / or LipE compared to other molecules active against that target.[24,25] Analysis of the published GSK pan-BET inhibitors through this lens showed that while the molecules had comparable LE (0.31 – 0.38), there was a more pronounced difference in the LipE values (Figure 3). I-BET567 (**3**) and I-BET469 (**4**) stood out compared to molibresib (**1**) and I-BET282E (**2**) with improved LipE values. Although these compounds were not all developed by fragment growth from the KAc mimetic, consideration of the KAc mimetic embedded within

each molecule and the relevant efficiencies of said KAc mimetic proved enlightening (Figure 3). To allow a normalized comparison, the corresponding KAc mimetic fragments **5-8** are shown attached to a phenyl ring. It is of note that fragments **5-8** are not expected to occupy the WPF shelf or ZA channel due to their size. The trajectory between KAc mimetic and optimized inhibitor all demonstrated a dramatic improvement in LipE values highlighting the large gains possible when growing to occupy the WPF shelf and ZA channel. In direct contrast, the LE values all dropped or at best, remained the same when moving between KAc mimetic and pan-BET candidate inhibitor. As the BRD4 BD1 potency of triazole **5** is < 4.3, the LE and LipE values shown in Figure 3 are based on a pIC_{50}: 4.2, the maximum theoretically possible and are included to aid comparison.
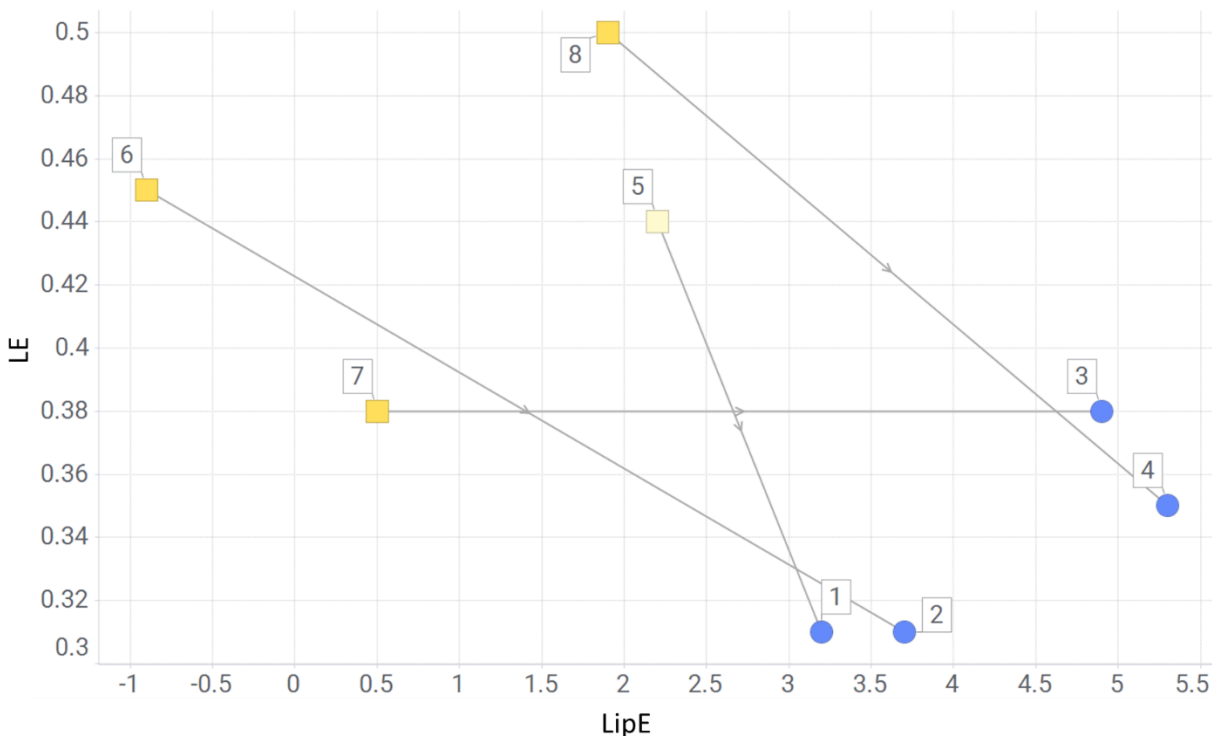

	5	**6**	**7**	**8**
BRD4 BD1 / BD2 pIC_{50}:	<4.3 / <4.3	4.3 / 3.8	3.6 / 3.9	5.5 / 5.0
BRD4 BD1 LE / LipE:	0.44 / 2.2	0.45 / -0.9	0.38 / 0.5	0.50 / 1.9

Figure 3. Visualization of LE and LipE values of compounds **1**–**8**. GSK pan-BET inhibitors are shown as blue circles and the corresponding KAc mimetics as yellow squares. Compound **5** is shown for comparison with the maximum theoretical LE and LipE derived from BRD4 BD1 pIC_{50} 4.2 as the measured BRD4 BD1 $pIC_{50} < 4.3$.

Learning from the trajectory analysis shown in Figure 3, the medicinal chemistry strategy was to identify a structurally distinct KAc mimetic fragment with high levels of LE as this parameter did not improve during optimization. Upon obtaining a co-crystal structure of the new KAc mimetic bound to a BET bromodomain, suitable vectors to access the WPF shelf and ZA channel would be identified, and the fragment grown to occupy these regions with concomitant gains in LipE. Through a focus on LipE throughout optimization, it was hypothesized that a candidate quality oral molecule could be rapidly identified with high LE and LipE.

Identification of an efficient KAc mimetic. Multiple successful fragment approaches to target bromodomains and in particular the BET family have been reported in the literature, which gave

the team confidence that a similar approach would be fruitful again.[26-29] To identify a structurally distinct and efficient KAc mimetic, a holistic data mining approach was taken. Following multiple historical internal screening campaigns and subsequent medicinal chemistry efforts, GSK had generated BRD4 BD1 data on ~50,000 compounds and it was this dataset that was extensively mined at the outset of this effort. Initially, compounds that fell into chemotypes previously worked on, or known in the literature were removed and the remaining compounds filtered to those with measurable activity in the BRD4 BD1 assay. Triaging the resultant 8000 compounds via LE > 0.3 and subsequent clustering gave 460 compounds. Orthogonal confirmation of BRD4 BD1 binding through SPR reduced the number to 270 which were then triaged by visual inspection to deliver several fragment hits of potential interest. In particular, benzoazepinone **9** stood out with both an encouraging LE of 0.46, LipE: 3.0 and a structure that appeared plausible as an KAc mimetic (Figure 4a). Crystallography of **9** bound to BRD2 BD2 was actioned which subsequently confirmed both the compound structure and the predicted binding mode as an KAc mimetic (Figure 4b). The lactam carbonyl in **9** makes the canonical hydrogen-bonding interaction directly with Asn429 (BRD2 BD2 numbering) and a through water interaction with Tyr386. The N-methyl group protrudes into a region at the base of the pocket adjacent to the highly conserved network of water molecules. The semi-saturation of the benzoazepinone positions the aryl ring towards the WPF shelf, but neither of the pendant methoxy groups make any interaction with this lipophilic region despite the 7-position methoxy being closest to doing so (Figure 4c). In a similar fashion, compound **9** does not occupy the ZA channel either, although the 5-position of the benzoazepinone ring offered a probable vector.
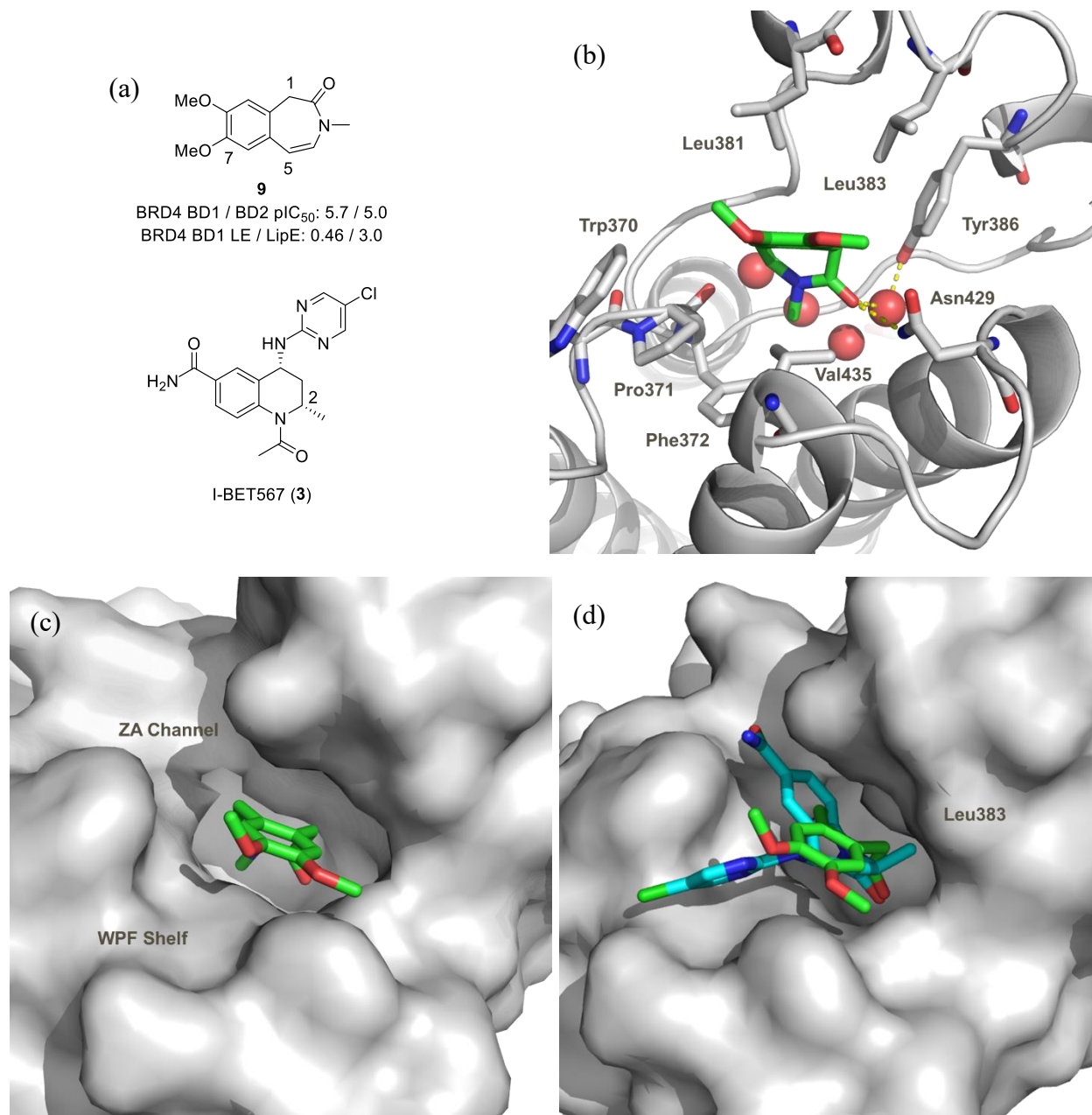
Figure 4. (a) Structure of compounds **9** and **3**; (b) Crystal structure of **9** (green) bound to BRD2 BD2 (grey) (pdb: xxxx). Water molecules are shown as red spheres and hydrogen bonds are marked in yellow; (c) As (b) but with protein surface shown; (d) As (c) but with I-BET567 (**3**) (blue) bound to BRD4 BD1 overlaid (pdb: xxxx).

Comparison of the structures of fragment **9** bound to BRD2 BD2 with pan-BET inhibitor I-BET567 (**3**) bound to BRD4 BD1 highlighted an opportunity to improve potency through the

addition of a single methyl group: I-BET567 (**3**) occupies a shallow hydrophobic pocket adjacent to Leu383 with a methyl group appended to the 2-position of the THQ ring which drives BRD4 activity across this chemotype.[30] Compound **9** did not occupy this pocket and overlaying the two structures highlighted the 1-position of the benzoazepinone ring as a probable vector (Figure 4d). It was anticipated that this would not only drive potency, but also LE due to the addition of only a single heavy atom. Indeed, the replacement of a hydrogen atom with a methyl group is a well-documented approach to achieve rapid gains in activity, typically via conformational restriction and / or interaction with a hydrophobic region of the protein.[31] Confirming the design hypothesis, addition of a methyl group to the 1-position of fragment **9** to give *(R/S)*-**10** resulted in a 100-fold eudysmic ratio of the separated enantiomers with the more potent enantiomer demonstrating a 10-fold gain in potency at BRD4 BD1 / BD2 over **9** (absolute stereochemistry was assigned by crystallography, vide infra). This gain of potency also led to a dramatic increase in LE, together with a more marginal gain in LipE due to the increased lipophilicity of the additional methyl group. A similar profile was observed for the saturated matched molecular pairs *(R/S)*-**11** with a 16-fold eudysmic ratio demonstrating a clear preference for one of the methyl group enantiomers at BRD4 BD1 / BD2. However, more generally, olefin saturation was not well tolerated with the more potent enantiomer of **11** being less active than the starting fragment **9**. Interestingly, a profound difference in lipophilicity was observed between **10** and **11** with the saturated pair far more polar than the semi-saturated analogues.

Table 1. Profiling of compounds **9**, *(R/S)*-**10** and *(R/S)*-**11**

	structure	BRD4 BD1 / BD2 FRET pIC_{50}	BRD4 BD1 LE / LipE[a]	chromLog$D_{pH7.4}$
9	MeO, MeO benzoazepinone structure	5.7 / 5.0	0.46 / 3.0	2.6

(S)-**10**	MeO, MeO structure	4.9 / 4.3	0.37 / 1.4	3.4
(R)-**10**	MeO, MeO structure	6.8 / 6.2	0.51 / 3.4	3.4
(S)-**11**	MeO, MeO structure	4.2 / 3.8	0.32 / 1.7	2.5
(R)-**11**	MeO, MeO structure	5.4 / 4.8	0.41 / 2.8	2.6

[a] LipE = BRD4 BD1 pIC_{50} − chromLog$D_{pH7.4}$; LE = (1.37 × BRD4 BD1 pIC_{50}) / heavy atom count

Crystallography of the more potent enantiomer of **10** and **11** bound to BRD2 BD2 allowed determination of the absolute stereochemistry of the methyl group at the 1-position in both molecules as *R* (Figure 5). As expected, the carbonyl group of (R)-**10** makes the canonical direct hydrogen bonding interaction to Asn429 and a through water interaction to Tyr386 (Figure 5a). Confirming the design hypothesis, the (R)-methyl group occupies a shallow hydrophobic pocket adjacent to Leu383. The structure of the saturated molecular matched pair (R)-**11** adopts a similar conformation to (R)-**10** despite the increased flexibility afforded by reduction of the olefin (Figure 5b). While the same hydrogen bonding interactions with the protein are observed, the (R)-**11** pendant aryl ring is tilted closer to the WPF shelf than with (R)-**10**, however no interaction is made with this lipophilic region. Comparison of the bound structures of **9**, (R)-**10** and (R)-**11** reveals a striking overlay of the KAc mimetics despite the presence of the additional methyl group at the 1-position (Figure 5c). A conformational analysis carried out using mixed torsional/low mode sampling in Macromodel (Maestro v2014-4) showed that the bioactive conformation of (R)-**10** corresponds very closely to the minimum energy conformation of the ligand. In contrast, the minimum energy conformation of (R)-**11** was 7.2 kJ mol^{-1} lower in energy than the bioactive conformation. This energy difference corresponds to ~1.2 logs of binding affinity in close

agreement with the difference in pIC$_{50}$ of the two molecules, suggesting that the lower potency of

(*R*)-**11** is primarily driven by the strain energy associated with adapting its bioactive conformation.
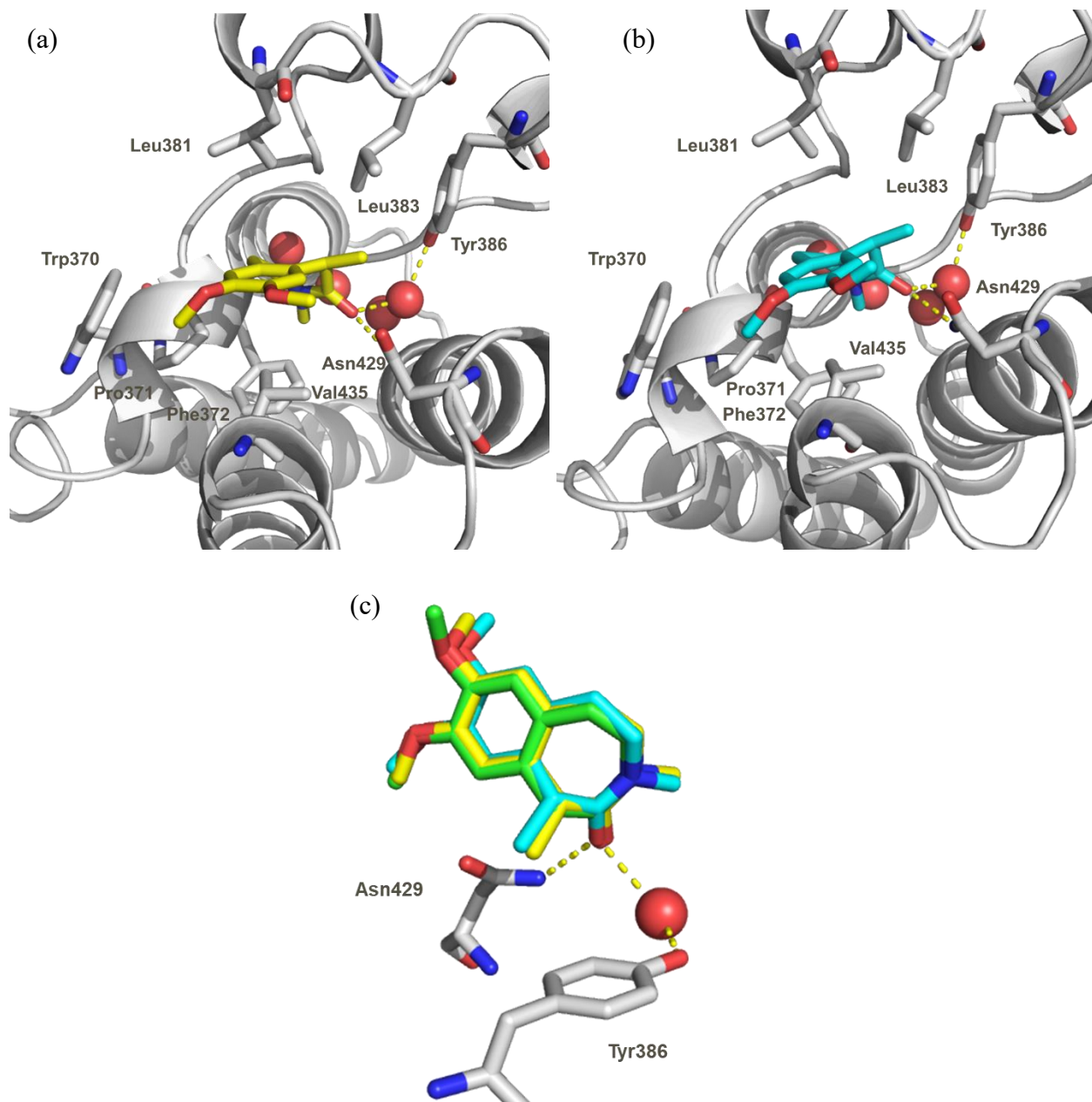

Figure 5. (a) Crystal structure of (*R*)-**10** (yellow) bound to BRD2 BD2 (grey) (pdb: xxxx). Water

molecules are shown as red spheres and hydrogen bonds are marked in yellow; (b) Crystal structure

of (*R*)-**11** (blue) bound to BRD2 BD2 (grey) (pdb: xxxx). Water molecules are shown as red

spheres and hydrogen bonds are marked in yellow; (c) Overlay of crystal structures of **9** (green,

pdb: xxxx), (R)-**10** (yellow, pdb: xxxx) and (R)-**11** (blue, pdb: xxxx) bound to BRD2 BD2 with only Asn429 and Tyr386 shown for clarity in gey (pdb: xxxx).

With a promising and efficient KAc mimetic identified in (R)-**10**, further profiling was undertaken to build an early understanding on liabilities and potential challenges in the development of this fragment into an orally bioavailable pan-BET candidate quality molecule (Table 2).

Table 2. Profile of (R)-**10**

(R)-**10**
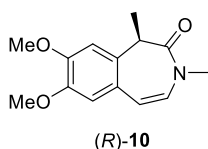
BRD4 BD1 / BD2 pIC_{50}	6.8 / 6.2
BRD4 BD1 LE / LipE[a]	0.51 / 3.4
hWB MCP-1 pIC_{50}	6.0
chromLog$D_{pH7.4}$	3.4
CYP3A4 pIC_{50}	<4.4
CYP3A4 MDI	No
hERG pIC_{50}	<4.3
AMP (nm/s)	890
CLND / FaSSIF solubility (μg/mL)	≥139 / >1000
rat / dog / human hepatocyte CL_{int} (mL/min/g tissue)	6.35 / 2.64 / <0.45

[a] LipE = BRD4 BD1 pIC_{50} – chromLog$D_{pH7.4}$; LE = (1.37 × BRD4 BD1 pIC_{50}) / heavy atom count

Consistent with the BRD4 BD1 / BD2 activity, (R)-**10** showed hWB MCP-1 inhibition at 1 μM, which not only provides evidence of cellular target engagement, but also a clinically relevant biomarker of BET bromodomain inhibition.[32] Pleasingly, there was no evidence of CYP3A4 metabolism dependent inhibition or activity at the hERG ion channel, and both passive permeability and solubility were encouragingly high. However, in vitro clearance studies revealed marked instability in rat and dog hepatocyte incubations which would need to be improved during optimization. To aid in the understanding of soft spots, in silico MetaSite prediction highlighted

the two methoxy groups and the amide methyl as the most likely sites of metabolism (SI, Figure
S1).[33]

Exploring WPF shelf and ZA channel occupation. As mentioned above, pan-BET inhibitors
typically occupy both the WPF shelf and the ZA channel of the BET bromodomains for BET
potency and selectivity over non-BET bromodomains (Figure 2). Analysis of the crystal structure
of (*R*)-**10** bound to BRD2 BD2 (Figure 4d and Figure 5c) indicated that the benzoazepinone 7-
position would be suitable to access the BET WPF shelf and the 5-position most suitable to access
the ZA channel. Accordingly, an exploratory approach was taken to rapidly build an
understanding of SAR from these vectors with some key compounds shown in Table 3. To better
understand how LipE could be optimally impacted, diverse substituents with a wide range of
lipophilicities were chosen at both vectors. Due to the multiple synthetic routes used to access the
targets (vide infra), the data shown in Table 3 is measured on 1-position racemates, single unknown
enantiomers and single known enantiomers. Where the molecules are racemic, '*rac-*' is used
before the compound number. Where the molecules have unknown stereochemistry at the 1-
position, data for the most potent separated enantiomer is shown and the stereochemistry assumed
to be (*R*).
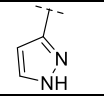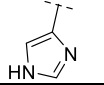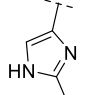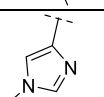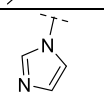
Removal of both methoxy groups from (*R*)-**10** gave unsubstituted **12** which had the highest LE
seen to date in this effort and due to the retrospective trajectory analysis already carried out (Figure
3), gave the chemistry team confidence that a high-quality molecule could be delivered from this
ligand efficient template (Table 3). There was also a drop in LipE compared to (*R*)-**10**, but as **12**
is a fragment, LE is the more relevant metric and the team was confident that considerable gains
in LipE could be gained through optimization.[34] To this end and to engage the WPF shelf from the
7-position, it was hypothesized that a sulfone, oxygen or sp3 hybridized carbon linker would

16

provide a reasonable geometry to position a substituent onto the shelf. Saturated groups were desired from this vector to keep the PFI ≤ 6 and maintain the encouraging developability properties seen to date with this series.[22] There is ample precedent for saturated groups interacting beneficially with the WPF shelf and it was thought this approach would provide more flexibility for exploring the narrow ZA channel with aromaticity if required.[16,35] Growing from **12** with the re-addition of the 7-methoxy group to give **13** improved BRD4 BD1 / BD2 potency and LipE while lipophilicity remained the same. Matched molecular pair ethyl substituted **14** further increased activity, together with a large increase in lipophilicity which significantly impacted the LipE. Growing the 7-methoxy had a marginal impact on potency with diol **18** standing out due to its dramatically improved BRD4 BD1 LipE compared to *rac*-**15**, **16** and *rac*-**17** due to reduced lipophilicity. It is of note that even with the low lipophilicity of diol **18** (chromLog$D_{\text{pH7.4}}$ 1.3) acceptable passive permeability together with activity in the hWB assay was observed. Growing via a carbon linker with more polar groups than ethyl **14** had a beneficial impact on potency with cyclic ether **19** demonstrating BRD4 BD1 pIC$_{50}$ > 7 for the first time with the benzoazepinone KAc mimetic, together with an improved LipE. Introduction of a moderately basic benzylic amine was detrimental to potency, with particularly reduced activity at BRD4 BD2 observed with pyrrolidine **21**. Alcohols **22-24** and sulfone **25** were all well tolerated with diols **23** and **24** standing out due to improved BRD4 BD1 LipE, although at the cost of reduced passive permeability. While the groups investigated from the 7-position only spanned a 10-fold BRD4 BD1 potency range, the results demonstrated that a ~60,000-fold lipophilicity range was largely well tolerated from this vector.

Table 3. Exploration of 7- and 5-position vectors
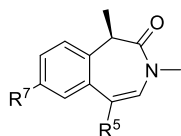
	R^7	R^5	BRD4 BD1/BD2 FRET pIC_{50}	hWB MCP-1 pIC_{50}	BRD4 BD1 LE / LipE[a]	Chrom Log$D_{pH\ 7.4}$	CLND (µg/mL)	AMP (nm/s)
12[b]	H	H	5.8 / 5.3	5.3	0.57 / 1.5	4.3	≥86	1000
13	OMe	H	6.2 / 5.8	-	0.53 / 1.9	4.3	-	880
14	Et	H	6.7 / 6.2	-	0.58 / 0.8	5.9	-	730
rac-15	OEt	H	6.3 / 6.0	5.5	0.51 / 1.3	5.0	≥120	700
16[b]	MeO~~~O (structure)	H	6.5 / 6.1	6.0	0.47 / 2.4	4.0	≥128	840
rac-17	HO~~~O (structure)	H	6.6 / 6.1	6.2	0.45 / 3.0	3.6	≥131	740
18	HO, HO~~~O (structure)	H	6.4 / 5.9	6.2	0.44 / 5.1	1.3	≥142	42
19[b]	tetrahydropyran (structure)	H	7.2 / 6.5	6.2	0.47 / 1.7	5.4	≥111	710
20	morpholine (structure)	H	6.8 / 6.2	6.4	0.44 / 3.5	3.3	≥142	775
21[b]	pyrrolidine (structure)	H	6.3 / 5.1	5.8	0.43 / 4.8	1.5	≥97	360
22[b]	HO (structure)	H	6.4 / 5.8	6.0	0.52 / 3.8	2.6	≥108	240
23	HO, HO (structure)	H	6.4 / 5.7	6.2	0.46 / 5.2	1.2	≥209	30
24	HO, OH (structure)	H	6.4 / 5.7	6.0	0.49 / 5.3	1.1	≥101	27
25[b]	sulfone (structure)	H	6.7 / 5.9	6.4	0.49 / 3.6	3.1	-	420
26[b]	sulfone (structure)	Me	7.1 / 6.6	6.8	0.49 / 3.7	3.4	≥131	150
27[b]	sulfone (structure)	O, NH2 (structure)	5.8 / 5.5	5.7	0.36 / 4.7	1.1	82	10
rac-28	sulfone (structure)	Ph	6.6 / 6.3	5.8	0.36 / 1.5	5.1	≥146	1000
rac-29	sulfone (structure)	pyridinyl (structure)	6.2 / 5.8	5.9	0.34 / 3.4	2.8	128	350
30	sulfone (structure)	pyrazole (structure)	7.4 / 7.1	7.4	0.41 / 4.6	2.8	≥222	145
31[b]	OEt	pyrazole (structure)	8.0 / 8.1	7.7	0.48 / 3.9	4.1	143	570
32[b]	OEt	pyrazole N-NH (structure)	8.2 / 8.4	7.6	0.51 / 4.7	3.4	≥115	370

|								
rac-**33**	OEt		7.5 / 7.7	6.9	0.47 / 3.7	3.8	≥99	540
34[b]	OEt		8.0 / 8.0	7.3	0.50 / 5.3	2.7	≥131	460
35[b]	OEt		7.9 / 7.7	7.8	0.47 / 4.8	3.1	≥135	400
36[b]	OEt		7.5 / 7.6	7.3	0.45 / 4.0	3.6	117	690
rac-**37**	OEt		4.4 / 4.6	-	0.27 / 0.1	4.3	≥65	580

[a] LipE = BRD4 BD1 pIC_{50} – chromLog$D_{pH7.4}$; LE = $(1.37 \times$ BRD4 BD1 $pIC_{50}) /$ heavy atom count; [b] more potent separated unknown enantiomer, assumed *R* stereochemistry based on analogue crystallography.

In parallel to the 7-position investigation, an exploration of the 5-position was in progress to gain additional potency through occupying the ZA channel. While fixing the 7-position as an ethyl substituted sulfone, in part due to synthetic ease, addition of a methyl group to the 5-position to give **26** demonstrated an encouraging jump in both biochemical and hWB potency. Primary amide **27** showed a 10-fold drop in potency, although due to 100-fold reduced lipophilicity, the LipE increased 10-fold over **26**. Passive permeability also dropped below the target criteria of 30 nm/s, presumably due to the reduced lipophilicity and/or increased number of hydrogen bond donors. 6-Membered aromatic rings were not well tolerated from the 5-position with benzene **28** and pyridine **29** shown as representative examples. However, 5-membered rings such as pyrazole **30** led to increases in both biochemical and hWB potency while maintaining desirable solubility and passive permeability. Ethoxy substituted matched molecular pair **31** maintained this trend with an example of the first compound with a BRD4 BD1 $pIC_{50} > 8$ confirming the design hypothesis that growing into the ZA channel would be a fruitful route to improve potency. Des-methyl **32** had similar levels of potency to N-methyl matched molecular pair **31** and due to decreased lipophilicity had increased LipE. 3-Substituted NH pyrazole *rac*-**33** and imidazoles **34-36** were well tolerated with
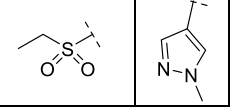
methyl imidazole **35** particularly active in the hWB MCP-1 assay. An activity cliff was seen with N-linked imidazole **37** with a profound drop in potency compared to C-linked isomer **34**.

With the starting point for this exploration, (*R*)-**10**, demonstrating marked instability in rat and dog hepatocyte incubations (Table 2), data was generated on more substituted analogues to understand how readily this challenge could be mitigated (Table 4). Morpholine substituted **20** still showed problematic rat and dog in vitro hepatocyte CL_{int}, while the human CL_{int} was maintained at <0.45 mL/min/g tissue. Although data is not available for the appropriate matched molecular pair, substitution of both the 5 and 7-position as in **26** resulted in a dramatic reduction of rat and dog hepatocyte CL_{int} demonstrating for the first time that moderate clearance in these species was obtainable from the benzoazepinone template. Although fraction unbound in hepatocytes was not measured at the time, the comparable lipophilicity between compounds **20** and **26** suggests that the CL_{int} change is likely to be driven by removing / blocking site(s) of metabolism rather than non-specific binding.[36] Pyrazole **30** demonstrated further improved dog hepatocyte stability together with moderate rat CL_{int}, whereas **31** with chromLog$D_{pH7.4}$: 4.1 highlighted the importance of controlling lipophilicity on this template if low hepatocyte clearance was to be achieved.

Table 4. Hepatocyte incubation CL_{int} for **20**, **26**, **30** and **31**
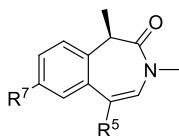
	R^7	R^5	chromLog$D_{pH7.4}$	rat / dog / human hepatocyte CL_{int} (mL/min/g tissue)
20	(morpholine ethyl)	H	3.3	23.76 / 3.37 / <0.45
26[a]	(ethyl sulfonyl)	Me	3.4	1.18 / 0.77 / <0.45

30	(ethyl methylsulfone structure)	(pyrazole ring)	2.8	2.44 / <0.65 / <0.45
31[a]	OEt	(pyrazole ring)	4.1	72.36 / <0.65 / 9.14

[a] more potent separated unknown enantiomer, assumed *R* stereochemistry based on analogue crystallography.

Exploiting SAR knowledge. Visualizing the relationship between potency, lipophilicity and lipophilic efficiency is a powerful method to interrogate these critical molecular attributes.[18] The compounds profiled in Table 3 were plotted with BRD4 BD1 on the y-axis, chromLog$D_{pH7.4}$ on the x-axis, and diagonal lines representing different LipE values (Figure 6). While there was no desirable LipE cut-off for this project, this visualization allows trends to be identified, aids in analysis and encourages teams to target improved LipE, rather than just improved potency. Alcohol substituents in the 7-position (colored blue), in particular diols **18**, **23** and **24**, while less potent than some other substituents, made efficient use of the lipophilicity budget with encouraging LipE values > 5. While there was a clear preference for 5-membered heteroaromatic rings in the 5-position (squares) from a potency lens, the chemistry team was also encouraged by LipE values amongst the highest seen to date with the benzoazepinone series e.g **34**. The same general trends are also seen when visualizing BRD4 BD2 pIC$_{50}$ against chromLog$D_{pH7.4}$ data with alcohols and 5-membered rings giving large gains in LipE relative to other groups when considering matched molecular pairs.
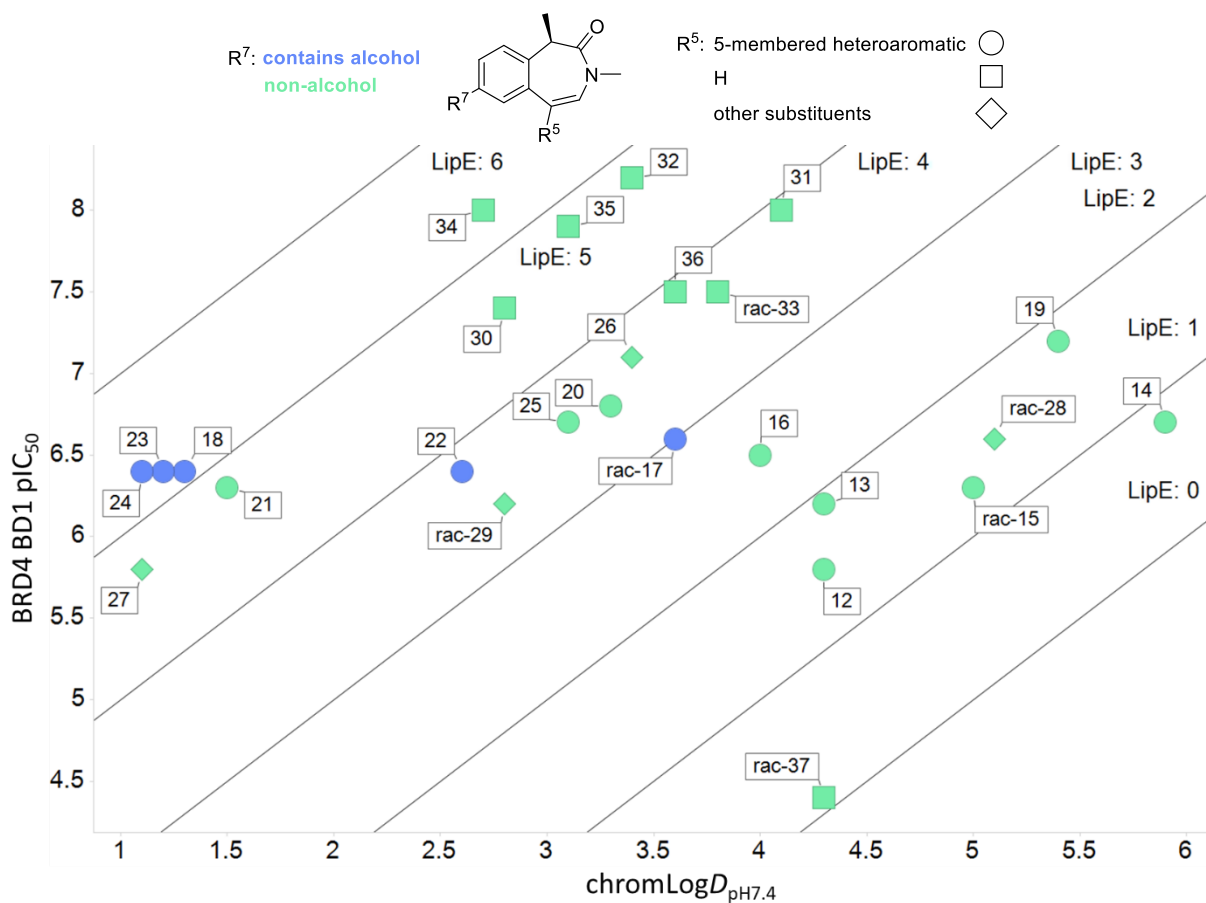
Figure 6. Plot of BRD4 BD1 pIC$_{50}$ against chromLog$D_{pH7.4}$ with diagonal lines representing LipE values for compounds in Table 3. Compound numbers are shown in boxes.

Having gained an understanding of the SAR at the 5- and 7-position, the chemistry team sought to exploit this knowledge by combining groups with the aim of delivering compounds which met the predetermined progression criteria. Although insufficient matched molecular pairs were available for a thorough Free-Wilson analysis,[37] with an understanding of the binding mode of the targets, the chemistry team was confident that at least partial additivity in the SAR would be observed. As such, 22 7-position and 35 5-position moieties that drove LipE were virtually enumerated as single enantiomers to give 770 potential targets. Attempts to triage the list down to a manageable number for synthesis via hard cut-offs using parameters such as lipophilicity and hydrogen bond donor count were unsuccessful with hundreds of compounds remaining. To

address this common challenge with virtual enumeration, a simple equal weighting multi-parameter scoring profile based on predicted or calculated physicochemical properties was used to identify benzoazepinone molecules more likely to be orally bioavailable (Figure 7).
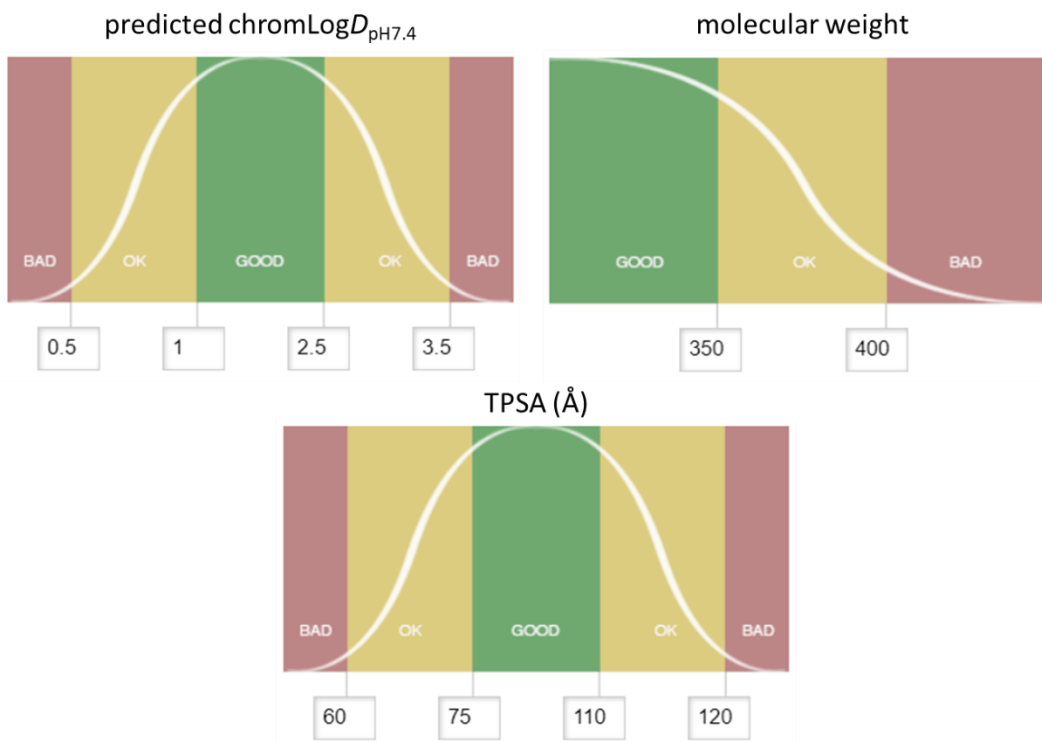
Figure 7. Multi-parametric scoring profile desirability parameters for predicted chromLog$D_{pH7.4}$, molecular weight, and topological polar surface area.

Key to the success of any given multi-parameter score is the determination of 'desirable' for a given property.[38] ChromLog$D_{pH7.4}$ < 1 was scored as less desirable to try and drive passive permeability.[18] The upper boundary was set to deliver stable hepatocyte CL$_{int}$ and meet the pre-defined progression criteria of PFI ≤ 6 due to the presence of two aromatic rings in the majority of the targets. Due to the combinatorial nature of the virtual enumeration, some molecules had undesirable molecular weight, so a target < 400 was set as desirable to drive towards developable chemical space. Topological polar surface area (TPSA) < 110 was designated to drive passive

23

permeability,[39] whereas the lower end of 75 was chosen to try and mitigate adverse toxicological outcomes.[40] Application of the resultant multiparametric scoring function to the 770 virtually enumerated targets gave a range of 0.963 – 0.002 with 1 being the optimal score. This score, together with an assessment of synthetic tractability was leveraged to identify 40 targets for synthesis, the BRD4 BD1 potency and lipophilicity of which are visualized on a LipE plot (Figure 8).

As seen previously in exploring the SAR on the benzoazepinone template, compounds with 7-position alcohols and 5-position 5-membered heterocycles, in particular NH and NMe pyrazoles, were not only the most potent, but also the most efficient. Of note is how inefficient 7-position non-alcohol substituents are when combined with a variety of 5-position groups, with the most efficient compound in this set (LipE: 5.3) still 50-fold less efficient than compound **38** which contains a 7-position alcohol substituent (LipE: 7.0).
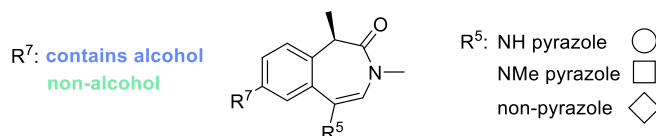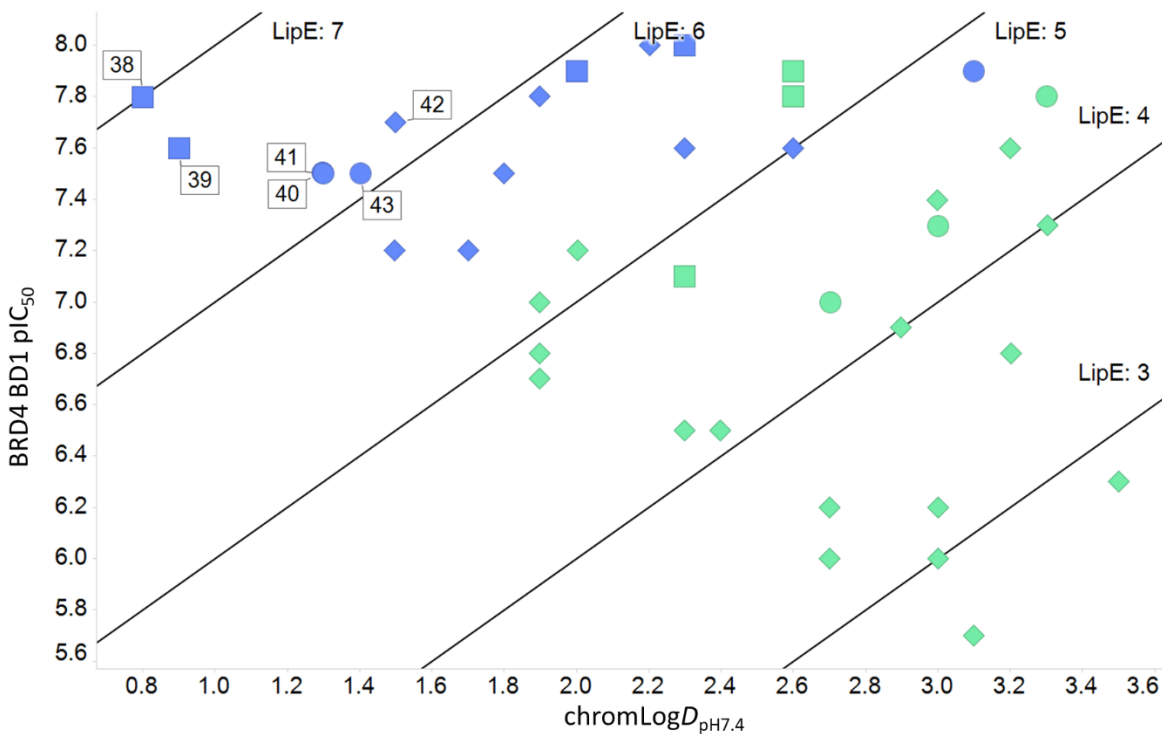
Figure 8. Plot of BRD4 BD1 pIC_{50} against $chromLogD_{pH7.4}$ for exploitative SAR compounds with diagonal lines representing LipE values. Compound numbers are shown in boxes where appropriate.

The structures and profiles of the most lipophilic efficient compounds accessed (**38-43**) in this set are shown in Table 5. All these compounds met the predetermined BRD4 BD1 / BD2 potency criteria (target $pIC_{50} > 7.0$) which translated into hWB MCP-1 activity above the desired threshold (target $pIC_{50} > 6.7$). FaSSIF solubility was encouraging with all compounds more soluble than the target of 100 µg/mL. However, somewhat predictably due to the high polarity of the compounds, passive permeability was less encouraging with only the epimeric diols **40** and **41** meeting the target criteria of > 30 nm/s. However, the low level of drop-off between the biochemical and whole blood assay for all the compounds did suggest that cellular penetration was certainly occurring, even if there was a potential risk of poor oral bioavailability for compounds **38**, **39**, **42** and **43**. At this point, **42** and **43** were down prioritised due to unmeasurable passive permeability

with **38** and **39** progressing towards in vivo pharmacokinetic studies to better understand the passive permeability risk of these compounds. The low polarity for diols **38-41** (chromLog$D_{pH7.4}$ 0.8-1.3) translated into low to moderate hepatocyte in vitro CL_{int} across rat, dog and human which gave further encouragement for in vivo studies. This low to moderate CL_{int} profile was a noticeable improvement over the hepatocyte incubation total stability observed with (*R*)-**10** (Table 2) and the exploration benzoazepinones **20**, **26**, **30** and **31** (Table 4) indicating the required improvements in metabolic stability that had been achieved during the optimization efforts.

Table 5. Profile of compounds **38-43**
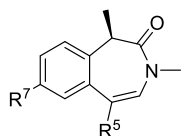
	R^7	R^5	BRD4 BD1/BD2 FRET pIC$_{50}$	hWB MCP-1 pIC$_{50}$	BRD4 BD1 LE / LipE[a]	chro mLog $D_{pH7.4}$	FaSSIF (µg/mL)	AMP (nm/s)	rat / dog / human hepatocyte CL$_{int}$ (mL/min/g tissue)
38			7.8 / 7.6	7.4	0.46 / 7.0	0.8	>1000	8	<0.8 / <0.65 / 0.52
39			7.6 / 7.4	7.5	0.45 / 6.7	0.9	417	7	<0.8 / - / <0.45
40			7.5 / 7.5	7.4	0.43 / 6.2	1.3	>1000	31	<0.8 / 1.12 / <0.45
41			7.5 / 7.2	7.4	0.43 / 6.2	1.3	>1000	31	<0.8 / <0.65 / <0.45
42			7.7 / 7.5	7.4	0.44 / 6.2	1.5	≥185[b]	<3	- / - / -
43			7.5 / 7.0	7.5	0.41 / 6.1	1.4	≥208[b]	<3	- / - / -

[a] LipE = BRD4 BD1 pIC$_{50}$ − chromLog$D_{pH7.4}$; LE = (1.37 × BRD4 BD1 pIC$_{50}$) / heavy atom count; [b] CLND solubility

Confirming the expected impact of poor in vitro passive permeability on oral bioavailability, epimeric diols **38** and **39** both showed oral bioavailability < 20% despite encouraging solubility

and total clearance (Table 6). The matched molecular pairs to NH pyrazoles **38** and **39**, methyl pyrazoles **40** and **41** had both improved rat oral bioavailability and lower total and unbound clearance, together with similar moderate total and unbound volumes of distribution and terminal half-lives. However, consistent with the in vitro hepatocyte CL_{int} data, a separation between epimeric diols **40** and **41** was seen in dog pharmacokinetic studies where **41** had reduced total and unbound clearance compared to **40**. Additionally, **41** showed an improved oral bioavailability in dog (79%) compared to **40** (39%), as well as a longer half-life. It is hypothesized that the oral bioavailability observed with diols **38-41** may be aided by intramolecular hydrogen bonding masking the polarity of the alcohols.[41] On the basis of the rat and dog pharmacokinetic experiments, **38-40** were down prioritised and **41** was progressed into downstream studies.

Table 6. Pharmacokinetic profile of compounds **38-41** following intravenous infusion and oral administration in male wistar han rat and beagle dog[a]
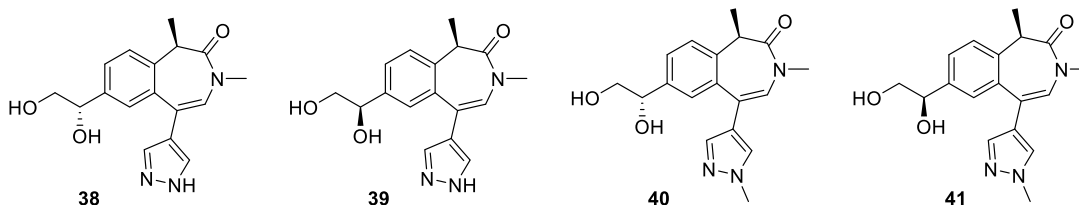
Cpd	Species	Dose iv[b] / po[c] (mg/kg)	CL_b (mL/min/kg)	$CL_{b,u}$ (mL/min/kg)	V_{ss} (L/kg)	V_{ss_u} (L/kg)	$t\frac{1}{2}$ (h)	Fpo (%)	fu_b
38	rat	1.0 / 3.1	43	75	1	1.8	0.41	19	0.57
39	rat	2.1 / 2.9	37	-	1.5	-	0.76	13	-
40	rat	1.0 / 3.1	19	31	1.1	1.8	0.97	66	0.61
	dog	0.4 / 1.5[d]	45	87	1.7	3.3	0.5	39	0.52
41	rat	1.0 / 3.0	26	38	1.3	1.9	0.74	67	0.68
	dog	0.5 / 1.5[d]	28	60	2.7	5.7	1.4	79	0.47

[a] PO values are mean n = 3 and IV n = 1 unless otherwise stated; [b] IV dose 1 h infusion in DMSO and (10%, w/v) Kleptose HPB in saline (2%:98% v/v or 5%:95% v/v); [c] PO dose vehicle: 1% (w/v) methylcellulose (400 cps) (aq); [d] n = 1

Profiling **41** against CYP3A4 did not show any evidence of direct or metabolism dependent inhibition (Table 7). The risk of hERG inhibition was also low and importantly **41** was negative in the mutagenicity Ames assay with and without the presence of S9 mix.

Throughout the medicinal chemistry optimization effort, there had been internal discussions about the benzoazepinone core structure and whether there were inherent developability risks associated with both the potentially epimerizable chiral methyl group in the 1-position and the electron rich olefin of the *N*-acyl enamine. Indeed, the nucleophilicity of the olefin is utilized via bromination in the synthesis of compounds with substituents in the 5-position (Scheme 5). Methyl epimerisation had also been observed during the synthesis of some targets, although this was only seen with the combination of forcing reaction conditions and an electron withdrawing group at C-7 which presumably lowered the pKa of the C-1 proton (Scheme 3). To understand these potential risks, a range of stability experiments were carried out: Profiling **41** at 40 °C pH 10 media, pH 6 media and simulated gastric fluid (SGF) with and without the presence of hydrogen peroxide as an oxidant did not reveal any compound degradation and glutathione trapping was also negative. The combination of these results provided reason to believe that **41**, and by extension the benzoazepinone core itself, was not fundamentally unstable or undevelopable.

Table 7. Further profiling of compound **41**[a]
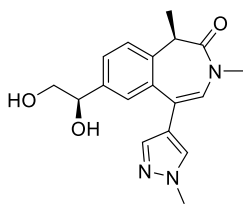
BRD4 BD1 / BD2 pIC$_{50}$	7.5 / 7.2
BRD4 BD1 LE / LipE	0.43 / 6.2
hWB MCP-1 pIC$_{50}$	7.4
chromLog$D_{pH7.4}$ / PFI	1.3 / 3.3
AMP (nm/s)	31
FaSSIF solubility (µg/mL)	> 1000
CYP3A4 pIC$_{50}$	< 4.4
CYP3A4 MDI	no
hERG pIC$_{50}$	< 4.3
Ames ± S9	negative
pH 10, 6, SGF ± H$_2$O$_2$ (half-life)	> 1000 h
GSH trapping	negative

[a] LipE = BRD4 BD1 pIC_{50} – chromLog$D_{pH7.4}$; LE = (1.37 × BRD4 BD1 pIC_{50}) / heavy atom count

BROMOscan profiling of **41** against 24 members of the human bromodomain family revealed activity against all members of the BET bromodomain family as expected (pKd 8.5 – 7.8) with the closest off target bromodomains CREBBP and TRIM24 (pKd 5.9) (SI, Table S2).[42] Screening **41** in the GSK enhanced cross-screening panel of pharmacologically relevant off-target liability assays revealed a profile supporting further development (SI, Table S3).

Crystallography of **41** in complex with BRD2 BD2 was obtained to confirm the mechanism of action as an KAc mimetic and better understand the interactions being made with the protein. As expected, based on previous co-crystal structures with this chemotype, the carbonyl group of the benzoazepinone ring made the canonical hydrogen-bonding interaction with Asn429 and a through water interaction with Tyr386 (Figure 9a). As seen with the structure of (*R*)-**10** bound to BRD2 BD2 (Figure 5), the chiral methyl group in the 1-position protrudes into the hydrophobic pocket adjacent to Leu383. Confirming the design hypothesis, substitution from the 7-position leads to engagement of the WPF shelf (Figure 9c). As might be expected, the polar diol points towards bulk solvent, making a through water interaction with Asp384 and the carbon chain rests on a lipophilic region. The two oxygen groups are orientated 2.8 Å apart, suggestive of an intramolecular hydrogen-bond which may help explain the observed passive permeability and oral exposure seen with this polar molecule.[43] This crystal structure challenges the dogma that lipophilic groups are required for activity when occupying the WPF shelf. It is clear that polar substituents can be tolerated in this region of the protein, as long as they are carefully chosen. Also confirming the initial design hypothesis, substitution from the 5-position placed the pyrazole ring into the ZA channel with a 29.1 ° dihedral angle with the enamide olefin. Interestingly the pyrazole C-5 carbon is 3.5 Å from the Pro371 backbone carbonyl and in the correct orientation to engage

through a hydrogen-bond (Figure 9b).[44] This, albeit slightly long, interaction may partly explain

the efficiency of the pyrazole ring from this vector (Figure 8). Overlaying the structures of **41** and

(*R*)-**10** highlight that although the key KAc mimetic hydrogen-bonding interactions have not

shifted, extension into the ZA channel and WPF shelf have caused the benzoazepinone ring to tilt

resulting in a 1.2 Å translation of the 7-carbon between the two ring systems (Figure 9d).
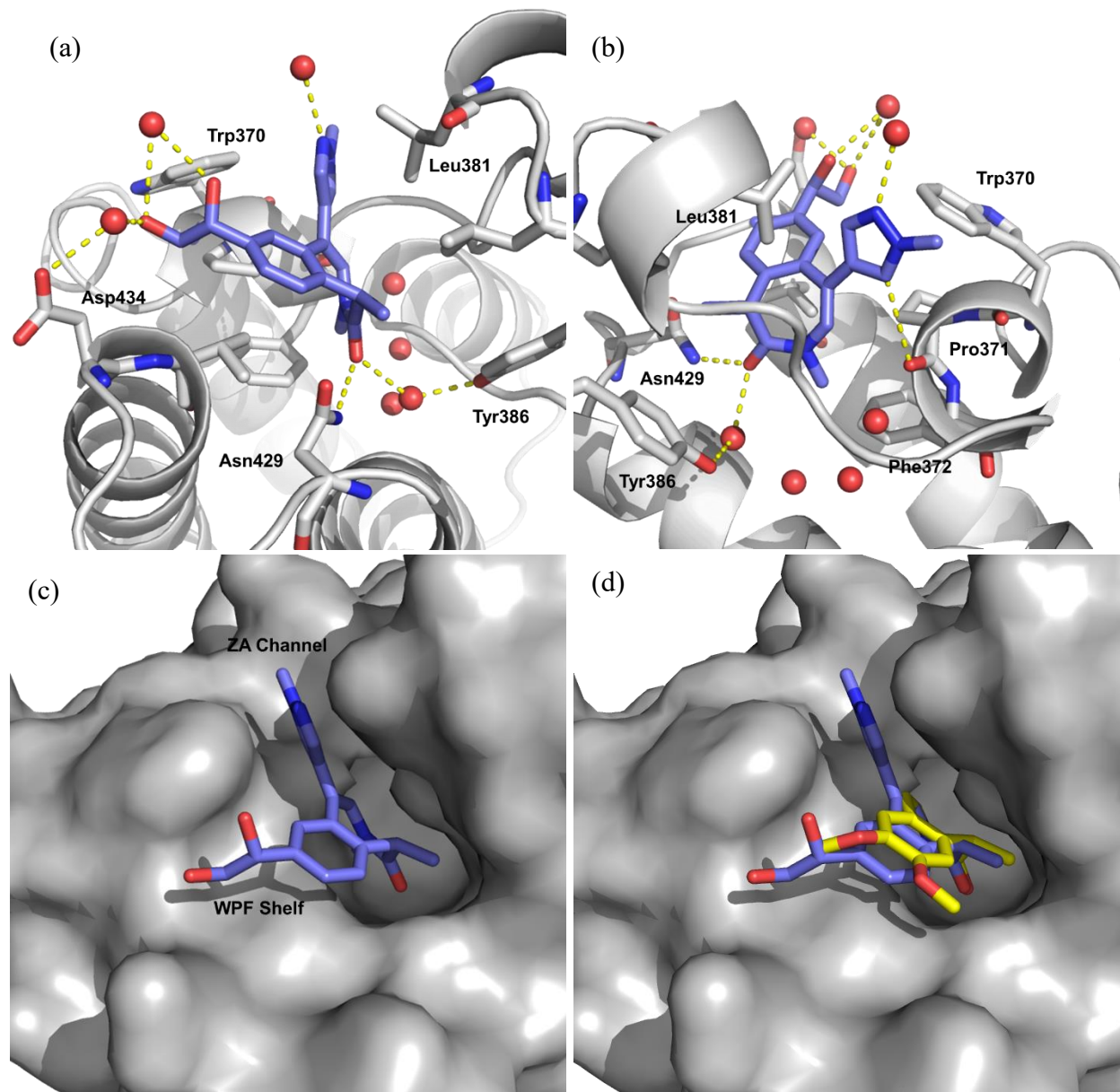
Figure 9. (a) Crystal structure of **41** (dark blue) bound to BRD2 BD2 (grey) (pdb: xxxx). Water molecules are shown as red spheres and hydrogen bonds are marked in yellow; (b) as (a), but in an alternative orientation; (c) as (a) but with the protein surface (grey) shown; (d) as (c), but with (*R*)-**10** (yellow) (pdb: xxxx) overlayed.

With data supportive of progression in hand, an early human dose prediction for **41** was generated using hWB MCP-1 potency data and a single species scaling approach while correcting for fraction unbound.[45,46] A target coverage of IC_{90} for 4 h was chosen to impact pro-inflammatory mediators based on internal knowledge generated via in vivo PKPD studies with other pan-BET bromodomain inhibitors. This target gave an encouraging once daily predicted human dose of 5 and 18 mg as allometrically scaled from rats and dogs respectively.

Efficiency Reanalysis. The medicinal chemistry strategy was to identify a highly ligand efficient KAc mimetic and then optimize based on LipE while occupying the WPF shelf and ZA channel for selectivity and potency against the BET family of bromodomains. Visualizing the LipE and LE trajectory from KAc mimetic **12** and lead molecule **41** highlights how successful this approach was with the benzoazepinone series (Figure 10). KAc mimetic **12** is more ligand efficient (0.57) than any of the other mimetics that have been used in GSK's portfolio of pan-BET inhibitors (**5-8**). Although the LipE for **12** is not as high as other KAc mimetics, the design strategy addressed this with a 50,000-fold improvement in LipE to deliver **41** that has the highest LipE (6.3) and LE (0.43) of the candidate quality GSK pan-BET inhibitors disclosed to date (**1-4**). Interestingly, this visualization highlights clearly an almost identical LE and LipE trajectory between KAc mimetic, and candidate observed for **6** to I-BET282E (**2**) and **12** to **41**. Analysis has shown that within a target class, the compounds that are more likely to become drugs are differentiated from other molecules by improved LE and/or LipE which is encouraging for any future development of **41**.[25]
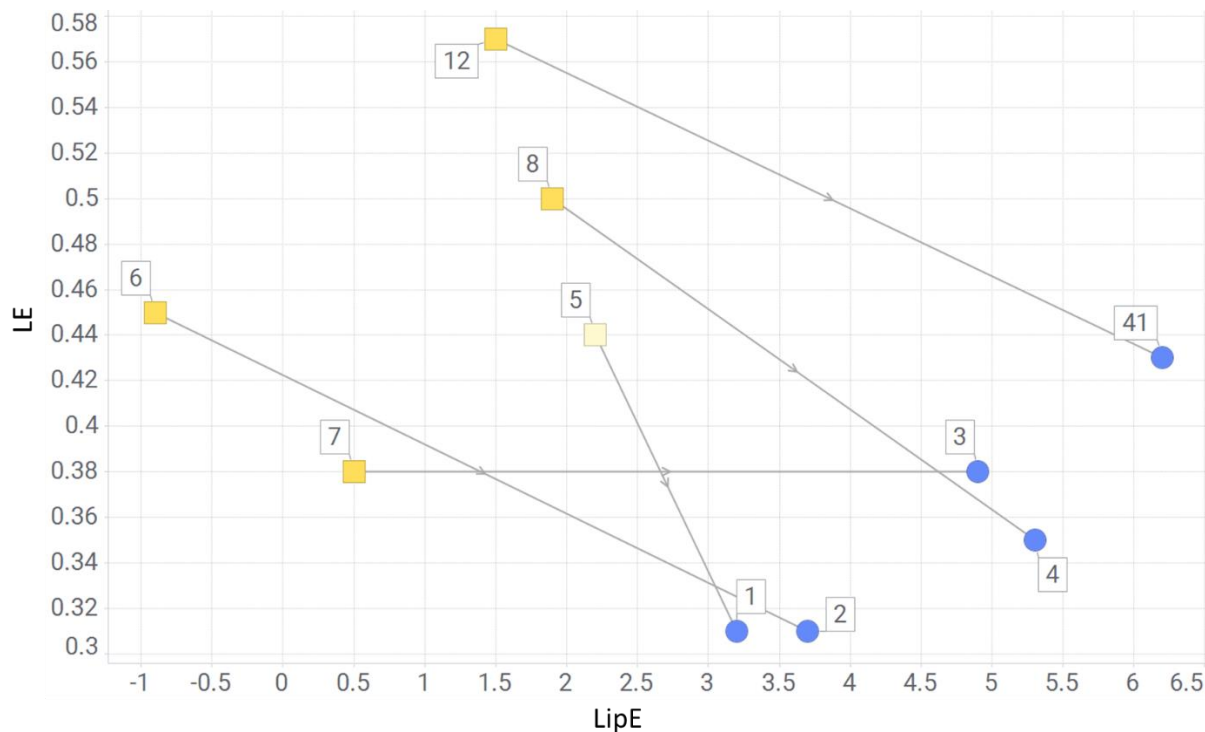
Figure 10. Visualization of LE and LipE values. GSK pan-BET inhibitors are shown as blue circles and the corresponding KAc mimetics as yellow squares. Compound **5** is shown with the maximum theoretical LE and LipE values as BRD4 BD1 $pIC_{50} < 4.3$.

Chemistry. Benzoazepinone hit **9** was purchased for the GSK compound collection. Synthesis of 1-methyl targets (*R/S*)-**10** and (*R/S*)-**11** began with amide bond formation via acid chloride formation from commercially available carboxylic acid **44** (Scheme 1). This was followed by a Brønsted acid-mediated cyclisation with the bis-methoxy activated aryl ring to form the benzoazepinone ring of *rac*-**10**. Chiral SFC purification provided the separated enantiomers (*S*)-**10** and (*R*)-**10**, the absolute configuration of which was assigned following crystallography (Figure 5). Hydrogenation of *rac*-**10** followed by chiral SFC purification provided straightforward access to the saturated matched molecular pairs (*S*)-**11** and (*R*)-**11**. In a similar fashion to the synthesis of *rac*-**10**, amide bond formation with commercially available acid **46** provided acetal **47**.

Aluminium chloride mediated cyclisation closed the 7-membered ring to give *rac*-**12** which was then purified by chiral SFC to provide ligand efficient fragment **12**.

Scheme 1. Synthesis of (*R*/*S*)-**10**, (*R*/*S*)-**11** and **12**[a]

44, R: OMe
46, R: H

45, R: OMe
47, R: H

rac-**10**, R: OMe
rac-**12**, R: H

(*R*)-**10**, R: OMe
12, R: H
+
(*S*)-**10**, R: OMe

(*R*)-**11**
+
(*S*)-**11**
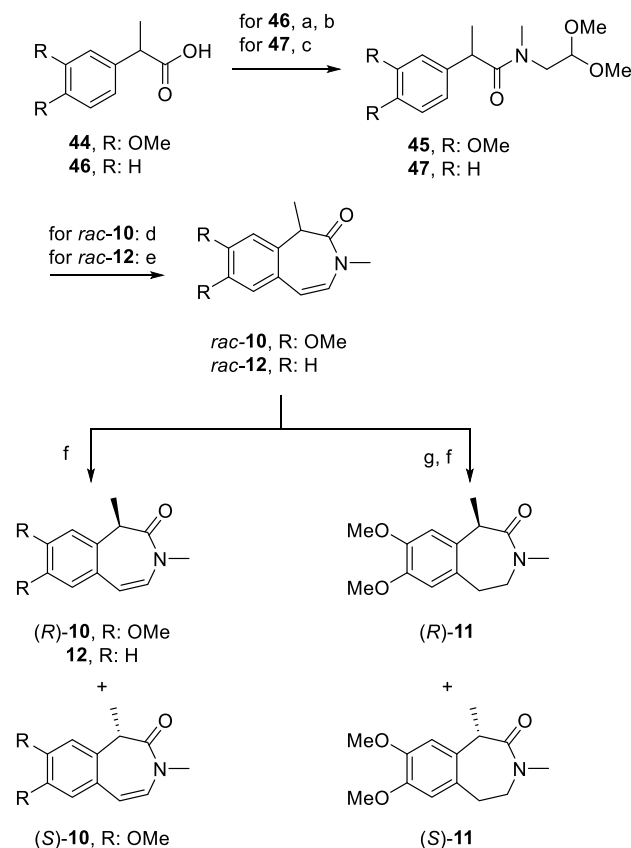
[a]Reagents and conditions: (a) SOCl$_2$, CH$_2$Cl$_2$, 0 °C to rt, 2 h; (b) 2,2-dimethoxy-*N*-methylethanamine, NEt$_3$, CH$_2$Cl$_2$, 0 °C to rt, 1 h, 38% over two steps; (c) T3P, 2,2-dimethoxy-*N*-methylethanamine, DIPEA, THF, 70 °C, 16 h, 66%; (d) AcOH, HCl, 0 °C to rt, 24 h, 45%; (e) AlCl$_3$, CH$_2$Cl$_2$, 0 °C to rt, 3 h, 24%; (f) chiral SFC purification; (g) 10% Pd/C, H$_2$, EtOH, rt, 24, 77%.

With the desired absolute stereochemistry at C-1 known to be *R*, a chiral synthesis of the benzoazepinone core was carried out utilizing a chiral Evans oxazolidinone alkylation as the key stereodetermining step (Scheme 2).[47] The required N-Acyl oxazolidinone derived from phenylalanine was accessed from commercially available carboxylic acid **48** via mixed anhydride formation. The chiral enolate was then generated with NaHMDS and trapped with methyl iodide

to give **49** with an 86% diastereomeric excess as determined by ^{1}H NMR analysis. Peroxide

mediated hydrolysis was followed by amide bond formation with methylamine to give **50**. Suzuki

coupling with the requisite pinacol boronic ester provide cyclisation precursor **51** which underwent

acid mediated condensation to provide **13** in 83% enantiomeric excess, consistent with the 86%

diastereomeric excess observed with **49**. Subsequent recrystallization in acetonitrile successfully

increased the enantiomeric excess of **13** to >99%.

Scheme 2. Synthesis of **13**[a]
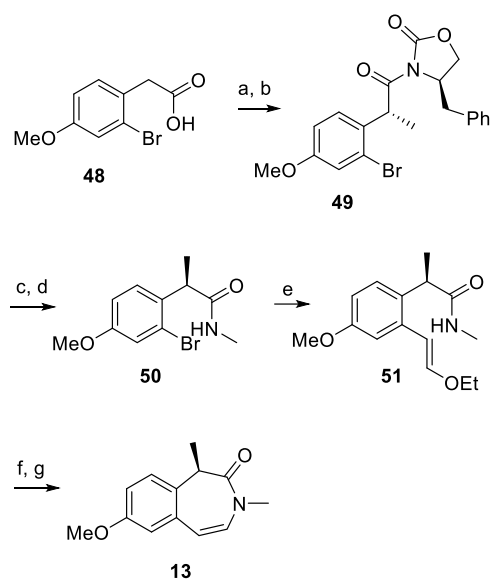
[a]Reagents and conditions: (a) PivCl, (*R*)-4-benzyloxazolidin-2-one, NEt$_3$, toluene, 110 °C, 24 h, 75%; (b) NaHMDS, MeI, THF, –78 °C to rt, 24 h, 81%, 86% d.e.; (c) LiOH, H$_2$O$_2$, THF, H$_2$O, 0 °C to rt, 25 h, 92%; (d) MeNH$_2$ in THF, HATU, DIPEA, DMF, rt, 45 min, 81%; (e) (*E*)-2-(2-ethoxyvinyl)-4,4,5,5-tetramethyl-1,3,2-dioxaborolane, K$_2$CO$_3$, Pd(PPh$_3$)$_4$, 1,4-dioxane, H$_2$O, 120 °C, 2 h, 81%; (f) 4 M HCl in 1,4-dioxane, 70 °C, 1 h, 82%, 83% e.e.; (g) recrystallisation in MeCN 71%, 99% e.e.

7-Bromo substituted (*R*)-benzoazepinone **54** was an important synthetic intermediate used in the

synthesis of multiple target molecules and to ensure material was available, the synthesis of **54**

was carried out on a decagram scale (Scheme 3). In contrast to the 86% d.e. obtained in the

synthesis of **49** (Scheme 2), Evans auxiliary mediated diastereoselective alkylation provided **52** as

a single diastereomer as judged by ^{1}H NMR analysis. Lithium peroxide mediated hydrolysis and

subsequent amide formation gave acetal **53** which was smoothly cyclized to key intermediate **54** under Lewis acid conditions. Negishi cross-coupling provided ethyl substituted **14** and Suzuki cross-coupling provided morpholine **20**. The forcing copper catalyzed sulfonylation conditions (120 °C, 48 h) used to access **25** resulted in complete racemization of the product, presumably due to the electron withdrawing nature of the 7-position sulfone. Subsequent chiral SFC purification of *rac*-**25** was then utilized to deliver **25** with >96% ee. Suzuki-Miyaura cross coupling with pinacol vinylboronate provided styrene **55** which underwent unoptimized dihydroxylation with oxone to give **24** as an epimeric mixture. Miyaura borylation of **54** was followed by oxidation with m-CPBA to provide 7-phenol **57**. Alkylation with dimethyloxirane under forcing conditions at 120 °C resulted in racemization of the C-1 chiral center to furnish *rac*-**17**. In contrast, room temperature alkylation with diethyl bromomalonate was followed by global ester reduction with sodium borohydride to deliver diol **18** with the chiral center intact. Palladium catalyzed enolate arylation with 7-bromo **54** at 110 °C gave malonate **56** without racemization, highlighting the relationship between the 7-position substituent and likelihood of epimerisation. Subsequent global ester reduction of **56** provided target diol **23**.

Scheme 3. Synthesis of **14**, *rac*-**17**, **18**, **20** and **23-25**[a]

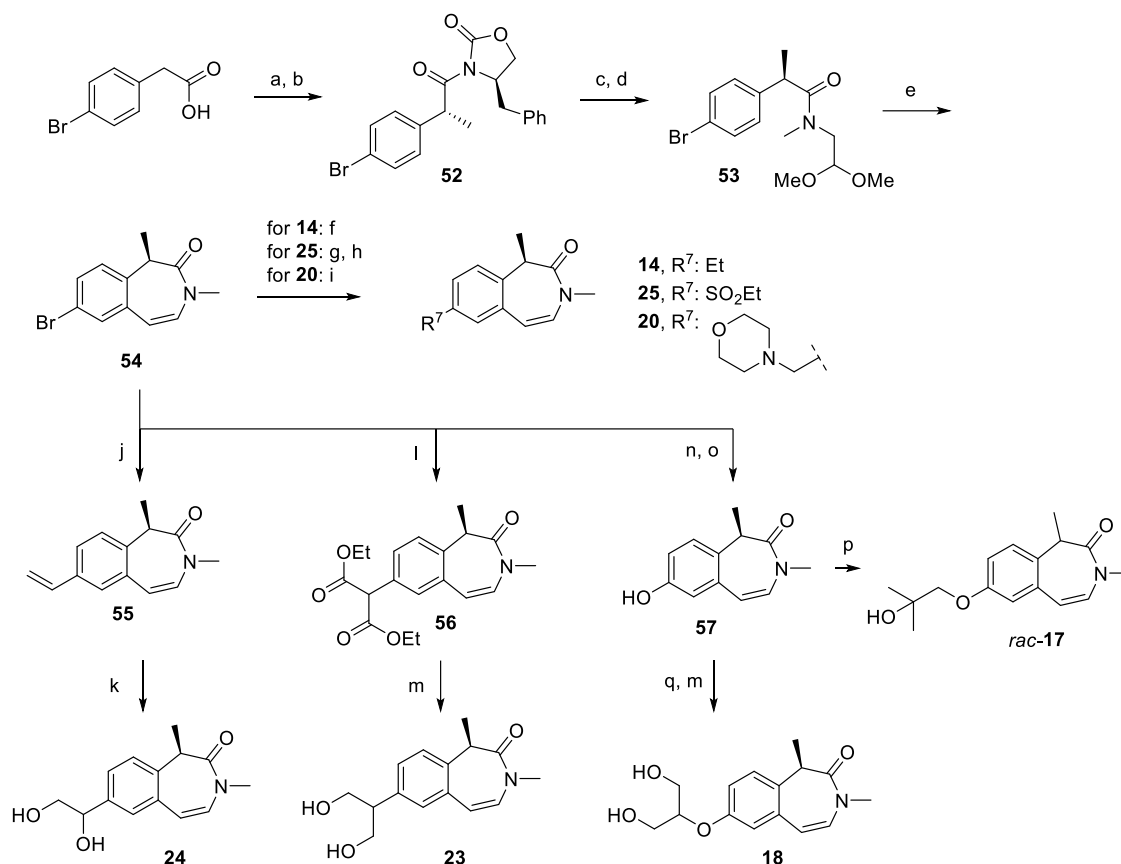ᵃReagents and conditions: (a) PivCl, (*R*)-4-benzyloxazolidin-2-one, NEt₃, toluene, 110 °C, 16 h, 53%; (b) NaHMDS, MeI, THF, –78 °C to rt, 16 h, 88%, single diastereomer; (c) LiOH, H₂O₂, THF, H₂O, 0 °C, 1 h, 96%; (d) T3P, 2,2-dimethoxy-*N*-methylethanamine, DIPEA, 2-MeTHF, 80 °C, 1 h, 86% (e) AlCl₃, CH₂Cl₂, 0 °C to rt, 16 h, 30%; (f) EtI, Zn, LiCl, Pd(amphos)Cl₂, THF, 100 ºC, 1 h, 34%; (g) EtSO₂Na, L-proline, CuI, Na₂CO₃, DMSO, 120 °C, 48 h, 46%; (h) chiral SFC purification; (i) potassium trifluoro(morpholinomethyl)borate, Pd(OAc)₂, XPhos, Cs₂CO₃, *i*-PrOH, H₂O, 100 °C, 1 h, 85%; (j) pinacol vinylboronate, Pd(PPh₃)₄, K₂CO₃, 1.4-dioxane, H₂O, 120 °C, 16 h, 78%; (k) oxone, H₂O, 70 °C, 3 h, 18%; (l) diethylmalonate, Pd(Pt-Bu₃)₂, K₃PO₄, toluene, 110 °C, 18 h, 67%; (m) NaBH₄, THF, MeOH, rt, 4 h; (n) bis(pinacolato)diboron, KOAc, PdCl₂(dppf), 1,4-dioxane, 85 °C, 16 h; (o) mCPBA, EtOH, H₂O, rt, 47 h, 82% over 2 steps; (p) 2,2-dimethyloxirane, K₂CO₃, DMF, 120 °C, 5 h, 16%; (q) diethyl bromomalonate, K₂CO₃, DMF, 4 h, 59%.

Compared to the stereocontrolled synthesis of **54** (Scheme 3Scheme 3. Synthesis of **14**, *rac*-**17**, **18**, **20** and **23**-**25**ᵃ), the synthesis of *rac*-**54** was more straightforward, achieved in only two steps from the commercially available 2-(4-bromophenyl)propanoic acid via amide formation and acetal cyclisation (Scheme 4). Due to this rapid and scalable route, *rac*-**54** was readily available to the medicinal chemistry team and was utilized to access several targets exploring WPF shelf

occupation from the 7-position via cross-coupling chemistry with the option to separate the enantiomers by HPLC or SFC chiral purification if required. Palladium catalyzed etherification with potassium hydroxide in ethanol provided 7-ethoxy *rac*-**15** in a 21% yield. Kumada coupling provided *rac*-**19** which was then separated by chiral SFC to deliver the two enantiomers, the more active of which was assigned with (*R*)-stereochemistry based on X-ray crystallography with (*R*)-**10** and (*R*)-**11** (Figure 5). Suzuki-Miyaura cross coupling of *rac*-**54** with the requisite Molander trifluoroborate salt followed by chiral SFC purification provided straightforward access to benzylamine **21**. Palladium catalyzed vinylation of *rac*-**54** provided *rac*-**55** which underwent a smooth hydroboration-oxidation sequence to provide primary alcohol *rac*-**22**. Purification via chiral HPLC furnished both enantiomers, the more active of which was assigned as **22**. Completing the synthesis of the 7-position exploration chemistry, Miyaura borylation of *rac*-**54** provided the intermediate boronic ester which underwent oxidation with hydrogen peroxide and sodium hydroxide to access phenol *rac*-**57**. Subsequent etherification and chiral purification provided **16** with >99% ee.

Scheme 4. Synthesis of *rac*-**15**, **16**, **19**, **21** and **22**[a]
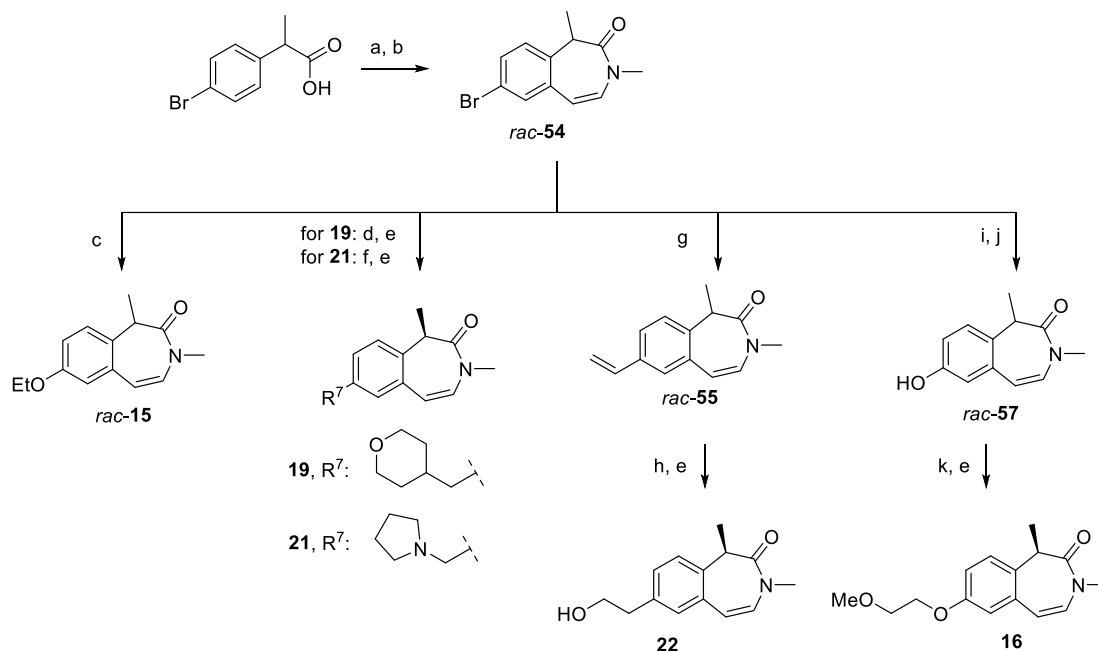
^{a}Reagents and conditions: (a) T3P, 2,2-dimethoxy-N-methylethanamine, DIPEA, THF, 80 °C, 4 h, 72%; (b) AlCl$_3$, CH$_2$Cl$_2$, 0 °C to rt, 24 h, 30%; (c) KOH, Pd$_2$dba$_3$, BippyPhos, EtOH, 85 °C, 3 h, 21%; (d) ((tetrahydro-2H-pyran-4-yl)methyl) bromide, Mg, I$_2$, 1,2-dibromoethane, THF, 85 °C, 2.4 h to rt, then added to rac-**60**, PdCl$_2$(dppf)·CH$_2$Cl$_2$, THF, 85 ºC, 12 h; (e) chiral purification; (f) potassium 1- trifluoroboratomethylpyrrolidine, Pd(OAc)$_2$, XPhos, Cs$_2$CO$_3$, THF, H$_2$O, 130 °C, 20 min; (g) pinacol vinylboronate, Pd(PPh$_3$)$_4$, K$_2$CO$_3$, 1.4-dioxane, H$_2$O, 120 °C, 30 min, 70%; (h) BH$_3$·THF, THF, rt, 90 min, then H$_2$O$_2$, NaOH, rt, 16, then BH$_3$·THF, rt, 4 h; (i) bis(pinacolato)diboron, KOAc, PdCl$_2$(dppf).CH$_2$Cl$_2$, 1,4-dioxane, 100 °C, 2 h, 52%; (j) H$_2$O$_2$, NaOH, 0 °C to rt, 2 h, 76%; (k) NaH, 1-chloro-2-methoxyethane, DMF, 0 °C to rt, 16 h.

To explore the SAR in the ZA channel, substitution of the 5-position of the benzoazepinone ring was required. To achieve this goal, the latent reactivity of the embedded enamide was utilized via bromination with phenyltrimethylammonium tribromide (PTAB) which delivered bromo intermediate **58** in 87% yield and with excellent chemoselectivity (Scheme 5). **58** served as a key intermediate for the synthesis of targets **26-30** via Palladium-catalyzed cross-coupling chemistry. Suzuki-Miyaura methylation was followed by chiral purification to provide **26**. Negishi cyanation followed by hydrolysis with H$_2$SO$_4$ provided rac-**27** which was separated by chiral purification to give **27**. Suzuki-Miyaura cross-coupling with the appropriate boronic acids provided rac-**28-30** and chiral SFC purification was used to isolate **30** with > 98% ee.

Scheme 5. Synthesis of **26–30**[a]

26, R^5: Me
27, R^5: CONH$_2$

rac-**28**, R^5: Ph
rac-**29**, R^5: 4-pyridiyl

30, R^5:
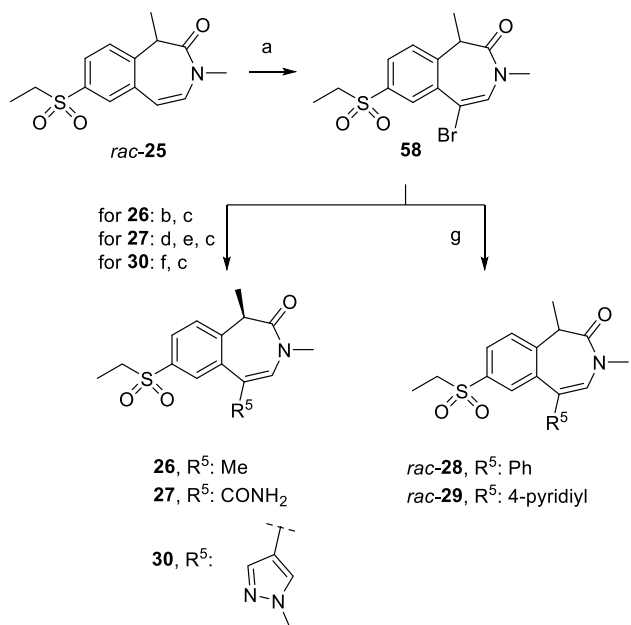
[a]Reagents and conditions: (a) PTAB, MeCN, rt, 1 h, 87%; (b) B$_3$(OMe)$_3$, K$_2$HPO$_4$, X-Phos Pd cycle, 1,4-dioxane, H$_2$O, 90 °C, 16 h, 92%; (c) chiral purification; (d) Zn(CN)$_2$, Pd(PPh$_3$)$_4$, DMF, 150 °C, 30 min, 52%; (e) H$_2$SO$_4$, rt, 12 h; (f) 1-methyl-4-(4,4,5,5-tetramethyl-1,3,2-dioxaborolan-2-yl)-1H-pyrazole, K$_2$HPO$_4$, X-Phos Pd cycle, 1,4-dioxane, H$_2$O, 90 °C, 16 h, 92%. (g) Aryl boronic acid, PdCl$_2$(dppf), K$_2$CO$_3$, i-PrOH, H$_2$O, 80 °C, 1 h.

In a similar fashion to that shown in Scheme 5 and utilizing the same innate reactivity of the enamide, C-5 bromination of rac-**15** with NBS provided key intermediate **59** in 89% yield (Scheme 6). Suzuki-Miyaura cross coupling with **59** was used to access **31**, **32** and rac-**33**, with Buchwald-Hartwig coupling utilized to form the critical C-N bond in **37**. To gain access to a wider variety of halide-heteroaryl building blocks for Suzuki-Miyaura chemistry, an umpolung approach was taken with the initial formation of a boronic ester in the 5-position. This proved a useful intermediate with straightforward cross-coupling chemistry with the appropriate heteroaryl bromides delivering racemic product which then underwent chiral purification to provide **34-36**.

Scheme 6. Synthesis of **31-37**[a]
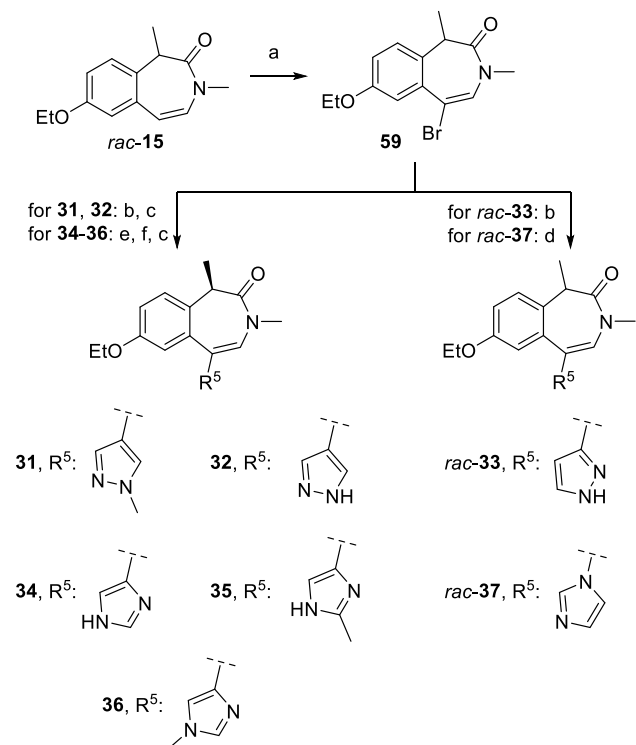
^aReagents and conditions: (a) NBS, MeCN, rt, 5 h, 89%; (b) pyrazole boronic ester or acid, Pd(PPh$_3$)$_4$, K$_2$CO$_3$, i-PrOH, H$_2$O, 100 °C; (c) chiral purification; (d) imidazole, Pd$_2$dba$_3$, DavePhos, NaOt-Bu, 1,4-dioxane, 100 to 140 °C, 1%; (e) bis(pinacolato)diboron, Pd(OAc)$_2$, t-BuPPh$_2$, KOAc, 1,4-dioxane, 70 °C, 60%; (f) bromo-imdazole, Pd source, base, solvent.

To access diols **38** and **40** with the required (*S*)-secondary alcohol, **55** served as a critical intermediate for ligand controlled Sharpless asymmetric dihydroxylation with AD-mix-α to provide **60** in 61% yield as a single diastereomer (Scheme 7). The absolute (*S*)-alcohol stereochemistry of **60** was assigned via the Sharpless mnemonic and this determination was reinforced by the crystallographic confirmation of **41** as (*R*)-alcohol stereochemistry which was synthesized using AD-mix-β (Figure 9).[48] Bromination of **60** with PTAB was followed by Suzuki-Miyaura cross coupling with the appropriately substituted pyrazole boronic acid to provide **38** and **40**. The synthesis of **39** and **41** proceeded in the same manner, expect for the use of AD-mix-β to access epimeric diol **61** with (*R*)-alcohol stereochemistry.

Scheme 7. Synthesis of **38-41**^a

To access ether **42**, phenol **57** served as a useful nucleophile and was smoothly alkylated to provide a TBS protected intermediate in 60% yield (Scheme 8). Subsequent C-5 bromination with PTAB resulted in concomitant TBS deprotection, presumably due to the acidic nature of the reaction, to give primary alcohol **62**. Miyaura borylation was followed by Suzuki-cross coupling with SEM protected imidazole **63** to provide **42** in an unoptimized 11% yield.

Scheme 8. Synthesis of **42**[a]

The final target, diol **43**, was accessed from intermediate **56** via C-5 bromination and Suzuki-Miyaura cross coupling to give bis-ester **64** in 37% yield over two steps (Scheme 9). Global ester reduction with sodium borohydride provided 1,3-diol **43**.

Scheme 9. Synthesis of **43**[a]
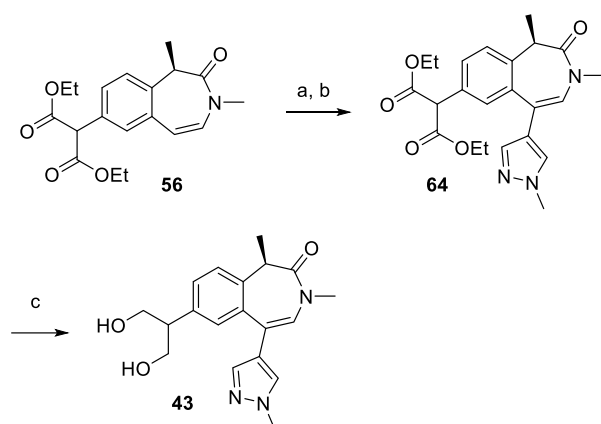
[a]Reagents and conditions: (a) NBS, CCl$_4$, 60 °C, 2 h; (b) pyrazole boronic ester, XPhos G2, K$_3$PO$_4$, 1,4-dioxane, H$_2$O, 100 °C, 18 h, 37% over two steps; (c) NaBH$_4$, THF, H$_2$O, rt, 4 h, 15%.

CONCLUSION

In conclusion, we report the trajectory analysis from KAc mimetic to pan-BET bromodomain inhibitor for several of GSK's reported pan-BET candidate molecules through an efficiency lens. This highlighted the importance of identifying a ligand efficient KAc mimetic as lipophilic efficiency can be readily gained throughout optimisation via occupation of the WPF shelf and ZA channel. From initial hit **9**, the highly ligand efficient benzoazepinone **12** was identified through occupation of a shallow hydrophobic pocket in the protein with a methyl group. Subsequent structure guided design enabled exploration of the WPF shelf and ZA channel in parallel to identify groups that delivered gains in LipE. Exploiting the SAR knowledge through the combination of

LipE preferred groups led to the identification of **41** (I-BET432, GSK3740432), an oral candidate quality pan-BET bromodomain inhibitor with a 5-18 mg QD early predicted human dose.

EXPERIMENTAL SECTION

Physicochemical Properties. Artificial membrane permeability, chromatographicLog$D$ at pH 7.4, FaSSIF solubility and CLND solubility were measured using published protocols.[49]

Chemistry methods. All solvents were purchased from Sigma Aldrich (anhydrous solvents) and commercially available reagents were used as received. All reactions were followed by TLC analysis (TLC plates GF254, Merck) or LCMS (liquid chromatography mass spectrometry) using a Waters ZQ instrument. NMR spectra were recorded at ambient temperature unless otherwise stated using standard pulse methods on any of the following spectrometers and signal frequencies: Bruker AV-400 (^{1}H = 400 MHz, ^{13}C = 100.6 MHz), Bruker AV-500 (^{1}H = 500 MHz, ^{13}C = 125.8 MHz), Bruker AVII+ 600 (^{1}H = 600 MHz, ^{13}C = 150.9 MHz). Chemical shifts are reported in ppm and are referenced to tetramethylsilane (TMS) or the following solvent peaks: CDCl$_3$ (^{1}H = 7.27 ppm, ^{13}C = 77.00 ppm), DMSO-d_6 (^{1}H = 2.50 ppm, ^{13}C = 39.51 ppm) and CD$_3$OD (^{1}H = 3.31 ppm, ^{13}C = 49.15 ppm). Coupling constants are quoted to the nearest 0.1 Hz and multiplicities are given by the following abbreviations and combinations thereof: s (singlet), d (doublet), t (triplet), q (quartet), m (multiplet), br (broad). Column chromatography was performed on pre-packed silica gel columns using biotage SP4, Isolera One or Teledyne ISCO apparatus. High resolution mass spectra (HRMS) were recorded on a Micromass Q-Tof Ultima hybrid quadrupole time-of-flight mass spectrometer, with analytes separated on an Agilent 1100 Liquid Chromatograph equipped with a Phenomenex Luna C18(2) reversed phase column (100 mm × 2.1 mm, 3 µm packing diameter). LC conditions were 0.5 mL/min flow rate, 35 °C, injection volume 2-5 µL. Gradient

elution with (A) H_2O containing 0.1% (v/v) formic acid and (B) acetonitrile containing 0.1% (v/v) formic acid. Gradient conditions were initially 5% B, increasing linearly to 100% B over 6 min, remaining at 100% B for 2.5 min then decreasing linearly to 5% B over 1 min followed by an equilibration period of 2.5 min prior to the next injection. LCMS analysis was carried out on a Waters Acquity UPLC instrument equipped with a BEH column (50 mm × 2.1 mm, 1.7 μm packing diameter) and Waters micromass ZQ MS using alternate-scan positive and negative electrospray. Analytes were detected as a summed UV wavelength of 210 – 350 nm. Liquid phase methods were used:

Formic – 40 °C, 1 mL/min flow rate. Gradient elution with the mobile phases as (A) H_2O containing 0.1% volume/volume (v/v) formic acid and (B) acetonitrile containing 0.1% (v/v) formic acid. Gradient conditions were initially 1% B, increasing linearly to 97% B over 1.5 min, remaining at 97% B for 0.4 min then increasing to 100% B over 0.1 min

Formic B – 35 °C, 0.6 mL/min flow rate. Gradient elution with the mobile phases as (A) H_2O containing 0.1% volume/volume (v/v) formic acid and (B) acetonitrile containing 0.1% (v/v) formic acid. Gradient conditions were initially 97% B, dropping to 2% between 0.4 and 3.2 min, then increaseing back to 97% B between 3.8 and 4.2 min, maintaining at 97% B until 4.5 min.

Formic C – 35 °C, 0.6 mL/min flow rate. Gradient elution with the mobile phases as (A) H_2O containing 0.1% volume/volume (v/v) formic acid and (B) acetonitrile containing 0.1% (v/v) formic acid. Gradient conditions were initially 97% B, deceasing lineraly from 1.8 min to 3.8 min to 70%, then decreasing to 50% between 3.8 min and 4.5 min. Then between 4.5 min and 5 min, %B decreased to 5% where it remained until 6 min and then increased linerally to 97% until 7 min.

Formic D – 35 °C, 0.45 mL/min flow rate. Gradient elution with the mobile phases as (A) H_2O containing 0.05% volume/volume (v/v) formic acid and (B) acetonitrile containing 0.05% (v/v)

formic acid. Gradient conditions were initially 97% B, deceasing lineraly from 0.4 min to 4 min to 2%, then increasing from 4.5 min to 5 min to 97% where is remained until 5.5 min.

High pH – 40 °C, 1 mL/min flow rate. Gradient elution with the mobile phases as (A) 10 mM aqueous ammonium bicarbonate solution, adjusted to pH 10 with 0.88 M aqueous ammonia and (B) acetonitrile. Gradient conditions were initially 1% B, increasing linearly to 97% B over 1.5 min, remaining at 97% B for 0.4 min then increasing to 100% B over 0.1 min.

Mass-directed automatic purification (MDAP) was carried out using a Waters ZQ MS using alternate-scan positive and negative electrospray and a summed UV wavelength of 210–350 nm. Two liquid phase methods were used:

Formic – Sunfire C18 column (100 mm × 19 mm, 5 µm packing diameter, 20 mL/min flow rate) or Sunfire C18 column (150 mm × 30 mm, 5 µm packing diameter, 40 mL/min flow rate). Gradient elution at ambient temperature with the mobile phases as (A) H_2O containing 0.1% volume/volume (v/v) formic acid and (B) acetonitrile containing 0.1% (v/v) formic acid.

TFA – Xselect CSH column (150 mm × 30 mm, 5 µm packing diameter, 30 mL/min flow rate). Gradient elution at ambient temperature with the mobile phases as (A) H_2O containing 0.1% volume/volume (v/v) TFA and (B) acetonitrile containing 0.1% (v/v) TFA.

High pH – Xbridge C18 column (100 mm × 19 mm, 5 µm packing diameter, 20 mL/min flow rate) or Xbridge C18 column (150 mm × 30 mm, 5 µm packing diameter, 40 mL/min flow rate). Gradient elution at ambient temperature with the mobile phases as (A) 10 mM aqueous ammonium bicarbonate solution, adjusted to pH 10 with 0.88 M aqueous ammonia and (B) acetonitrile.

The purity of all compounds tested was determined by LCMS and ^{1}H NMR to be >95% apart from **24** (85% purity), *rac*-**29** (92% purity) and *rac*-**37** (94% purity).

N-(2,2-Dimethoxyethyl)-2-(3,4-dimethoxyphenyl)-N-methylpropanamide (45). To a stirred solution of 2-(3,4-dimethoxyphenyl)propanoic acid (**44**) (2.80 g, 13.32 mmol) in CH_2Cl_2 (10 mL), cooled to 0 °C, $SOCl_2$ (9.72 mL, 133 mmol) was added by dropwise addition at 0 °C for 10 min under N_2. The reaction was allowed to stir rt for 2 h and then then evaporated to give a yellow oil (2.90 g) which was used immediately. The oil was dissolved in CH_2Cl_2 (30 mL) and cooled to 0 °C under N_2. NEt_3 (1.77 mL, 12.68 mmol) was added over 10 min followed by 2,2- dimethoxy-N-methylethanamine (1.82 g, 15.22 mmol). The resultant mixture was stirred at rt for 1 h and then quenched with H_2O. The separated aqueous phase was washed with CH_2Cl_2 (3 × 40 mL). The organic phase was dried (Na_2SO_4) and concentrated under vacuo to give a residue. The residue was purified by flash column chromatography using 100-200 mesh silica gel eluting with 50% EtOAc / hexane. The appropriate fractions were combined and evaporated to give **45** (1.50 g, 38%). ^{1}H NMR (400 MHz, DMSO-d_6) δ 6.92–6.80 (m, 2H), 6.80–6.67 (m, 1H), 4.41 (t, J = 5.4 Hz, 1H), 4.08–3.93 (m, 1H), 3.76–3.68 (m, 6H), 3.60–3.36 (m, 1H), 3.33–3.15 (m, 7H), 2.93 - 2.80 (m, 3H), 1.36–1.16 (m, 3H); LCMS (formic B) $(M+H)^+$ = 312.1, R_t = 1.79 min (99%).

7,8-Dimethoxy-1,3-dimethyl-1,3-dihydro-2H-benzo[d]azepin-2-one (*rac*-10). Acetic acid (2.21 ml, 38.5 mmol) was added to a solution of **45** (1.50 g, 4.82 mmol) in conc. HCl (5.85 ml, 67.4 mmol) at 0 °C and the reaction mixture was slowly warmed to rt and stirred for 24 h. The reaction mixture was poured into H_2O and then the aqueous phase was extracted with Et_2O (3 × 50 mL). The organic solution was dried (Na_2SO_4) and concentrated under vacuo to give a residue. The residue was purified by flash column chromatography by using 100-200 mesh silica gel and eluting with 20% EtOAc / hexane. The appropriate fractions were combined and evaporated to give *rac*-**10** (540 mg, 45%). ^{1}H NMR (400 MHz, DMSO-d_6) δ 6.91 (s, 1H), 6.76 (s, 1H), 6.54–

6.30 (m, 2H), 3.77–3.73 (m, 3H), 3.29 (s, 3H), 3.17–3.01 (m, 4H), 1.49 (br s, 3H); LCMS (formic C) $(M+H)^+ = 248.1$, $R_t = 4.35$ min (99%).

(S)-7,8-Dimethoxy-1,3-dimethyl-1,3-dihydro-2H-benzo[d]azepin-2-one ((S)-10) and (R)-7,8-Dimethoxy-1,3-dimethyl-1,3-dihydro-2H-benzo[d]azepin-2-one ((R)-10). *Rac*-**10** was dissolved in MeOH and purified by chiral SFC to give (S)-**10** and (R)-**10**. Chiral SFC: Lux Amylose-2 (250 ×30 mm), 50% CO_2 / MeOH, total Flow: 90.0 g/min, back pressure: 100 bar, UV: 226 nm, stack time: 5.5 min, load / injection: 64 mg. (S)-**10** analytical data as *rac*-**10** above, chiral HPLC: Chiralpak AD-H (4.6 × 250 mm), solvent: 0.5% DIPEA in MeOH, temp: 30 °C, flow: 5 mL / min, $R_t = 1.39$ min (>99% ee). (R)-**10** analytical data as *rac*-**10** above, chiral HPLC: Chiralpak AD-H (4.6 × 250 mm), solvent: 0.5% DIPEA in MeOH, temp: 30 °C, flow: 5 mL / min, $R_t = 2.81$ min (>99% ee).

(S)-7,8-Dimethoxy-1,3-dimethyl-1,3,4,5-tetrahydro-2H-benzo[d]azepin-2-one ((S)-11) and (R)-7,8-Dimethoxy-1,3-dimethyl-1,3,4,5-tetrahydro-2H-benzo[d]azepin-2-one ((R)-11). A stirred solution of *rac*-**10** (450 mg, 1.82 mmol) in dry EtOH (20 mL) under N_2 was degassed for 15 min. 10% Pd/C (150 mg, 1.82 mmol) was added and stirred at rt for 24 h under H_2 balloon pressure. The reaction mixture was filtered through a celite pad, the pad was washed with EtOH (3 × 20 mL) and filtrate concentrated under vacuo to give a residue. The residue was purified by flash column chromatography using 100-200 mesh silica gel eluting with 50% EtOAc / hexane. The appropriate fractions were combined and evaporated under reduced pressure to give *rac*-**11** (350 mg, 77%). The material was dissolved in MeOH and purified by chiral SFC to give (S)-**11** and (R)-**11**. Chiral SFC Chiralpak AD-H (250 ×30 mm), 70% CO_2 / MeOH, total Flow: 100.0 g/min, back pressure: 100 bar, UV: 214 nm, stack time: 4.5 min, load / injection: 32 mg. (S)-**11**: ¹H NMR (400 MHz, DMSO-d_6) δ 6.72 (s, 1H), 6.69 (s, 1H), 4.34 (q, $J = 6.9$ Hz, 1H), 4.13 (ddd, J

= 4.8, 10.1, 14.9 Hz, 1H), 3.73 (s, 3H), 3.71 (s, 3H), 3.52–3.31 (m, 1H), 3.15–2.91 (m, 2H), 2.85 (s, 3H), 1.36 (d, J = 7.0 Hz, 3H); LCMS (formic B) (M+H)$^+$ = 250.1, R_t = 1.61 min (99%); Chiral HPLC: Chiralpak AD-H (4.6 × 250 mm), solvent: 0.5% DIPEA in MeOH, temp: 29.8 °C, flow: 3 mL / min, R_t = 4.81 min (>98% ee). (*R*)-**11** analytical data as for *S*-**11**; Chiral HPLC: Chiralpak AD-H (4.6 × 250 mm), solvent: 0.5% DIPEA in MeOH, temp: 29.8 °C, flow: 3 mL / min, R_t = 7.13 min (>98% ee).

N-(2,2-Dimethoxyethyl)-N-methyl-2-phenylpropanamide (47). To a solution of 2-phenylpropanoic acid (**46**) (25.00 g, 166 mmol) in THF (250 mL) was added 2,2-dimethoxy-*N*-methylethanamine (23.80 g, 200 mmol) and DIPEA (116 mL, 666 mmol) followed by T3P in EtOAc (132 g, 416 mmol) under N$_2$. The reaction mixture was maintained at 70 °C for 16 h and then evaporated to dryness. The residue was diluted with H$_2$O (500 mL) and washed with EtOAc (2 × 250 mL). The separated organic layer was washed with brine (500 ml), dried (Na$_2$SO$_4$) and concentrated under vaccum to give **47** as a colorless oil (30 g, 66%). ^{1}H NMR (400 MHz, CDCl$_3$) δ 7.36–7.20 (m, 5H), 4.49 (t, J = 5.5 Hz, 1H), 4.15–4.01 (m, 1H), 3.88 (q, J = 6.9 Hz, 1H), 3.61–3.45 (m, 1H), 3.42–3.28 (m, 6H), 2.98–2.93 (m, 3H), 1.44 (d, J = 6.8 Hz, 3H); LCMS (formic B) (M+H)$^+$ = 252.2, R_t = 1.99 min (92%).

(*R*)-1,3-Dimethyl-1,3-dihydro-2H-benzo[d]azepin-2-one (12). To a suspension of AlCl$_3$ (53.1 g, 398 mmol), in CH$_2$Cl$_2$ (100 mL), at 0 °C, a solution of **47** (10 g, 39.8 mmol) in CH$_2$Cl$_2$ (50 ml) was added over 10 min. The reaction mixture was maintained at 0 °C and then the reaction was allowed to warm to rt for 3 h. The reaction mixture was quenched with ice (500 ml) at 0 °C and then the aqueous layer was extracted with CH$_2$Cl$_2$ (2 × 300 mL). The separated organic phase was washed with brine (300 ml), dried over (Na$_2$SO$_4$) and concentrated under reduced pressure to give a residue. The residue was purified by column chromatography using 60-120 silicagel using 10%

EtOAc in petroleum ether. Appropriate fractions were combined and evaporated under reduced pressure to give *rac*-**12** (2.00 g, 24%). *Rac*-**12** was dissolved in MeOH and purified by chiral SFC to give **12**. Chiral SFC: Chiralpak AD-H (250 ×30 mm), 50% CO_2 / 0.5% DIPA in MeOH, total flow: 90.0 g/min, back pressure: 100 bar, UV: 224 nm, stack time: 2.5 min, load / injection: 11 mg. ^{1}H NMR (400 MHz, DMSO-d_6) δ 7.42–7.22 (m, 4H), 6.62–6.41 (m, 2H), 3.27–3.11 (m, 1H), 3.03 (s, 3H), 1.50 (br d, J = 6.4 Hz, 3H); LCMS (formic B) $(M+H)^+$ = 187.9, R_t = 1.97 min (99%); chiral SFC: Chiralpak AD-H (4.6 × 250 mm), solvent: 0.5% DIPEA in MeOH, temp: 29.9 °C, flow: 3 mL / min, R_t = 3.83 min, undesired enantiomer R_t = 2.39 min (>99% ee).

(*R*)-4-Benzyl-3-(2-(2-bromo-4-methoxyphenyl)acetyl)oxazolidin-2-one. 2-(2-Bromo-4-methoxyphenyl)acetic acid **(48)** (25.30 g, 103 mmol), *(R)*-4-benzyloxazolidin-2-one (12.40 g, 69.7 mmol) and triethylamine (40 mL, 287 mmol) were stirred in toluene (175 mL) under N_2 at 80 °C for 5 min. Then, a solution of pivaloyl chloride (12.50 mL, 101 mmol) in toluene (25 mL) was added over 5 min to the reaction mixture at 80 °C. At the end of addition, the reaction mixture was heated at 110 °C for 24 h. The reaction mixture was then concentrated under reduced pressure to give a brown oil. The oil was partitioned between EtOAc and a saturated solution of sodium bicarbonate. The layers were separated. The aqueous layer was re-extracted with EtOAc. The organic layers were combined, dried through a phase separator, and concentrated under reduced pressure to give a yellow oil. The oil was purified by silica column chromatography, eluting with a gradient of 0-60% EtOAc in cyclohexane. The relevant fractions were concentrated under reduced pressure to give the title compound as a yellow oil (23.50 g, 75%). ^{1}H NMR (400 MHz, CDCl$_3$) δ 7.36–7.24 (m, 3H), 7.23–7.19 (m, 2H), 7.17 (d, J = 2.8 Hz, 1H), 7.16 (d, J = 2.8 Hz, 1H), 6.86 (dd, J = 8.6, 2.8 Hz, 1H), 4.75–4.64 (m, 1H), 4.42 (d, J = 18.2 Hz, 1H), 4.30 (d, J = 18.2 Hz, 1H), 4.25 (d, J = 7.8 Hz, 1H), 4.21 (dd, J = 9.3, 3.2 Hz, 1H), 3.80 (s, 3H), 3.35 (dd, J = 13.3, 3.2

Hz, 1H), 2.80 (dd, J = 13.3, 9.3 Hz, 1H); LCMS (high pH) (M)$^-$ = 402.3, 404.3, R$_t$ = 1.27 min (79%).

(*R*)-4-Benzyl-3-((*R*)-2-(2-bromo-4-methoxyphenyl)propanoyl)oxazolidin-2-one (49). (*R*)-4-Benzyl-3-(2-(2-bromo-4-methoxyphenyl)acetyl)oxazolidin-2-one (6.80 g, 14.4 mmol) was dissolved in THF (45 mL) under N$_2$ and cooled to –78 °C. A 1 M solution of NaHMDS in THF (17.2 mL, 17.2 mmol) was added dropwise to the reaction mixture. The reaction mixture was stirred for 1.5 h at –78 °C. MeI (2.69 mL, 43.1 mmol) was added and the reaction mixture was stirred 1 h at –78 °C to rt. The reaction mixture was quenched with a saturated solution of ammonium chloride. The organic solvent was concentrated under reduced pressure. The residual solution was extracted twice with EtOAc. The organic layers were combined, dried through a phase separator and concentrated under reduced pressure to give a yellow oil. The crude oil was dissolved in THF (45 mL) and cooled under N$_2$ to –78 °C. Then a 1 M solution of NaHMDS in THF (17.2 mL, 17.2 mmol) was added dropwise and left to stir at –78 °C for 15 min. The mixture was allowed to warm up to rt for 15 min and then recooled to –78 °C. MeI (2.69 mL, 43.1 mmol) was added. The reaction mixture was allowed to slowly warm up to rt and was stirred for 6 h at rt. MeI (2.69 mL, 43.1 mmol) was added and the reaction was stirred overnight at rt. The reaction mixture was quenched with a saturated solution of ammonium chloride. The organic solvent was concentrated under reduced pressure. The residue was partitioned between EtOAc and H$_2$O. The aqueous layer was extracted with EtOAc. The organic layers were combined, dried through a phase separator, and concentrated under reduced pressure to give a yellow oil. The oil was purified by silica column chromatography, eluting with a gradient of 0-80% EtOAc in cyclohexane. The fractions were concentrated under reduced pressure to give **49** as a yellow oil (5.38 g, 81%, 86% d.e. by ^{1}H NMR). ^{1}H NMR (400 MHz, CDCl$_3$) δ 7.36–7.20 (m, 6H), 7.12 (d, J = 2.7 Hz, 1H),

6.86 (dd, J = 8.6, 2.7 Hz, 1H), 5.27 (q, J = 7.1 Hz, 1H), 4.71–4.63 (m, 1H), 4.16 (d, J = 5.1 Hz, 2H), 3.78 (s, 3H), 3.32 (dd, J = 13.3, 3.3 Hz, 1H), 2.80 (dd, J = 13.3, 9.7 Hz, 1H), 1.55 (d, J = 6.8 Hz, 3H). NMR showed 7% of the other diastereomer (R)-4-benzyl-3-((S)-2-(2-bromo-4-methoxyphenyl)propanoyl)oxazolidin-2-one. This ratio was determined at the benzylic CH$_3$ doublet at 1.55 ppm (major diastereomer) and 1.51 ppm (minor diastereomer); LCMS (high pH) $(M+H)^+$ = 418.5, 420.5, R_t = 1.33 min (98%).

(R)-2-(2-Bromo-4-methoxyphenyl)propanoic acid. H_2O_2 (2 mL, 35% aq., 23.2 mmol) was added to a solution of LiOH (1.11 g, 46.3 mmol) in H_2O (8 mL) at 0 °C and the solution was stirred for 5 min. This solution was added to a solution of **51** (5.38 g, 11.6 mmol) in THF (20 mL) at 0 °C. The reaction mixture was stirred for 7 h at rt. H_2O_2 (2 mL, 35% aq., 23.2 mmol) was added and the reaction mixture was further stirred at rt for 18 h. The reaction mixture was quenched with 10% sodium thiosulfate solution and was concentrated under reduced pressure. The residual solution was diluted with EtOAc. The layers were separated. The aqueous layer was acidified to pH 1 with a 2 M aqueous solution of HCl and then extracted with EtOAc. The organics were combined, dried through a phase separator, and concentrated under reduced pressure to give the title compound as a yellow solid (5.53 g, 92%). LCMS (high pH) $(M)^-$ = 257.2, 259.2, R_t = 0.54 min (84%).

(R)-2-(2-Bromo-4-methoxyphenyl)-N-methylpropanamide (50). (R)-2-(2-Bromo-4-methoxyphenyl)propanoic acid (5.53 g, 50% pure by weight, 10.7 mmol) was taken in DMF (30 mL) and HATU (4.50 g, 11.7 mmol) and DIPEA (5.60 mL, 32.0 mmol) were added. The reaction mixture was stirred under N_2 at rt for 5 min. A 2 M solution of methanamine in THF (13.30 mL, 26.7 mmol) was added and the reaction mixture was stirred at rt for 45 min. The reaction mixture was diluted with EtOAc and brine. The layers were separated. The aqueous layer was extracted

with EtOAc. The organics were combined, washed with brine, dried through a phase separator, and concentrated under reduced pressure to give a yellow oil. The oil was purified by silica column chromatography, eluted with a gradient of 0-60% EtOAc in cyclohexane. The appropriate fractions were concentrated under reduced pressure to give **50** as a yellow oil (3.22 g, 81%). ^{1}H NMR (400 MHz, CDCl$_3$) δ 7.33 (d, J = 8.8 Hz, 1H), 7.11 (d, J = 2.7 Hz, 1H), 6.87 (dd, J = 8.8, 2.7 Hz, 1H), 5.39 (br. s, 1H), 3.96 (q, J = 7.1 Hz, 1H), 3.79 (s, 3H), 2.76 (d, J = 4.9 Hz, 3H), 1.47 (d, J = 7.1 Hz, 3H); LCMS (high pH) (M+H)$^+$ = 272.2, 274.3 R$_t$ = 0.88 min (88%).

(*R*,*E*)-2-(2-(2-Ethoxyvinyl)-4-methoxyphenyl)-*N*-methylpropanamide (51). (*E*)-2-(2-ethoxyvinyl)-4,4,5,5-tetramethyl-1,3,2-dioxaborolane (100 mg, 0.51 mmol), **50** (94 mg, 0.31 mmol), K$_2$CO$_3$ (80 mg, 0.58 mmol) and Pd(PPh$_3$)$_4$ (18 mg, 0.016 mmol) were stirred in 1,4-dioxane (5 mL) and H$_2$O (1 mL) under N$_2$ at 120 °C for 2 h. The reaction mixture was cooled to rt and concentrated under reduced pressure to give a brown residue. The residue was partitioned between EtOAc and H$_2$O. The layers were separated. The aqueous layer was re-extracted with EtOAc. The organics were combined, dried through a phase separator, and concentrated under reduced pressure to give a yellow oil. The oil was purified by silica column chromatography, eluting with a gradient of 0-100% EtOAc in cyclohexane. The appropriate fractions were concentrated under reduced pressure to give **51** as a yellow oil (78 mg, 81%). ^{1}H NMR (400 MHz, CDCl$_3$) δ 7.20 (d, J = 8.6 Hz, 1H), 6.83 (d, J = 2.7 Hz, 1H), 6.80 (d, J = 12.7 Hz, 1H), 6.75 (dd, J = 8.6, 2.7 Hz, 1H), 5.92 (d, J = 12.7 Hz, 1H), 5.30 (br. s, 1H), 3.89 (q, J = 7.1 Hz, 2H), 3.80 (s, 3H), 3.73 (q, J = 7.1 Hz, 1H), 2.70 (d, J = 4.5 Hz, 3H), 1.49 (d, J = 7.1 Hz, 3H), 1.34 (t, J = 7.1 Hz, 3H); LCMS (high pH) (M+H)$^+$ = 264.5, R$_t$ = 0.94 min (100%).

(*R*)-7-Methoxy-1,3-dimethyl-1,3-dihydro-*2H*-benzo[*d*]azepin-2-one (13). A solution of **51**(78 mg, 0.25 mmol) in a 4 M solution of HCl in 1,4-dioxane (5 mL, 20.0 mmol) was stirred

under N_2 at 70 °C for 1 h. The reaction mixture was diluted with EtOAc and H_2O. The layers were separated. The aqueous layer was extracted with EtOAc. The organics were combined, dried through a phase separator, and concentrated under reduced pressure to give an orange oil. The oil was purified by silica column chromatography, eluting with a gradient of 0-100% EtOAc in cyclohexane. The appropriate fractions were concentrated under reduced pressure to give **13** as a yellow solid (47 mg, 82%, 83% ee). LCMS (high pH) $(M+H)^+ = 218.4$, $R_t = 0.95$ min (100%); chiral HPLC: Chiralpak AD column, 25 cm, rt, 25% EtOH in heptane, injection volume 0.3 µL) $R_t = 9.39$ min, 91.3%, other enantiomer $R_t = 6.84$ min, 8.6%. In a separate experiment, **13** (3.6 g, 15.74 mmol, 83% ee) was suspended in warm MeCN (5 mL). The mixture was heated at reflux for a few min. The entire material dissolved. The mixture was then left to slowly cool to rt (for 3 h) allowing the slow formation of white crystals. The supernatant was removed with a pipette. The solid was rinsed with Et_2O twice. The supernatant was removed with a pipette, affording **13** as white crystals (2.56 g, 71%, >99% ee). ^1H NMR (400 MHz, $CDCl_3$) δ 7.22 (d, $J = 8.8$ Hz, 1H), 6.95 (dd, $J = 8.8$, 2.8 Hz, 1H), 6.76 (d, $J = 2.8$ Hz, 1H), 6.37 (d, $J = 9.1$ Hz, 1H), 6.28 (d, $J = 9.1$ Hz, 1H), 3.80 (s, 3H), 3.23 (br. s, 1H), 3.11 (s, 3H), 1.61 (s, 3H). LCMS (high pH) $(M+H)^+ = 218.0$, $R_t = 0.96$ min (100%); chiral HPLC: Chiralpak AD column, 25 cm, rt, 20% EtOH in heptane, injection volume 0.2 µL) $R_t = 9.83$ min, 99.6%, other enantiomer $R_t = 7.09$ min, 0.4%.

(*R*)-4-Benzyl-3-(2-(4-bromophenyl)acetyl)oxazolidin-2-one. To a solution of 2-(4-bromophenyl)acetic acid (**55**) (1000 g, 4650 mmol) and (*R*)-4-benzyloxazolidin-2-one (742 g, 4185 mmol) in toluene (10000 mL), was added NEt_3 (1944 mL, 113950 mmol). The reaction mixture was heated at 80 °C, then pivaloyl chloride (859 mL, 6975 mmol) was added slowly at the same temperature. The temperature was increased to 110 °C and stirred for 16 h. The reaction was quenched with 1 N HCl solution and extracted with EtOAc (2 × 1000 mL). The organic phase

was washed with saturated aq. $NaHCO_3$, dried over Na_2SO_4, filtered, and concentrated *in vacuo* to give the crude product. The crude product was purified by recrystallization by using Et_2O (2 x 1000 mL) and *n*-hexane (2 x 1000 mL) to give the title compound as a pale-yellow solid (980 g, 53%). ^{1}H NMR (400 MHz, DMSO-d_6) δ ^{1}H NMR (400 MHz, DMSO-d$_6$) δ = 7.63–7.45 (m, 2H), 7.34–7.19 (m, 5H), 7.19–7.08 (m, 2H), 4.78–4.55 (m, 1H), 4.35 (t, J = 8.6 Hz, 1H), 4.29–4.09 (m, 3H), 3.07 - 2.83 (m, 2H); LCMS (formic method E) $(M+H)^+$ = 374.1, 376.0, R_t = 3.36 min (93%).

(*R*)-4-Benzyl-3-((*R*)-2-(4-bromophenyl)propanoyl)oxazolidin-2-one (52). To a solution of MeI (5.96 mL, 95 mmol) in anhydrous THF (100 mL) stirred under N_2 at –78 °C was added a solution of NaHMDS (22.01 mL, 1 M in THF, 22.01 mmol), then reaction mixture was stirred for 2 h at the same temperature. (*R*)-4-Benzyl-3-(2-(4-bromophenyl)acetyl)oxazolidin-2-one (10.0 g, 22.01 mmol) was added over 15 min and the reaction mixture was stirred at rt for 16 h. The reaction mixture was quenched with saturated NH_4Cl (100 mL), then extracted with EtOAc (3 × 150 mL). The combined organic layers were washed with H_2O and brine, dried over Na_2SO_4, filtered, and concentrated *in vacuo* to give the crude product. The crude product was added to a silica gel 60-120 column and purified by column chromatography eluting with EtOAc in *n*-hexane (15%). The appropriate fractions were combined and concentrated *in vacuo* to give **52** as a yellow gum (8.0 g, 88%). ^{1}H NMR (400 MHz, CDCl$_3$) δ 7.50–7.39 (m, 2H), 7.37–7.15 (m, 7H), 5.08 (q, J = 7.0 Hz, 1H), 4.59 (tdd, J = 2.9, 7.1, 9.9 Hz, 1H), 4.18–4.03 (m, 2H), 3.34 (dd, J = 3.3, 13.4 Hz, 1H), 2.80 (dd, J = 9.8, 13.3 Hz, 1H), 1.61–1.45 (m, 3H); LCMS (formic method E) $(M+H)^+$ = 388.1, 390.1, R_t = 3.24 min (94%).

(*R*)-2-(4-Bromophenyl)propanoic acid. To a solution of **52** (75 g, 143 mmol) in THF (350 mL) and H_2O (175 mL) at 0 °C was added dropwise a solution of lithium peroxide [prepared by adding 30% H_2O_2 (73 mL, 715 mmol) to LiOH (3.42 g, 143 mmol) in H_2O (160 mL)]. The

reaction mixture was stirred for 0 °C for 1 h. The reaction mixture was cooled to the 0 °C, then quenched with saturated aqueous Na_2SO_3 (500 mL). The solvent was removed *in vacuo*. The residue was extracted with CH_2Cl_2 (2 × 500 mL). The aqueous layer was acidified (pH 2-3) with conc. HCl (10 mL) and then extracted with EtOAc (2 × 700 mL). The combined organic layers were washed with brine (700 mL). The separated organic layer was dried with anhydrous Na_2SO_4, filtered, and concentrated under reduced pressure to give the title compound as pale-yellow solid (32.0 g, 96 %). ^{1}H NMR (400 MHz, DMSO-d_6) δ 12.36 (br s, 1H), 7.59–7.43 (m, 2H), 7.33–7.19 (m, 2H), 3.68 (q, J = 7.2 Hz, 1H), 1.35 (d, J = 7.2 Hz, 3H); LCMS (formic method E) (M+H)$^+$ = 227.0, 228.9, R_t = 2.57 min (99%).

(*R*)-2-(4-Bromophenyl)-N-(2,2-dimethoxyethyl)-N-methylpropanamide (53). To a stirred solution of (*R*)-2-(4-bromophenyl)propanoic acid (40.0 g, 175 mmol) in dry 2-MeTHF (400 mL), was added 2,2-dimethoxy-*N*-methylethanamine (27.1 mL, 210 mmol) and DIPEA (122 mL, 698 mmol) at rt. The reaction mixture was cooled to 0 °C, then T3P (50% by weight solution in EtOAc, 157 mL, 262 mmol) was added slowly. The reaction mixture was stirred at 80 °C for 1 h. The reaction mixture was cooled to rt and diluted with H_2O (400 mL) and EtOAc (400 mL). The layers were separated and the aqueous extracted with EtOAc (300 mL). The combined organic layers were washed with brine (500 mL). The organic layer was separated, dried with anhydrous Na_2SO_4, filtered, and concentrated under reduced pressure to give **53** as brown liquid (50.0 g, 86%) which was used without further purification. ^{1}H NMR (400 MHz, CDCl$_3$) δ 7.52–7.28 (m, 2H), 7.24–7.07 (m, 2H), 4.48 (t, J = 5.5 Hz, 1H), 3.86 (q, J = 6.9 Hz, 1H), 3.61–3.45 (m, 1H), 3.43–3.30 (m, 7H), 3.00–2.89 (m, 3H), 1.41 (d, J = 6.8 Hz, 3H); LCMS (formic method E) (M+H)$^+$ = 329.1, 331.1, R_t = 2.38 min (99%).

(R)-7-Bromo-1,3-dimethyl-1H-benzo[d]azepin-2(3H)-one (54). Aluminium chloride (615 g, 4615 mmol) in CH_2Cl_2 (3000 mL), was added to a solution of **53** (200 g, 462 mmol) in CH_2Cl_2 (300 mL) at 0 °C and the reaction mixture was slowly warmed to rt and stirred for 16 h. The reaction mixture was poured in 6 N HCl (1000 mL) at 0 °C by dropwise addition. The aqueous residue was washed with CH_2Cl_2 (2 × 1000 mL). The organic layer was dried over Na_2SO_4, filtered and filtrate was concentrated to give a brown liquid. The liquid was purified by column chromatography (silica gel 100-200 column) eluting with EtOAc in *n*-hexane (23%). The appropriate fractions were combined and concentrated *in vacuo* to give the **54** (38 g, 30%) as a white solid. ^{1}H NMR (400 MHz, DMSO-d_6) δ 7.49 (dd, J = 8.3, 2.0 Hz, 1H), 7.39 (d, J = 2.0 Hz, 1H), 7.18 (d, J = 8.3 Hz, 1H), 6.33 (s, 2H), 3.23 (br. s, 1H), 3.12 (s, 3H), 1.62 (d, J = 5.9 Hz, 3H); LCMS (formic method E) $(M+H)^+$ = 265.9, 267.9, R_t = 2.90 min (96%).

(R)-7-Ethyl-1,3-dimethyl-1,3-dihydro-2H-benzo[d]azepin-2-one (14). To a dried-under-vacuum microwave vial was added **54** (300 mg, 1.13 mmol), zinc (275 mg, 4.21 mmol), Pd(amphos)Cl$_2$ (65 mg, 0.09 mmol), LiCl (4.5 mL, 0.5 M in THF, 2.25 mmol) and iodoethane (0.34 mL, 4.23 mmol). The vial was sealed, degassed and backfilled with N_2 × 3 and stirred at 100 °C for 1 h. The reaction mixture was filtered through celite and flushed through with H_2O (20 mL) and EtOAc (20 mL). The organic phase was dried by passing through a hydrophobic frit and evaporated to dryness to yield a brown oil, which was subsequently purified by flash column chromatography (50 g SNAP cartridge, 0–25% 3:1 EtOAc:EtOH in cyclohexane). The relevant fractions were pooled and evaporated to dryness to give **14** as a clear oil (88 mg, 34%). ^{1}H NMR (400 MHz, CDCl$_3$) δ 7.46–7.28 (m, 2H), 7.24–7.08 (m, 1H), 6.47–6.37 (m, 1H), 6.32–6.30 (m, 1H), 3.28 (br s, 1H), 3.20–3.07 (m, 3H), 2.73–2.61 (m, 2H), 1.78–1.70 (m, 3H), 1.32–1.20 (m, 3H); LCMS (formic) $(M+H)^+$ = 216.2, R_t = 1.15 min (97%).

(*R*)-7-(Ethylsulfonyl)-1,3-dimethyl-1*H*-benzo[*d*]azepin-2(3*H*)-one (25). To a mixture of **54** (400 mg, 1.50 mmol) and sodium ethanesulfinate (2.62 g, 22.60 mmol) in DMSO (4 mL) was added *L*-proline (35 mg, 0.30 mmol), CuI (29 mg, 0.15 mmol) and Na_2CO_3 (478 mg, 4.51 mmol) at rt. Then the reaction mixture was stirred at 120 °C for 48 h. The reaction mixture was cooled to rt and then diluted with H_2O (50 mL) and EtOAc (100 mL). The separated organic phase was washed with brine (50 mL), dried with anhydrous Na_2SO_4, filtered, and concentrated under reduced pressure. The crude product was purified by column chromatography (silica gel), eluting with 1:1 hexane-EtOAc. The collected fractions were concentrated under reduced pressure to give *rac*-**25** as an off-white solid (200 mg, 46%). 70 mg of *rac*-**25** was then separated by chiral SFC (Column: Lux Amylose-2 (250 × 30 mm); 50% CO_2, 50% MeOH, flow 60 g/min, back pressure 100 bar; UV 226 nm; 20 × 3 mg injections). Fractions from the second peak were concentrated under reduced pressure to give **25** (26 mg, 6%, >96% ee). ^{1}H NMR (400 MHz, DMSO-d_6) δ 7.87 (s, 1H), 7.86 (d, J = 7.9 Hz, 2H), 7.56 (d, J = 8.8 Hz, 1H), 6.75–6.58 (m, 2H), 3.40–3.18 (m, 3H), 3.06 (s, 3H), 1.55 (br d, J = 6.6 Hz, 3H), 1.10 (t, J = 7.3 Hz, 3H); LCMS (formic B) $(M+H)^+$ = 280.1, R_t = 1.70 min (98%); Chiral SFC: LuxCellulose-2 (4.6 × 250 mm), MeOH, flow rate: 4 g / min, 40% modified, 100 bar, 30.2 °C, R_t = 3.88 min (98.2%), undesired enantiomer R_t = 3.28 min.

(*R*)-1,3-Dimethyl-7-(morpholinomethyl)-1,3-dihydro-2H-benzo[d]azepin-2-one (20). **54** (1.00 g, 3.76 mmol), potassium trifluoro(morpholinomethyl)borate (1.17 g, 5.64 mmol), and Cs_2CO_3 (3.67 g, 11.27 mmol) were added to a microwave vial. *i*-PrOH (15 mL) and H_2O (5 mL) were added to the vial, which was purged with N_2 for 5 min prior to the addition of $Pd(OAc)_2$ (25 mg, 0.11 mmol) and XPhos (0.11 g, 0.23 mmol). After a further 5 min purge with N_2, the vial was capped and heated in the microwave at 100 °C for 30 min. Further potassium trifluoro(morpholinomethyl)borate (900 mg, 4.35 mmol), $Pd(OAc)_2$ (25 mg, 0.11 mmol) and

XPhos (0.11 g, 0.23 mmol) were added to the reaction mixture, which was purged with N_2 by evacuation-refill. The vial was heated in the microwave at 100 °C for a further 30 min. The mixture was filtered, and the solvent removed in vacuo, before extracting the residue in EtOAc (100 mL) and washing with saturated $NaHCO_3$ solution (100 mL). The aqueous layer was extracted with EtOAc (50 mL) and the product extracted from the combined organic layers with 1M HCl solution (2 × 50 mL). The acidic aqueous layer was neutralised to pH~10 with NaOH pellets, and the product reextracted into EtOAc (2 × 50mL). This was passed through a hydrophobic frit, and the solvent removed under reduced pressure to give **20** as a pale-yellow oil (920 mg, 85%). ^{1}H NMR (400 MHz, MeOH-d_4) δ 7.46–7.35 (m, 1H), 7.34–7.25 (m, 2H), 6.56 (d, J = 8.8 Hz, 1H), 6.48 (d, J = 9.3 Hz, 1H), 3.73–3.62 (m, 4H), 3.53 (s, 2H), 3.31–3.18 (m, 1H), 3.11 (s, 3H), 2.50–2.38 (m, 4H), 1.60 (br s, 3H); LCMS (high pH) (M+H)$^+$ = 287.3, R_t = 0.90 min (100%).

(*R*)-1,3-Dimethyl-7-vinyl-1H-benzo[d]azepin-2(3*H*)-one (55). A mixture of **54** (4.00 g, 15.03 mmol), 4,4,5,5-tetramethyl-2-vinyl-1,3,2-dioxaborolane (3.82 mL, 22.54 mmol), K_2CO_3 (5.19 g, 37.6 mmol) and Pd(PPh$_3$)$_4$ (0.87 g, 0.75 mmol) in 1,4-dioxane (60 mL) and H_2O (20 mL) was heated at 120 °C for 16 h. The reaction was allowed to cool to rt and then concentrated *in vacuo* to give a yellow solid. The resulting residue was dissolved in EtOAc (100 mL) and washed with H_2O (100 mL). The organic layers were extracted with EtOAc (2 × 100 mL) and the organic layers combined to give a yellow/orange solution, which became red and then brown. The combined organic layers were passed through a hydrophobic frit and concentrated *in vacuo* to a dark brown oil. The crude product was dissolved in CH_2Cl_2 and loaded onto a 120 g silica cartridge. This was purified by column chromatography, eluting with EtOAc in cyclohexane (0-35%). The appropriate fractions were combined and concentrated *in vacuo* to give **55** (2.62 g, 78%) as an orange/yellow solid. ^{1}H NMR (400 MHz, MeOH-d_4) δ 7.52 (dd, J = 1.7, 8.1 Hz, 1H), 7.37 (d, J = 2.0 Hz, 1H),

7.29 (d, J = 8.3 Hz, 1H), 6.85–6.66 (m, 1H), 6.57 (d, J = 8.8 Hz, 1H), 6.48 (d, J = 9.3 Hz, 1H), 5.81 (dd, J = 1.0, 17.6 Hz, 1H), 5.26 (dd, J = 1.0, 10.8 Hz, 1H), 3.31–3.22 (m, 1H), 3.13 (s, 3H), 1.72–1.54 (m, 3H); LCMS (high pH) (M+H)$^+$ = 214.2, R_t = 1.10 min (100%).

(1R)-7-(1,2-Dihydroxyethyl)-1,3-dimethyl-1,3-dihydro-2H-benzo[d]azepin-2-one (24). To a 50 mL round-bottomed flash was added, in sequence, acetone (5 mL), **55** (100 mg, 0.47 mmol) and H_2O (10 mL). The reaction was heated to 70 °C, and then oxone (576 mg, 0.94 mmol) was added portion wise. The reaction was left to stir under N_2 at 70 °C for 3 h. The reaction was allowed to cool to rt and was quenched portion wise with excess saturated sodium sulphite solution. The reaction mixture was extracted into n-butanol (2 × 50 mL) and the organic phase was dried by passing through a hydrophobic frit. The solvent was removed in vacuo and the resultant yellow oil was purified by flash column chromatography (0-60% 3:1 EtOAc in EtOH / cyclohexane) to give **24** as a clear oil (23 mg, 18%). ^{1}H NMR (400 MHz, CDCl$_3$) δ 7.41–7.27 (m, 3H), 6.45 (d, J = 9.3 Hz, 1H), 6.33 (br d, J = 8.3 Hz, 1H), 4.90–4.80 (m, 1H), 3.84–3.60 (m, 2H), 3.35–3.20 (m, 1H), 3.13 (d, J = 1.5 Hz, 3H), 2.50–2.30 (br.s, 2H), 1.77–1.55 (m, 3H); LCMS (high pH) (M+H)$^+$ = 246.1, R_t = 0.62 min (85%).

Diethyl (R)-2-(1,3-dimethyl-2-oxo-2,3-dihydro-1H-benzo[d]azepin-7-yl)malonate (56). To a stirred solution of **54** (1.00 g, 3.76 mmol) in toluene (10 mL), were added diethyl malonate (0.69 ml, 4.51 mmol) and K$_3$PO$_4$ (2.39 g, 11.27 mmol). The reaction mixture was degassed under N_2 atmosphere for 15 min. After that Pd(Pt-Bu$_3$)$_2$ (0.04 g, 0.08 mmol) was added. The reaction mixture was stirred at 110 °C for 18 h in sealed tube. The reaction mixture was quenched with H_2O and extracted with EtOAc (2 × 50 mL). The combined organic layer was washed with brine, dried with anhydrous Na$_2$SO$_4$, filtered, and concentrated under vacuum. The residue was purified by column chromatography using 100-200 silica gel eluting with 15% EtOAc in hexane, the

appropriate fractions were combined and evaporated to give **56** (900 mg, 67%). ^{1}H NMR (400 MHz, DMSO-d_6) δ 7.41 (dd, J = 1.7, 8.1 Hz, 1H), 7.34 (d, J = 2.0 Hz, 1H), 7.29 (d, J = 8.3 Hz, 1H), 6.57 (d, J = 9.3 Hz, 1H), 6.49 (d, J = 8.8 Hz, 1H), 4.97 (s, 1H), 4.22–4.08 (m, 4H), 3.22 (br.s, 1H), 3.05 (s, 3H), 1.51 (br d, J = 6.8 Hz, 3H), 1.19 (dt, J = 1.0, 7.1 Hz, 6H); LCMS (formic B) $(M+H)^+$ = 346.3, R_t = 2.89 min (96%).

(R)-7-(1,3-Dihydroxypropan-2-yl)-1,3-dimethyl-1,3-dihydro-2H-benzo[d]azepin-2-one (23). To a stirred solution of **56** (550 mg, 1.59 mmol) in THF (15 mL) and MeOH (5 mL) was added NaBH$_4$ (482 mg, 12.74 mmol) portionwise at rt and stirred for 4 h. The solvent was removed under vacuum, the resulting residue quenched with H$_2$O (20 mL) and extracted with EtOAc (2 × 50 mL). The combined organic phase was washed with brine (30 mL), dried over anhydrous Na$_2$SO$_4$, filtered, and concentrated under vacuum. The resultant residue was purified by column chromatography using 100-200 silica gel eluting with 50% EtOAC in hexane. The appropriate fractions were combined and evaporated under reduced pressure to give **23** as an off-white solid (163 mg, 39%). ^{1}H NMR (400 MHz, MeOH-d_4) δ 7.37–7.21 (m, 3H), 6.57 (d, J = 9.3 Hz, 1H), 6.46 (d, J = 8.8 Hz, 1H), 3.91–3.75 (m, 4H), 3.28 (br.s, 1H), 3.10 (s, 3H), 2.99 (quin, J = 6.6 Hz, 1H), 1.68–1.54 (m, 3H); LCMS (formic D) $(M+H)^+$ = 262.2, R_t = 1.36 min (99%).

(R)-7-Hydroxy-1,3-dimethyl-1,3-dihydro-2H-benzo[d]azepin-2-one (57). To a round bottomed flask was added a solution of **54** (4.00 g, 15.03 mmol) in anhydrous 1,4-dioxane (30 mL), and the solution was degassed with N$_2$. 4,4,4',4',5,5,5',5'-octamethyl-2,2'-bi(1,3,2-dioxaborolane) (11.45 g, 45.1 mmol) and KOAc (4.43 g, 45.1 mmol) were added, and the resulting solution was stirred under N$_2$ for 15 min before adding PdCl$_2$(dppf) (1.10 g, 1.503 mmol). The resultant suspension was heated to 85 °C overnight. The reaction mixture was cooled to rt, sat. aq. NH$_4$Cl (50 mL) and EtOAc (50 mL) were added. The separated aqueous layer was diluted with

brine (30 mL) and then washed with EtOAc (3 × 25 mL). The combined organic layer was washed with H_2O (30 mL), brine (40 mL), filtered through celite, dried through a hydrophobic frit and then concentrated under vacuum to give a black solid which was used without further purification. The black solid was dissolved in EtOH (60 mL) and H_2O (30 mL) and mCPBA (3.37 g, 77% by weight in H_2O, 15.04 mmol) was added. Following stirring under N_2 at rt for 2 h, mCPBA (3.37 g, 77% by weight in H_2O, 15.04 mmol) was added and stirring continued for a further 5 h. mCPBA (3.37 g, 77% by weight in H_2O, 15.04 mmol) was added and the reaction stirred under N_2 at rt overnight. Further mCPBA (320 mg, 77% by weight in H_2O, 1.43 mmol) was added and stirring continued for 24 h. The reaction was quenched slowly with saturated $NaHCO_3$ (140 mL) until neutral pH was reached. The mixture was diluted with EtOAc (100 mL), the layers were separated, and the aqueous layer was washed with EtOAc (4 × 100 mL). The combined organic phase was added to saturated aq. sodium sulphite and stirred until Merckoquant Peroxide Test paper showed no trace of peroxides. The organic layer was separated from the sat. aq. sodium sulphite and then concentrated under vacuum to afford a brown solid. The crude solid was purified by column chromatography eluting with *t*-BuOMe / cyclohexane (15-100%). The appropriate fractions were combined and concentrated under vacuum to afford **57** as a white solid (2.51 g, 82% over 2 steps). Data matches *rac*-**57** below.

7-(2-Hydroxy-2-methylpropoxy)-1,3-dimethyl-1H-benzo[d]azepin-2(3H)-one (*rac*-17). A microwave vial was charged with **57** (50 mg, 0.25 mmol), K_2CO_3 (54 mg, 0.39 mmol) and 2,2-dimethyloxirane (0.05 mL, 0.57 mmol) in DMF (1 mL). The mixture was heated at 120 °C for 1 h under microwave irradiation and then for a further 4 h at 120 °C. The reaction mixture was evaporated under a stream of N_2 to give an orange solid. The solid was dissolved in 2:1 MeOH / H_2O and purified by MDAP (high pH). The appropriate fractions were combined and evaporated

under reduced pressure to give *rac*-**17** as a colorless gum (11 mg, 16%). ^{1}H NMR (400 MHz, DMSO-d_6) δ 7.16 (d, J = 8.8 Hz, 1H), 6.98 (dd, J = 2.9, 8.8 Hz, 1H), 6.90 (d, J = 2.4 Hz, 1H), 6.52 (d, J = 9.3 Hz, 1H), 6.44 (d, J = 9.3 Hz, 1H), 4.59 (s, 1H), 3.77–3.65 (m, 2H), 3.27–3.09 (m, 1H), 3.03 (s, 3H), 1.47 (br d, J = 6.8 Hz, 3H), 1.24–1.16 (m, 6H); LCMS (formic) (M+H)$^+$ = 276.2, R_t = 0.86 min (100%).

Diethyl (R)-2-((1,3-dimethyl-2-oxo-2,3-dihydro-1H-benzo[d]azepin-7-yl)oxy)malonate. To a stirred solution of **57** (500 mg, 2.46 mmol) in DMF (5 mL), was added K$_2$CO$_3$ (1020 mg, 7.38 mmol) and diethyl bromo malonate (588 mg, 2.46 mmol) at rt. The mixture was stirred for 4 h, quenched with H$_2$O (20 mL) and extracted with EtOAc (2 × 50 mL). The combined organic layer was washed with brine (40 mL), dried with anhydrous Na$_2$SO$_4$, filtered, and concentrated under reduced pressure. The resultant material was purified by column chromatography using 100-200 silica gel eluting with 15% EtOAC in hexane. Appropriate fractions were combined and evaporated under reduced pressure to give the title compound as an oil (1.30 g, 59%). ^{1}H NMR (400 MHz, DMSO-d_6) δ 7.20 (d, J = 8.8 Hz, 1H), 7.02 (br dd, J = 2.4, 8.8 Hz, 1H), 6.94 (d, J = 2.6 Hz, 1H), 6.55 (br d, J = 9.2 Hz, 1H), 6.41 (br d, J = 9.0 Hz, 1H), 5.71 (s, 1H), 4.33–4.12 (m, 4H), 3.15 (br d, J = 12.7 Hz, 1H), 3.08–2.94 (m, 3H), 1.62–1.36 (m, 3H), 1.30–1.12 (m, 6H); LCMS (formic method H) (M+H)$^+$ = 362.1, R_t = 2.75 min (92%).

(R)-7-((1,3-Dihydroxypropan-2-yl)oxy)-1,3-dimethyl-1,3-dihydro-2H-benzo[d]azepin-2-one (18). To a stirred solution of diethyl (R)-2-((1,3-dimethyl-2-oxo-2,3-dihydro-1H-benzo[d]azepin-7-yl)oxy)malonate (150 mg, 0.42 mmol) in THF (10 mL) and MeOH (5 mL), was added NaBH$_4$ (126 mg, 3.32 mmol) portionwise at rt and stirred for 4 h. The solvent was removed under vacuum and the resulting residue quenched with H$_2$O (30 mL). The aqueous phase was extracted with EtOAc (2 × 50 mL). The combined organic phase was washed with brine (30 mL),

dried with anhydrous Na_2SO_4, filtered, and concentrated under vaccum. The resultant residue was purified by column chromatography using 100-200 silica gel eluting with 60% EtOAC in hexane. The appropriate fractions were combined and evaporated under reduced pressure to give **18** as a white solid (51 mg, 44%). ^{1}H NMR (400 MHz, DMSO-d_6) δ 7.14 (d, J = 8.6 Hz, 1H), 7.01 (dd, J = 2.5, 8.7 Hz, 1H), 6.92 (d, J = 2.4 Hz, 1H), 6.51 (d, J = 9.0 Hz, 1H), 6.41 (d, J = 9.2 Hz, 1H), 4.73 (dt, J = 2.3, 5.5 Hz, 2H), 4.24 (quin, J = 5.2 Hz, 1H), 3.56 (tq, J = 5.6, 11.5 Hz, 4H), 3.17 (br dd, J = 6.5, 11.7 Hz, 1H), 3.02 (s, 3H), 1.46 (br d, J = 6.1 Hz, 3H); LCMS (formic B) $(M+H)^+$ = 278.2, R_t = 1.39 min (99%).

2-(4-Bromophenyl)-N-(2,2-dimethoxyethyl)-N-methylpropanamide. To a stirred solution of 2-(4-bromophenyl)propanoic acid (68.8 g, 300 mmol) in dry THF (150 mL) under N_2, 2,2-dimethoxy-N-methylethanamine (46.7 mL, 360 mmol), T3P (50% by weight in EtOAc, 451 mL, 751 mmol) and DIPEA (210 mL, 1201 mmol) were added at rt, and then the solution was heated to 80 °C for 4 h. The reaction mixture was quenched with H_2O, the aqueous residue was washed with EtOAc (3 × 40 mL). The organic solution was dried (Na_2SO_4) and concentrated under vacuo to give a residue. The residue was purified by column chromatography using 100-200 mesh silica gel and eluting with 50% EtOAc in hexane to give the title compound (89.0 g, 72%). Data as for (*R*)-2-(4-bromophenyl)-N-(2,2-dimethoxyethyl)-N-methylpropanamide above.

7-Bromo-1,3-dimethyl-1H-benzo[d]azepin-2(3H)-one (*rac*-54). Aluminium chloride (81.00 g, 606 mmol) in CH_2Cl_2 (100 mL), was added to a solution of 2-(4-bromophenyl)-N-(2,2-dimethoxyethyl)-N-methylpropanamide (20.00 g, 60.6 mmol) in CH_2Cl_2 (50 mL) at 0 °C and the reaction mixture was slowly warmed to rt and stirred for 24 h. The reaction mixture was added via dropwise addition to 6 N HCl (100 mL) at 0 °C. The separated aqueous phase was washed with CH_2Cl_2 (3 × 100 mL). The combined organic solution was dried (Na_2SO_4) and concentrated

under vacuo. The resultant residue was purified by column chromatography using 100-200 mesh silica gel, eluting with 20% EtOAc in hexane to give *rac*-**54** (5.24 g, 30%). Data as for **54** above.

7-Ethoxy-1,3-dimethyl-1H-benzo[d]azepin-2(3H)-one (15). *Rac*-**54** (5.00 g, 18.79 mmol) and KOH (1.58 g, 28.2 mmol) were dissolved in EtOH (20 mL) in a round bottomed flask and placed under an atmosphere of N_2 by evacuation-refill. Pd_2dba_3 (86 mg, 0.09 mmol) and BippyPhos (190 mg, 0.38 mmol) were added, and the reaction heated at 85 °C under N_2 for 3 h. The solvent was removed under reduced pressure and the residue re-dissolved in EtOAc (100 mL) and passed through celite. The filtrate was then washed with H_2O and brine. The organic layer was passed through a hydrophobic frit and the solvent was removed under reduced pressure. The sample was loaded in MeOH and purified by column chromatography using a 400 g reverse phase (C18) column, eluting with an MeCN (+0.1% NH_3)-H_2O (+0.1% NH_3) solvent system (5-85%). The appropriate fractions were combined and evaporated *in vacuo* to give *rac*-**15** as a beige solid (905 mg, 21%). ^{1}H NMR (400 MHz, MeOH-d_4) δ 7.21 (d, J = 8.8 Hz, 1H), 6.99 (dd, J = 2.4, 8.8 Hz, 1H), 6.85 (d, J = 2.4 Hz, 1H), 6.59–6.41 (m, 2H), 4.05 (q, J = 7.2 Hz, 2H), 3.26 (br.s, 1H), 3.11 (s, 3H), 1.58 (br.s, 3H), 1.39 (t, J = 6.9 Hz, 3H); LCMS (high pH) $(M+H)^+$ = 232.1, R_t = 1.07 min (95%).

(R)-1,3-Dimethyl-7-((tetrahydro-2H-pyran-4-yl)methyl)-1H-benzo[d]azepin-2(3H)-one (19). Magnesium turnings (0.41 g, 16.9 mmol) in THF (15 mL), iodine (0.29 g, 1.13 mmol) and 1,2-dibromoethane (0.97 mL, 11.3 mmol) were combined, stirred, and the reaction mixture was heated to 85 °C for 20 min under N_2. A solution of ((tetrahydro-2H-pyran-4-yl)methyl) bromide (2.29 g, 11.3 mmol) in THF (15 mL) was added slowly and the reaction mixture stirred for 2 h at the same temperature and then cooled to rt. In another dry round bottom flask was prepared a suspension of *rac*-**54** (3.00 g, 11.3 mmol) in THF (15 mL), the solution was degassed for 20 min,

$PdCl_2(dppf)$-CH_2Cl_2 adduct (0.92 g, 1.13 mmol) was added under N_2, and the Grignard solution was added dropwise over 15 min. The reaction mixture was then heated to 85 °C for 12 h under N_2. The reaction mixture was cooled to rt, quenched with 5% aqueous ammonium chloride (5 mL) and then extracted with ethyl acetate (2 × 100 mL). The organic layer was washed with 20% NaCl, the organic layer collected, dried over Na_2SO_4, and concentrated under reduced pressure. The resultant residue was purified by flash chromatography, eluting with 25% EtOAc in hexane. The appropriate fractions were combined and evaporated under reduced pressure to give *rac*-**19**. The compound was further purified by chiral SFC (Column: Lux Cellulose-2 (250 x 30)mm, 5μ; 50% CO_2, 50% (0.5% DEA in methanol), flow 70 g/min, back pressure 100 bar; UV 212 nm; 20 x 7 mg injections). Fractions from the second peak were combined and evaporated to give **19** (22 mg, 1%, >90% ee). ^1H NMR (400 MHz, DMSO-d_6) δ = 7.27–7.08 (m, 3H), 6.52 (d, J = 9.2 Hz, 1H), 6.44 (d, J = 9.2 Hz, 1H), 3.85–3.72 (m, 2H), 3.29–3.10 (m, 4H), 3.02 (s, 3H), 1.71 (ddd, J = 3.8, 7.3, 11.2 Hz, 1H), 1.59–1.35 (m, 5H), 1.34–1.08 (m, 3H); LCMS (formic) $(M+H)^+$ = 286.1, R_t = 2.22 min (97%); Chiral SFC: Lux Cellulose-2 (4.6 x 250 mm), 0.5% DIPEA in MeOH, total flow: 4 g / min, 40% co-solvent, temp: 30 °C, 100 bar, UV: 210 nm, R_t = 4.25 min (96%), undesired enantiomer R_t = 3.54 min.

(*R*)-1,3-Dimethyl-7-(pyrrolidin-1-ylmethyl)-1,3-dihydro-2H-benzo[d]azepin-2-one (21). To a solution of *rac*-**54** (500 mg, 1.88 mmol) in THF (2 mL) and H_2O (0.2 mL), potassium 1-trifluoroboratomethylpyrrolidine (359 mg, 1.88 mmol) and Cs_2CO_3 (1.84 g, 5.64 mmol) were added and degassed for 15 min. Then $Pd(OAc)_2$ (13 mg, 0.06 mmol) and XPhos (54 mg, 0.11 mmol) was added and the reaction mixture heated to 130 °C for 20 min under microwave irradiation. The reaction mixture was quenched with H_2O and extracted with EtOAc (3 × 30 mL). The combined organic solution was dried (Na_2SO_4) and concentrated under vacuo. The resultant

residue was purified by flash column chromatography using 100-200 mesh silica gel eluting with 6% MeOH in CH_2Cl_2 to give *rac*-**21**. The compound was further purified by chiral SFC (Column: Chiralpak AS-H (250 x 30) mm; 85% CO_2, 15% (0.5% DIPEA in methanol), flow: 100 g/min, back pressure 100 bar; UV 210 nm; 130 × 7.5 mg injections). Fractions from the second peak were combined and evaporated to give **21** (61 mg, 12%, >98% ee). ^{1}H NMR (400 MHz, DMSO-d_6) δ 7.38–7.28 (m, 1H), 7.28–7.14 (m, 2H), 6.63–6.37 (m, 2H), 3.55 (s, 2H), 3.23–3.10 (m, 1H), 3.03 (s, 3H), 2.48–2.32 (m, 4H), 1.76–1.59 (m, 4H), 1.56–1.40 (m, 3H); LCMS (formic B) $(M+H)^+$ = 271.1, R_t = 1.20 min (99%); Chiral HPLC: Chiralpak AS-H (4.6 × 250 mm), 0.5% DIPEA in MeOH, total flow: 3 mL / min, 20% modifier, temp: 29.9 °C, 100 bar, R_t = 2.29 min (99.2%), undesired enantiomer R_t = 2.08 min.

1,3-Dimethyl-7-vinyl-1,3-dihydro-2H-benzo[d]azepin-2-one (*rac*-55). 4,4,5,5-Tetramethyl-2-vinyl-1,3,2-dioxaborolane (0.48 mL, 2.82 mmol), *rac*-**60** (500 mg, 1.88 mmol), Pd(PPh$_3$)$_4$ (109 mg, 0.09 mmol) and K_2CO_3 (649 mg, 4.70 mmol) were added to a microwave vial. 1,4-Dioxane (3 mL) and H_2O (1 mL) were added and the reaction heated to 120 °C for 30 min in the microwave at very high absorbance. The reaction was concentrated in vacuo and then partitioned between EtOAc (20 mL) and H_2O (20 mL). The separated aqueous phase was washed with EtOAc (2 × 10 mL). The combined organic phase was passed through a hydrophobic frit and then concentrated under reduced pressure. The resultant residue was purified by silica gel chromatography eluting with 0-30% EtOAc / cyclohexane. Appropriate fractions were combined and concentrated in vacuo to give *rac*-**54** (279 mg, 70%). ^{1}H NMR (400 MHz, CDCl$_3$) δ 7.47 (dd, *J* = 1.5, 8.1 Hz, 1H), 7.34–7.26 (m, 1H), 6.78–6.68 (m, 1H), 6.44 (d, *J* = 9.1 Hz, 1H), 6.32 (d, *J* = 9.1 Hz, 1H), 5.77 (dd, *J* = 1.0, 17.6 Hz, 1H), 5.28 (d, *J* = 11.6 Hz, 1H), 3.44–3.22 (m, 1H), 3.14 (s, 3H), 1.71–1.55 (m, 3H); LCMS (high pH) $(M+H)^+$ = 214.2, R_t = 1.10 min (100%).

(R)-7-(2-Hydroxyethyl)-1,3-dimethyl-1,3-dihydro-2H-benzo[d]azepin-2-one (22). BH_3-THF (0.19 mL, 0.19 mmol) was added to a stirring solution of *rac*-**55** (100 mg, 0.47 mmol) in THF (2 mL) and left to stir for 1.5 h at rt. NaOH (0.38 mL, 2 M aq., 0.75 mmol) and H_2O_2 (159 mg, 30% by weight in H_2O, 1.41 mmol) were added and the reaction stirred overnight. Further BH_3-THF (0.19 mL, 0.19 mmol) was added and the reaction left to stir for 4 h. 10% aq. Sodium sulphite solution (10 mL) was added. The mixture was dissolved in EtOAc (10 mL) and the separated aqueous phase extracted with EtOAc (2 × 10 mL). The combined organic phase was passed through a hydrophobic frit and evaporated under reduced pressure. The residue was purified by silica gel column chromatography eluting with 0-50% EtOAc/cyclohexane. Appropriate fractions were combined and evaporated under reduced pressure to give *rac*-**22**. In parallel a second reaction was carried out using *rac*-**64** (20 mg) with all other reagents and solvents scaled accordingly. The combined products were dissolved in 2:1 EtOH / n-heptane (3 mL) and purified by chiral HPLC: Regis (*R,R*) Whelk (250 × 21.2 mm), 0.6 mL injection volume, ambient temperature, 20 mL / min flow rate, 4:1 heptane / EtOH, The appropriate fractions were combined and evaporated to give **22** as a colorless solid (10 mg, 8%, >99% ee). ^1H NMR (400 MHz, $CDCl_3$) δ 7.29 (br.s, 2H), 7.15 (s, 1H), 6.42 (d, *J* = 8.8 Hz, 1H), 6.32 (d, *J* = 8.8 Hz, 1H), 3.88 (t, *J* = 6.6 Hz, 2H), 3.29 (br. s, 1H), 3.13 (s, 3H), 2.89 (t, *J* = 6.4 Hz, 2H), 1.75–1.59 (m, 3H), 1.53 (br s, 1H); LCMS (high pH) $(M+H)^+$ = 232.1, R_t = 0.78 min (100%); Chiral HPLC: Regis (*R,R*)-Whelk-0O1 (4.6 × 250 mm), 4:1 heptane / EtOH, flow rate: 1 mL / min, ambient temp, R_t = 14.12 min (99.9%), undesired enantiomer R_t = 17.89 min.

1,3-Dimethyl-7-(4,4,5,5-tetramethyl-1,3,2-dioxaborolan-2-yl)-1,3-dihydro-2H-benzo[d]azepin-2-one. To a stirred solution of *rac*-**54** (1 g, 3.76 mmol) in 1,4-dioxane (20 mL) was added potassium acetate (0.92 g, 9.39 mmol) and bis(pinacolato)diboron (2.39 g, 9.39 mmol)

at rt and the resulting suspension was degassed for 45 min. Then PdCl$_2$(dppf)-CH$_2$Cl$_2$ adduct (0.31 g, 0.376 mmol) was added and again degassed for 30 min. Then the solution was heated to 100 °C for 2 h under N$_2$. The reaction mixture was diluted with H$_2$O (30 ml) and EtOAc (50 mL), filtered through a celite bed and then the filtrate cake was washed with EtOAc (3 × 30 mL). The combined filtrate was separated, then the organic layer was washed with brine (2 × 20 mL). Then the organic layer was separated, dried over anhydrous Na$_2$SO$_4$ and concentrated under reduced pressure to afford a black gum. The gum was purified by column chromatography using silica gel (100-200 mesh), eluting with 20% EtOAc in petroleum ether. The appropriate fractions were combined and evaporated to give the title compound as a pale-yellow oil (750 mg, 52%). LCMS (formic B) (M+H)$^+$ = 314.2, R$_t$ = 2.61 min (82%).

7-Hydroxy-1,3-dimethyl-1,3-dihydro-2H-benzo[d]azepin-2-one (*rac*-57). To a cooled solution of 1,3-dimethyl-7-(4,4,5,5-tetramethyl-1,3,2-dioxaborolan-2-yl)-1,3-dihydro-2H-benzo[d]azepin-2-one (800 mg, 2.55 mmol) in THF (15 mL) was added aq. NaOH (7.66 mL, 2 M in H$_2$O 15.33 mmol) dropwise, then the reaction mixture was stirred at 0 °C for 10 min. H$_2$O$_2$ (1.31 mL, 30% weight in H$_2$O, 12.77 mmol) was added dropwise over 2 min at 0 °C and then the reaction mixture was stirred at rt for 2 h. The reaction mixture was acidified to pH 6.5 with 2 M aq. HCL(8 mL), diluted with H$_2$O (15 mL) and extracted with EtOAc (2 × 25 mL). The combined organic layers were washed with brine (2 × 15 mL), dried over anhydrous Na$_2$SO$_4$ and concentrated under reduced pressure to give a pale-yellow oil. In parallel a second reaction was run using 750 mg *rac*-**61** with all other reagents and solvents scaled accordingly. The crude product from both reactions was combined and purified by column chromatography using silica gel (100-200 mesh), eluting with 40% EtOAc in petroleum ether. The appropriate fractions were combined and evaporated under reduced pressure to give *rac*-**57** as a yellow solid (800 mg, 76%).

^{1}H NMR (400 MHz, DMSO-d_6) δ 9.40 (br s, 1H), 7.06 (d, J = 8.3 Hz, 1H), 6.81 (dd, J = 2.7, 8.6 Hz, 1H), 6.69 (d, J = 2.4 Hz, 1H), 6.47 (d, J = 9.3 Hz, 1H), 6.36 (d, J = 9.3 Hz, 1H), 3.12 (br s, 1H), 3.02 (s, 3H), 1.44 (br d, J = 6.4 Hz, 3H); LCMS (formic B) (M+H)$^+$ = 204.1, R_t = 1.64 min (96%).

(*R*)-7-(2-Methoxyethoxy)-1,3-dimethyl-1,3-dihydro-2H-benzo[d]azepin-2-one (16). To a suspension of NaH (118 mg, 60% by weight in mineral oil, 2.95 mmol) in DMF (10 mL) cooled to 0 °C was added *rac*-**57** (300 mg, 1.48 mmol). Following stirring for 15 min at the same temperature, 1-chloro-2-methoxyethane (209 mg, 2.21 mmol) was added dropwise. The reaction was then stirred at rt for 16 h under N$_2$. The mixture was quenched with H$_2$O (20 mL) and extracted with EtOAc (2 × 30 mL). The combined organic layer was washed with cold brine (3 × 20 mL), dried over anhydrous Na$_2$SO$_4$ and concentrated under reduced pressure to give a pale brown oil. In parallel a second reaction was run using 100 mg *rac*-**62** with all other reagents and solvents scaled accordingly. The crude product from both reactions was combined and purified by column chromatography using silica gel (100-200 mesh), eluting with 30% EtOAc in petroleum ether. The appropriate fractions were combined and evaporated under reduced pressure to give a pale-yellow oil. The oil was purified by preparative HPLC: purification conditions. Mobile Phase : A) 10 mm Ammonium bicarbonate Mobile Phase : B) Acetonitrile Column : sunfire C18 (150 × 19 mm), flow rate: 18 mL / min, solvent: 60% THF in MeCN, The appropriate fractions were collected and lyophilized to give *rac*-**16** as a white solid (90 mg, 17%). *Rac*-**16** (80 mg was taken and purified by chiral SFC to give **16** (28 mg). Chiral SFC: Lux Amylose-2 (250 ×30 mm), 50% CO$_2$ / 0.5% DIPEA in MeOH, total flow: 60.0 g/min, back pressure: 100 bar, UV: 223 nm, stack time: 3.3 min, load / injection: 2.5 mg. ^{1}H NMR (400 MHz, DMSO-d_6) δ 7.17 (d, J = 8.8 Hz, 1H), 6.99 (dd, J = 2.7, 8.6 Hz, 1H), 6.90 (d, J = 2.4 Hz, 1H), 6.53 (d, J = 8.8 Hz, 1H), 6.43 (d, J = 9.3 Hz, 1H),

4.21–4.01 (m, 2H), 3.69–3.62 (m, 2H), 3.32–3.29 (m, 3H), 3.17 (br.s, 1H), 3.03 (s, 3H), 1.47 (br d, J = 6.4 Hz, 3H); LCMS (formic B) $(M+H)^+$ = 262.1, R_t = 1.91 min (99%); chiral SFC: Lux Amylose-2 (4.6 × 250 mm), solvent: 0.5% DIPEA in MeOH, temp: 29.9 °C, flow: 3 mL / min, R_t = 5.72 min, undesired enantiomer R_t = 3.95 min (>99% ee).

5-Bromo-7-(ethylsulfonyl)-1,3-dimethyl-1H-benzo[d]azepin-2(3H)-one (58). A solution of phenyltrimethylaminotribromide (404 mg, 1.07 mmol) in MeCN (4 mL) was added to a solution of *rac*-**25** (300 mg, 1.07 mmol) in MeCN (6 mL) at rt under N_2. The reaction was stirred at rt for 1 h. H_2O (30 mL) was added, followed by EtOAc (30 mL). The organic layer was separated, and the aqueous phase washed with EtOAc (2 × 20 mL). The organic layers were combined, passed through a hydrophobic frit and concentrated in vacuo to give **58** as an off white solid (370 mg, 87%). ^{1}H NMR (400 MHz, CDCl$_3$) δ 8.29 (d, J = 2.0 Hz, 1H), 7.97 (dd, J = 2.0, 8.3 Hz, 1H), 7.53 (d, J = 8.8 Hz, 1H), 6.97 (s, 1H), 3.57–3.45 (m, 1H), 3.21–3.10 (m, 5H), 1.85–1.61 (m, 3H), 1.42–1.26 (m, 3H); LCMS (formic) $(M+H)^+$ = 358.0, 360.0, R_t = 0.94 min (78%).

(R)-7-(Ethylsulfonyl)-1,3,5-trimethyl-1H-benzo[d]azepin-2(3H)-one (26). A solution of **58** (200 mg, 0.56 mmol) in 1,4-dioxane (7 mL) and H_2O (0.7 mL) was degassed for 10 min under N_2 and then 2,4,6-trimethyl-1,3,5,2,4,6-trioxatriborinane (210 mg, 1.68 mmol), potassium hydrogen phosphate (292 mg, 1.68 mmol) and X-Phos Pd cycle (44 mg, 0.06 mmol) were added. The reaction mixture was stirred at 90 °C for 16 h, cooled to rt and diluted with H_2O (30 mL) and EtOAc (60 mL). The layers were separated, and the organic layer was washed with brine (30 mL), dried with anhydrous Na_2SO_4, filtered and concentrated under reduced pressure. The crude product was added to a silica gel (100-200 mesh) column and eluted with hexane/EtOAc (30/70). Appropriate fractions were combined and concentrated under reduced pressure to give *rac*-**26** (150 mg, 92%). The racemic compound was dissolved in MeOH and purified by chiral SFC

purification: Lux Amylose-2 (250 × 30) mm,5μ, % CO_2: 60 %, % Co solvent: 40% (100% MeOH),

total flow: 70.0 g/min, back pressure: 100.0 bar, UV: 210 nm, stack time: 3.5 min, load/inj : 5 mg.

The appropriate fractions were combined and evaporated under reduced pressure to give **26** as an

off-white solid (68 mg, >94% ee). ^{1}H NMR (400 MHz, DMSO-d_6) δ 8.00–7.83 (m, 2H), 7.55 (d,

J = 8.3 Hz, 1H), 6.67–6.54 (m, 1H), 3.39–3.31 (m, 3H), 2.97 (s, 3H), 2.26 (d, J = 0.9 Hz, 3H), 1.53

(d, J = 6.8 Hz, 3H), 1.11 (t, J = 7.3 Hz, 3H); LCMS (formic B) (M+H)$^+$ = 294.1, R_t = 1.82 min

(99%); Chiral SFC: LuxCellulose-2 (4.6 × 250 mm), MeOH, flow rate: 3 mg / min, 40% modified,

100 bar, 30.2 °C, R_t = 3.73 min (97.3%), undesired enantiomer R_t = 2.81 min.

7-(Ethylsulfonyl)-1,3-dimethyl-2-oxo-2,3-dihydro-1H-benzo[d]azepine-5-carbonitrile. To

a degassed solution of **58** (100 mg, 0.28 mmol) in DMF (5 mL), stirred under N_2 at rt was added

zinc cyanide (46 mg, 0.39 mmol) followed by Pd(PPh$_3$)$_4$ (23 mg, 0.02 mmol). The reaction mixture

was stirred at 150 °C for 30 min under microwave irradiation. The reaction mixture was diluted

with H_2O (20 mL) and the separated aqueous layer was extracted with EtOAc (2 × 30 mL). The

combined organic phase was washed with H_2O followed by brine (20 mL), dried over sodium

sulfate, filtered, and then concentrated under reduced pressure. The resultant residue was purified

by column chromatography using 100-200 silica gel eluting with 15% EtOAc in hexane. The

appropriate fractions were combined and evaporated under reduced pressure to give the title

compound (50 mg, 52%). ^{1}H NMR (400 MHz, CDCl$_3$) δ 8.17 (d, J = 1.8 Hz, 1H), 8.09–7.99 (m,

1H), 7.57 (br d, J = 8.3 Hz, 1H), 7.25–7.19 (m, 1H), 3.35–3.24 (m, 4H), 3.15 (q, J = 7.3 Hz, 2H),

1.82–1.57 (m, 3H), 1.36–1.21 (m, 3H); LCMS (formic method H) (M+H)$^+$ = 305.1, R_t = 2.23 min

(87%).

(*R*)-7-(Ethylsulfonyl)-1,3-dimethyl-2-oxo-2,3-dihydro-1H-benzo[d]azepine-5-

carboxamide (27). A solution of 7-(ethylsulfonyl)-1,3-dimethyl-2-oxo-2,3-dihydro-1H-

benzo[d]azepine-5-carbonitrile (200 mg, 0.66 mmol) in sulfuric acid (0.35 mL, 6.57 mmol) was stirred at rt for 12 h. The reaction mixture was diluted with H_2O (20 mL), the aqueous layer was basified with sat. aq. sodium bicarbonate solution and extracted with EtOAc (2 × 50 mL). The separated organic phase was washed with brine (20 mL), dried over sodium sulfate filtered, and concentrated under vacuum to give *rac*-**27**. The racemic material was purified by chiral SFC: Lux Amylose-2 (250 × 30) mm, 5μ, % CO_2: 70 %, % Co solvent: 30% (100% MeOH), total flow: 100.0 g/min, stack time: 4 min, load/inj: 27 mg. The appropriate fractions were combined and evaporated under reduced pressure to give **27** (56 mg, 26%, >96% ee). ^{1}H NMR (400 MHz, DMSO-d_6) δ 8.14–7.96 (m, 1H), 7.91 (dd, J = 1.9, 8.2 Hz, 1H), 7.77–7.49 (m, 2H), 7.48–7.25 (m, 2H), 3.44–3.33 (m, 1H), 3.28–3.18 (m, 2H), 3.09 (s, 3H), 1.56 (d, J = 6.8 Hz, 3H), 1.11 (t, J = 7.3 Hz, 3H); LCMS (formic B) (M+H)$^+$ = 323.1, R_t = 1.39 min (98%); Chiral SFC: LuxCellulose-2 (4.6 × 250 mm), MeOH, flow rate: 3 g / min, 30% modified, 100 bar, 30.3 °C, R_t = 4.20 min (98.2%), undesired enantiomer R_t = 2.42 min.

7-(Ethylsulfonyl)-1,3-dimethyl-5-phenyl-1,3-dihydro-2H-benzo[d]azepin-2-one (*rac*-**28**). A mixture of **58** (100 mg, 0.25 mmol), $PhB(OH)_2$ (46 mg, 0.38 mmol), K_2CO_3 (104 mg, 0.75 mmol) and $PdCl_2$(dppf) (9 mg, 0.01 mmol) in H_2O (0.75 mL) and *i*-PrOH (3 mL) was sealed in a microwave vial. The reaction mixture was heated at 80 °C for 1 h in a microwave reactor. The reaction mixture was allowed to cool to rt, diluted with EtOAc (10 mL), filtered through celite and concentrated in vacuo. The resulting residue was purified by MDAP (high pH). The appropriate fractions were combined, and solvent evaporated in vacuo to give *rac*-**28** as a yellow solid (41 mg, 46%). ^{1}H NMR (400 MHz, CDCl$_3$) δ 7.96 (dd, J = 2.0, 8.3 Hz, 1H), 7.73–7.53 (m, 2H), 7.48–7.35 (m, 3H), 7.35–7.25 (m, 2H), 6.72 (s, 1H), 3.52 (q, J = 6.8 Hz, 1H), 3.22 (s, 3H), 3.04 (q, J =

7.3 Hz, 2H), 1.79 (d, J = 7.3 Hz, 3H), 1.23 (t, J = 7.6 Hz, 3H); LCMS (high pH) (M+H)$^+$ = 356.1, R_t = 1.07 min (99%).

7-(Ethylsulfonyl)-1,3-dimethyl-5-(pyridin-4-yl)-1,3-dihydro-2H-benzo[d]azepin-2-one (*rac*-29). A mixture of **58** (100 mg, 0.25 mmol), pyridin-4-ylboronic acid (46 mg, 0.38 mmol), K_2CO_3 (104 mg, 0.75 mmol) and PdCl$_2$(dppf) (9 mg, 0.01 mmol) in H_2O (0.75 mL) and *i*-PrOH (3 mL) was sealed in a microwave vial. The reaction mixture was heated at 80 °C for 1 h in a microwave reactor. Then the reaction was heated at 90 °C for 1 h in the microwave reactor. The reaction mixture was allowed to cool to rt, diluted with EtOAc (10 mL), filtered through celite and concentrated in vacuo. The resulting residue was purified by MDAP (formic acid). The appropriate fractions were combined, and solvent evaporated in vacuo. The resulting residue was dissolved in MeOH (10 mL) and passed through a preconditioned (10 mL, MeOH) amino propyl column (5 g). The appropriate fractions were combined, and solvent evaporated in vacuo to give *rac*-**29** as a white solid (6 mg, 7%). ^{1}H NMR (400 MHz, CDCl$_3$) δ 8.67 (d, J = 4.7 Hz, 2H), 8.00 (dd, J = 2.0, 8.3 Hz, 1H), 7.72– 7.52 (m, 2H), 7.25 (d, J = 4.7 Hz, 2H), 6.85 (s, 1H), 3.61–3.40 (m, 1H), 3.25 (s, 3H), 3.07 (q, J = 7.3 Hz, 2H), 1.79 (d, J = 6.8 Hz, 3H), 1.25 (t, J = 7.6 Hz, 3H); LCMS (formic) (M+H)$^+$ = 357.1, R_t = 0.48 min (92%).

(*R*)-7-(Ethylsulfonyl)-1,3-dimethyl-5-(1-methyl-1H-pyrazol-4-yl)-1H-benzo[d]azepin-2(3H)-one (30). To a stirred solution of **58** (370 mg, 1.03 mmol) in 1,4-dioxane (10 mL) and H_2O (1 mL), was added 1-methyl-4-(4,4,5,5-tetramethyl-1,3,2-dioxaborolan-2-yl)-1H-pyrazole (430 mg, 2.07 mmol) and potassium hydrogen phosphate (658 mg, 3.10 mmol) at rt. Following degassing for 10 min under N_2, X-Phos Pd cycle (81 mg, 0.10 mmol) was added, and the mixture was degassed for 5 min at rt. The reaction was stirred for 16 h at 90 °C in sealed tube and then cooled to rt. The mixture was diluted with H_2O (50 mL) and EtOAc (100 mL). The separated

organic phase was washed with brine (50 mL), dried with anhydrous Na_2SO_4, filtered, and concentrated under reduced pressure. The crude product was added to a silica gel (100-200 mesh) column and eluted with CH_2Cl_2 / MeOH (97/3). The appropriate fractions were combined and concentrated under reduced pressure to give *rac*-**30** (340 mg, 92%). The racemic material was dissolved in MeOH and purified by chiral SFC: Chiralcel OJ-H (250 × 21) mm,5μ, % CO_2: 70.0%, % Co-solvent: 30.0% (100% MeOH), total flow: 60.0 g / min, back pressure: 100.0 bar, UV: 215 nm, stack time: 2.7 min, load / inj: 3.0 mg. The appropriate fractions were combined, evaporated, and lyophilized to give **30** (127 mg, >98% ee). ^{1}H NMR (400 MHz, DMSO-d_6) δ 7.94 (dd, J = 1.9, 8.2 Hz, 1H), 7.85–7.70 (m, 2H), 7.68–7.49 (m, 2H), 7.01 (s, 1H), 3.86 (s, 3H), 3.47–3.31 (m, 1H), 3.28–3.16 (m, 2H), 3.05 (s, 3H), 1.58 (d, J = 6.8 Hz, 3H), 1.09 (t, J = 7.3 Hz, 3H); LCMS (formic B) (M+H)$^+$ = 360.1, R_t = 1.67 min (99%); Chiral SFC: Chiralcel OJ-H (4.6 × 250 mm), MeOH, flow rate: 3 g / min, 30% modified, 100 bar, 29.5 °C, R_t = 2.84 min (99.1%), undesired enantiomer R_t = 2.07 min.

5-Bromo-7-ethoxy-1,3-dimethyl-1,3-dihydro-2H-benzo[d]azepin-2-one (59). Under N_2, *rac*-**15** (310 mg, 1.34 mmol) was dissolved in MeCN (13 mL) and treated with NBS (262 mg, 1.47 mmol). The reaction was stirred at rt for 5 h and then the solvent was removed under reduced pressure. The residue was loaded onto a 80 g silica column and eluted with EtOAc / cyclohexane (0-20%). Combination and evaporation of the desired fractions gave **59** as a colorless oil (370 mg, 89%). ^{1}H NMR (400 MHz, CDCl$_3$) δ 7.26–7.18 (m, 2H), 7.02 (dd, J = 2.9, 8.8 Hz, 1H), 6.84 (s, 1H), 4.09 (q, J = 6.8 Hz, 2H), 3.34 (d, J = 6.8 Hz, 1H), 3.17–3.04 (m, 3H), 1.72–1.60 (m, 3H), 1.45 (t, J = 7.1 Hz, 3H); LCMS (formic) (M+H)$^+$ = 310.0, 312.0, R_t = 1.21 min (92%).

(*R*)-7-Ethoxy-1,3-dimethyl-5-(1-methyl-1H-pyrazol-4-yl)-1,3-dihydro-2H-benzo[d]azepin-2-one (31). 59 (50 mg, 0.16 mmol), 1-methyl-4-(4,4,5,5-tetramethyl-1,3,2-dioxaborolan-2-yl)-1H-

pyrazole (50 mg, 0.24 mmol), and K_2CO_3 (56 mg, 0.40 mmol) were added to a microwave vial. *i*-PrOH (0.6 mL) and H_2O (0.2 mL) were added to the vial, which was purged with N_2 for 5 mins prior to the addition of $Pd(PPh_3)_4$ (6 mg, 0.005 mmol). After a further 5 min purge with N_2, the vial was capped and heated in the microwave at 100 °C for 1 h. The solvent was removed under a stream of N_2 and the residue dissolved in 1:1 MeOH:DMSO (3 mL) and passed through a syringe filter prior to purification by MDAP (high pH). The appropriate fractions were combined, and the solvent removed under a stream of N_2 to give *rac*-**31** as a white solid (31 mg, 63%). The solid was dissolved in EtOH (1.5 mL) and purified by chiral HPLC: Chiralpak AD-H (250 mm × 25 mm, 5 μm), 10% EtOH in heptane, 30 mL / min, wavelength: 215 nm. The appropriate fractions were combined and evaporated under reduced pressure to give **31** as a colorless glass (8 mg, >98% ee).
^{1}H NMR (400 MHz, MeOH-d_4) δ 7.67 (s, 1H), 7.58 (s, 1H), 7.28 (d, $J = 8.8$ Hz, 1H), 7.05 (dd, $J = 2.7, 8.6$ Hz, 1H), 6.86 (d, $J = 2.4$ Hz, 1H), 6.79 (s, 1H), 4.00–3.91 (m, 5H), 3.36–3.30 (m, 1H), 3.10 (s, 3H), 1.61 (d, $J = 6.8$ Hz, 3H), 1.42–1.28 (m, 3H); LCMS (high pH) $(M+H)^+ = 312.3$, $R_t = 0.97$ min (99%); chiral HPLC: Chiralpak AD-H (250 mm × 4.6 mm), 10% EtOH in heptane, 1 mL / min, wavelength: 215 nm, $R_t = 17.98$ min (99.4%), undesired enantiomer $R_t = 15.73$ min.

(*R*)-7-Ethoxy-1,3-dimethyl-5-(1H-pyrazol-4-yl)-1,3-dihydro-2H-benzo[d]azepin-2-one (32). 59 (210 mg, 0.68 mmol), 4-(4,4,5,5-tetramethyl-1,3,2-dioxaborolan-2-yl)-1H-pyrazole (197 mg, 1.02 mmol), and K_2CO_3 (234 mg, 1.69 mmol) were added to a microwave vial. *i*-PrOH (2.40 mL) and H_2O (0.80 mL) were added to the vial, which was placed under an atmosphere of N_2 by evacuation-refill prior to the addition of $Pd(PPh_3)_4$ (23 mg, 0.02 mmol). After a replenishing the atmosphere of N_2, the vial was capped and heated in the microwave at 100 °C for 1 h. Further (1H-pyrazol-4-yl)boronic acid (91 mg, 0.81 mmol) and $Pd(PPh_3)_4$ (23 mg, 0.02 mmol) were added, the N_2 atmosphere replenished by evacuation-refill, and the reaction mixture heated in the

microwave at 100 °C for 1 h. Again further (1H-pyrazol-4-yl)boronic acid (91 mg, 0.81 mmol) and Pd(PPh$_3$)$_4$ (23 mg, 0.02 mmol) were added, the N$_2$ atmosphere replenished by evacuation-refill, and the reaction mixture heated in the microwave at 100 °C for 1 h. The solvent was removed under reduced pressure, and the residue extracted with EtOAc (50 mL) and filtered through celite, rinsing with further EtOAc. Following evaporation, the residue was dissolved in 1:1 MeOH:DMSO (6 mL) and purified by MDAP (high pH). The appropriate fractions were combined and the solvent evaporated in vacuo to give *rac*-**32** as a white solid (75 mg, 38%). The solid was dissolved in 4:1 EtOH/CH$_2$Cl$_2$ (2.5 mL) and purified by chiral HPLC: Chiralpak IA (250 mm × 30 mm, 5 μm), 15% EtOH in heptane (+0.2% isopropylamine), 30 mL / min, wavelength: 215 nm. The appropriate fractions were combined and evaporated under reduced pressure to give **32** as a white solid (29 mg, >99% ee). ^{1}H NMR (400 MHz, MeOH-d_4) δ 7.71 (br s, 2H), 7.29 (d, *J* = 8.8 Hz, 1H), 7.06 (dd, *J* = 2.9, 8.8 Hz, 1H), 6.85 (d, *J* = 2.9 Hz, 1H), 6.83 (s, 1H), 3.97 (dq, *J* = 1.2, 6.9 Hz, 2H), 3.45–3.36 (m, 1H), 3.12 (s, 3H), 1.62 (d, *J* = 7.3 Hz, 3H), 1.35 (t, *J* = 7.1 Hz, 3H); LCMS (high pH) (M+H)$^+$ = 298.2, R$_t$ = 0.87 min (100%); chiral HPLC: Chiralpak IA (250 mm × 4.6 mm), 15% EtOH in heptane (+0.2% isopropylamine), 1 mL / min, wavelength: 215 nm, R$_t$ = 12.78 min (99.4%), undesired enantiomer R$_t$ = 9.31 min.

7-Ethoxy-1,3-dimethyl-5-(1H-pyrazol-5-yl)-1,3-dihydro-2H-benzo[d]azepin-2-one (*rac*-33). **59** (50 mg, 0.16 mmol), (1H-pyrazol-3-yl)boronic acid (54 mg, 0.48 mmol), and K$_2$CO$_3$ (56 mg, 0.40 mmol) were added to a microwave vial. *i*-PrOH (0.60 mL) and H$_2$O (0.20 mL) were added to the vial, which was purged with N$_2$ for 5 min prior to the addition of Pd(PPh$_3$)$_4$ (6 mg, 0.005 mmol). After a further 5 min purge with N$_2$, the vial was capped and heated in the microwave at 100 °C for 1 h. The solvent was removed under a stream of N$_2$, the residue dissolved in 1:1 MeOH:DMSO (3 mL) and passed through a syringe filter prior to MDAP (high pH) purification.

The appropriate fractions were combined, and the solvent was removed under a stream of N_2 to give *rac*-**33** as a colorless glass (17 mg, 48%). ^{1}H NMR (400 MHz, MeOH-d_4) δ 7.68 (br s, 1H), 7.29 (d, *J* = 8.8 Hz, 1H), 7.06 (dd, *J* = 2.7, 8.6 Hz, 1H), 6.98 (s, 1H), 6.78 (br s, 1H), 6.39 (d, *J* = 2.4 Hz, 1H), 3.95 (q, *J* = 7.2 Hz, 2H), 3.46–3.35 (m, 1H), 3.15 (s, 3H), 1.63 (d, *J* = 6.8 Hz, 3H), 1.38–1.29 (m, 3H); LCMS (high pH) (M+H)$^+$ = 298.2, R$_t$ = 0.93 min (100%).

7-Ethoxy-1,3-dimethyl-5-(4,4,5,5-tetramethyl-1,3,2-dioxaborolan-2-yl)-1,3-dihydro-2H-benzo[d]azepin-2-one. **59** (883 mg, 2.85 mmol), 4,4,4',4',5,5,5',5'-octamethyl-2,2'-bi(1,3,2-dioxaborolane) (1.08 g, 4.27 mmol), Pd(OAc)$_2$ (32 mg, 0.14 mmol), *tert*-butyldiphenylphosphine (69 mg, 0.29 mmol) and KOAc (1.12 g, 11.39 mmol) were added to a microwave vial and the vial sealed. The reagents were placed under an atmosphere of N_2 by evacuation-refill and then dissolved in 1,4-dioxane (15 mL) before the atmosphere of N_2 was again replenished. The reaction was stirred at 70 °C for 90 min and then reheated to 70 °C for a further 1 h. The solvent was removed under reduced pressure and the residue redissolved in EtOAc (100 mL). The solution was washed with saturated aqueous sodium hydrogen carbonate solution (100 mL), brine (50 mL) and the combined aqueous layer extracted with further EtOAc (50 mL). The combined organic layer was passed through celite and the solvent removed under reduced pressure. The residue was loaded in CH_2Cl_2 and purified by gradient elution column chromatography using a 120 g silica cartridge eluting with EtOAc in cyclohexane (0% to 20%). The appropriate fractions were combined and evaporated in vacuo to give the title compound as an off-white solid (612 mg, 60%). ^{1}H NMR (400 MHz, MeOH-d_4) δ 7.18 (d, *J* = 8.8 Hz, 1H), 7.16 (d, *J* = 2.4 Hz, 1H), 7.08 (s, 1H), 6.96 (dd, *J* = 2.7, 8.6 Hz, 1H), 4.13–4.02 (m, 2H), 3.20–3.10 (m, 4H), 1.57 (d, *J* = 6.8 Hz, 3H), 1.44–1.34 (m, 15H); LCMS (formic) (M+H)$^+$ = 358.2, R$_t$ = 1.32 min (96%).

(*R*)-7-Ethoxy-5-(1H-imidazol-4-yl)-1,3-dimethyl-1,3-dihydro-2H-benzo[d]azepin-2-one

(34). 7-Ethoxy-1,3-dimethyl-5-(4,4,5,5-tetramethyl-1,3,2-dioxaborolan-2-yl)-1,3-dihydro-2H-benzo[d]azepin-2-one (306 mg, 0.86 mmol), 4-bromo-1H-imidazole (84 mg, 0.57 mmol), tripotassium phosphate (242 mg, 1.14 mmol), XPhos G2 precat (31 mg, 0.04 mmol) and XPhos (19 mg, 0.04 mmol) were added to a microwave vial. The vial was capped and placed under an atmosphere of N_2 by evacuation-refill. 1,4-Dioxane (0.40 mL) and H_2O (0.10 mL) were then added to the vial. After replenishing the atmosphere of N_2, the vial was heated to 100 °C in the microwave for 1 h. Further 4-bromo-1H-imidazole (84 mg, 0.57 mmol), XPhos G2 precat (31 mg, 0.04 mmol) and XPhos (19 mg, 0.04 mmol) were added, the atmosphere of N_2 replenished, and the vial heated in the microwave at 100 °C for a further 1 h. Again, 4-bromo-1H-imidazole (84 mg, 0.57 mmol), XPhos G2 precat (31 mg, 0.04 mmol) and XPhos (19 mg, 0.04 mmol) were added, the atmosphere of N_2 replenished, and the vial heated in the microwave at 100 °C for a further 1 h. Yet again, 4-bromo-1H-imidazole (84 mg, 0.57 mmol), XPhos G2 precat (31 mg, 0.04 mmol) and XPhos (19 mg, 0.04 mmol) were added, the atmosphere of N_2 replenished, and the vial heated in the microwave at 100 °C for a further 1 h. The solvent was removed under a stream of N_2, the resultant residue was dissolved in EtOAc and filtered through celite, washing with further EtOAc. The solvent was removed in vacuo, the sample redissolved in DMSO and purified by MDAP (high pH). Evaporation of solvent under reduced pressure gave *rac*-**34** as a white solid (12 mg, 7%). The solid was dissolved in EtOH (1 mL) and purified by chiral HPLC: Chiralpak AD-H (250 mm × 30 mm, 5 μm), 15% EtOH in heptane, 30 mL / min, wavelength: 215 nm. The appropriate fractions were combined and evaporated under reduced pressure to give **34** as a colorless glass (5 mg, >98% ee). ^{1}H NMR (400 MHz, MeOH-d_4) δ 7.75 (d, J = 1.0 Hz, 1H), 7.29 (d, J = 8.8 Hz, 1H), 7.11–7.02 (m, 2H), 6.99 (br s, 1H), 6.91 (br s, 1H), 3.99 (q, J = 6.8 Hz, 2H), 3.44–3.35 (m,

1H), 3.14 (s, 3H), 1.62 (d, J = 6.8 Hz, 3H), 1.36 (t, J = 6.8 Hz, 3H); LCMS (high pH) (M+H)$^+$ = 298.2, R_t = 0.82 min (100%); chiral HPLC: Chiralpak AD-H (250 mm × 4.6 mm), 15% EtOH in heptane, 1 mL / min, wavelength: 215 nm, R_t = 11.09 min (99.4%), undesired enantiomer R_t = 7.91 min.

(*R*)-7-Ethoxy-1,3-dimethyl-5-(2-methyl-1H-imidazol-5-yl)-1,3-dihydro-2H-benzo[d]azepin-2-one (35).   7-Ethoxy-1,3-dimethyl-5-(4,4,5,5-tetramethyl-1,3,2-dioxaborolan-2-yl)-1,3-dihydro-2H-benzo[d]azepin-2-one (313 mg, 0.88 mmol), 4-bromo-2-methyl-1H-imidazole (94 mg, 0.58 mmol), tripotassium phosphate (248 mg, 1.17 mmol), XPhos G2 precat (32 mg, 0.04 mmol) and XPhos (19 mg, 0.04 mmol) were added to a microwave vial. The vial was capped and placed under an atmosphere of N_2 by evacuation-refill. 1,4-Dioxane (0.40 mL) and H_2O (0.10 mL) were then added to the vial. After replenishing the atmosphere of N_2, the vial was heated to 100 °C in the microwave for 1 h. Further 4-bromo-2-methyl-1H-imidazole (94 mg, 0.58 mmol), XPhos (19 mg, 0.04 mmol) and XPhos G2 precat (32 mg, 0.04 mmol) were added, the atmosphere of N_2 replenished, and the vial heated in the microwave at 100 °C for a further 1 h. Again, further 4-bromo-2-methyl-1H-imidazole (94 mg, 0.58 mmol), XPhos (19 mg, 0.04 mmol) and XPhos G2 precat (32 mg, 0.04 mmol) were added, the atmosphere of N_2 replenished, and the vial heated in the microwave at 100 °C for a further 1 h. The solvent was removed under a stream of N_2, the residue was dissolved in EtOAc and filtered through celite, washing with further EtOAc. The solvent was removed in vacuo, the sample redissolved in 1:1 MeOH:DMSO (3 mL) and then purified by MDAP (high pH). Appropriate fractions were combined and evaporated under a stream of N_2 to give *rac*-**35** (70 mg, 39%). The residue was dissolved in 1:1 EtOH/heptane (1.5 mL) and purified by chiral HPLC: Chiralpak AD-H (250 mm × 30 mm, 5 μm), 10% EtOH in heptane (+0.2% isopropylamine), 30 mL / min, wavelength: 215 nm. The appropriate fractions

were combined and evaporated under reduced pressure to give **35** as an off-white solid (29 mg,

99% ee). ^{1}H NMR (400 MHz, MeOH-d_4) δ 7.28 (d, J = 8.3 Hz, 1H), 7.06 (dd, J = 2.4, 8.8 Hz,

1H), 6.97–6.91 (m, 2H), 6.87 (s, 1H), 3.99 (q, J = 7.2 Hz, 2H), 3.45–3.35 (m, 1H), 3.12 (s, 3H),

2.41 (s, 3H), 1.61 (d, J = 6.8 Hz, 3H), 1.39–1.33 (m, 3H); LCMS (high pH) (M+H)$^+$ = 312.2, R_t =

0.84 min (100%); chiral HPLC: Chiralpak AD-H (250 mm × 4.6 mm), 10% EtOH in heptane

(+0.2% isopropylamine), 1 mL / min, wavelength: 215 nm, R_t = 7.58 min (99.5%), undesired

enantiomer R_t = 5.95 min.

(*R*)-7-Ethoxy-1,3-dimethyl-5-(1-methyl-1H-imidazol-4-yl)-1,3-dihydro-2H-benzo[d]azepin-2-one (36). 7-Ethoxy-1,3-dimethyl-5-(4,4,5,5-tetramethyl-1,3,2-dioxaborolan-2-yl)-1,3-dihydro-2H-benzo[d]azepin-2-one (399 mg, 1.12 mmol) was dissolved in 1,4-dioxane (4

mL) and transferred to a microwave vial, to which was added 4-bromo-1-methyl-1H-imidazole

(150 mg, 0.93 mmol), K_2CO_3 (322 mg, 2.34 mmol) and Pd(PPh$_3$)$_4$ (32 mg, 0.03 mmol). The vial

was capped and placed under an atmosphere of N$_2$ by evacuation-refill and then heated in the

microwave at 100 °C for 1 h. Further 4-bromo-1-methyl-1H-imidazole (150 mg, 0.93 mmol) and

Pd(PPh$_3$)$_4$ (1077 mg, 0.93 mmol) were added to the reaction mixture, the vial resealed and the

atmosphere of N$_2$ replenished by evacuation-refill. The reaction mixture was returned to heating

in the microwave at 100 °C for 1 h. Further Pd(PPh$_3$)$_4$ (1077 mg, 0.93 mmol) was added to the

reaction mixture, the vial resealed and the atmosphere of N$_2$ replenished by evacuation-refill. The

reaction mixture was returned to heating in the microwave at 100 °C for 1 h. Again, further 4-bromo-1-methyl-1H-imidazole (80 mg, 0.50 mmol) and Pd(PPh$_3$)$_4$ (1077 mg, 0.93 mmol) were

added to the reaction mixture, the vial resealed and the atmosphere of N$_2$ replenished by

evacuation-refill. The reaction mixture was returned to heating in the microwave at 100 °C for 1

h. The solvent was removed under reduced pressure and the residue redissolved in EtOAc (50

mL). The solution was filtered through celite and rinsed with further EtOAc (100 mL). The solvent was removed from the filtrate under reduced pressure, the residue dissolved in 1:1 MeOH:DMSO (9 mL) and then purified by MDAP (high pH). The appropriate fractions were combined and the solvent evaporated under reduced pressure to give *rac-*36 as a pale pink solid (118 mg, 41%). The solid was dissolved in EtOH (3 mL) and purified by chiral HPLC: Chiralpak IC (250 mm × 30 mm, 5 µm), 15% EtOH in heptane (+0.2% isopropylamine), 30 mL / min, wavelength: 215 nm. The appropriate fractions were combined and evaporated under reduced pressure to give **36** as a white solid (48 mg, 96% ee). ^{1}H NMR (400 MHz, MeOH-d_4) δ 7.67 (s, 1H), 7.28 (d, J = 8.8 Hz, 1H), 7.09–6.95 (m, 4H), 4.00 (dq, J = 1.0, 7.0 Hz, 2H), 3.75 (s, 3H), 3.46–3.35 (m, 1H), 3.12 (s, 3H), 1.61 (d, J = 7.3 Hz, 3H), 1.36 (t, J = 6.8 Hz, 3H); LCMS (high pH) (M+H)$^+$ = 312.1, R_t = 0.90 min (100%); chiral HPLC: Chiralpak IC (250 mm × 4.6 mm), 15% EtOH in heptane (+0.2% isopropylamine), 1 mL / min, wavelength: 215 nm, R_t = 9.10 min (98%), undesired enantiomer R_t = 8.12 min.

7-Ethoxy-5-(1H-imidazol-1-yl)-1,3-dimethyl-1,3-dihydro-2H-benzo[d]azepin-2-one (*rac-*37). Imidazole (23 mg, 0.34 mmol) was added to a dried vial, to which was added 1,4-dioxane (1.5 mL) and the flask purged by sequential evacuation-refill cycles and placed under an atmosphere of N$_2$. NaOt-Bu (53 mg, 0.55 mmol) and **59** (100 mg, 0.32 mmol) were added, and the evacuation-refill cycle again repeated. The reaction mixture was stirred for 5 min, after which DavePhos (1 mg, 0.003 mmol) and Pd$_2$dba$_3$ (1 mg, 0.001 mmol) were added. On addition of the final reagents, the evacuation-refill cycle was repeated, and the reaction vessel heated to 100 °C. The reaction mixture was stirred at this temperature for 3 h. 1H-imidazole (110 mg, 1.61 mmol), Pd$_2$dba$_3$ (3 mg, 0.003 mmol) and DavePhos (3 mg, 0.006 mmol) were added, and the atmosphere of N$_2$ replenished by evacuation-refill. The vial was heated in the microwave at 100 °C for 30 min.

Further Pd_2dba_3 (15 mg, 0.02 mmol) and DavePhos (13 mg, 0.03 mmol) were added, and the atmosphere of N_2 replenished by evacuation-refill. The vial was heated in the microwave at 140 °C for 1 h. The solvent was removed under reduced pressure, redissolved in 1:1 MeOH:DMSO (3 mL) and purified by MDAP (TFA). The appropriate fractions were combined, and solvent removed under a stream of N_2. The residue was redissolved in 1:1 MeOH:DMSO (0.9 mL) and repurified by MDAP (high pH). The appropriate fractions were combined, and the solvent removed under a stream of N_2 to give **37** as a white solid (0.8 mg, 1%). ^{1}H NMR (400 MHz, MeOH-d_4) δ 8.57 (s, 1H), 8.21–8.10 (m, 1H), 7.53 (t, J = 1.5 Hz, 1H), 7.28 (d, J = 8.8 Hz, 1H), 7.23–7.14 (m, 1H), 7.11–6.92 (m, 2H), 4.09 (q, J = 6.8 Hz, 2H), 3.59 (d, J = 6.8 Hz, 1H), 2.81 (s, 3H), 1.67 (d, J = 6.8 Hz, 3H), 1.41 (t, J = 7.1 Hz, 3H); LCMS (high pH) $(M+H)^+$ = 298.1, R_t = 0.98 min (94%).

(*R*)-7-((*S*)-1,2-Dihydroxyethyl)-1,3-dimethyl-1H-benzo[d]azepin-2(3H)-one (60). AD-mix-α (2.70 g, 2.34 mmol) was added to a stirred solution of **55** (500 mg, 2.34 mmol) in *t*-BuOH (6 mL) and H_2O (6 mL). The resulting mixture was stirred at rt for 16 hours under N_2. The reaction was quenched by addition of sodium metabisulfite (3 g) and the mixture left stirring at rt for 1.5 h. The mixture was filtered, and the filtrate diluted with H_2O (10 mL) and EtOAc (10 mL). The organic layer was collected and the aqueous extracted with EtOAc (2 × 10 mL). The organic layers were combined, passed through a hydrophobic frit and concentrated in vacuo to give a pale yellow oil. The oil was purified by column chromatography by loading onto an 80 g silica cartridge (with CH_2Cl_2) and eluting with 10–100% EtOAc in cyclohexane. The appropriate fractions were combined and concentrated in vacuo to give **60** as a colorless oil (353 mg, 61%). ^{1}H NMR (400 MHz, MeOH-d_4) δ 7.44 (d, J = 8.6 Hz, 1H), 7.35 (s, 1H), 7.29 (d, J = 8.1 Hz, 1H), 6.55 (br d, J =

9.1 Hz, 1H), 6.45 (br d, J = 9.1 Hz, 1H), 4.77–4.70 (m, 1H), 3.65–3.59 (m, 2H), 3.30–3.21 (m,

1H), 3.11 (s, 3H), 1.59 (br s, 3H); LCMS (high pH) $(M+H)^+$ = 248.1, R_t = 0.61 min (100%).

(R)-5-Bromo-7-((S)-1,2-dihydroxyethyl)-1,3-dimethyl-1H-benzo[d]azepin-2(3H)-one.   A

solution of phenyltrimethylaminotribromide (537 mg, 1.43 mmol) in MeCN (2.5 mL) was added

to a solution of **60** (353 mg, 1.43 mmol) in MeCN (5 mL). The reaction was left stirring at rt under

N_2, for 1 h. The resulting yellow solution was diluted with H_2O (10 mL) and EtOAc (10 mL). The

organic layer was separated and the aqueous phase washed with EtOAc (2 × 10 mL). The combined

organic layers were passed through a hydrophobic frit and concentrated in vacuo to give an orange

oil. The oil was dissolved in CH_2Cl_2 and loaded onto a silica cartridge (40 g) then purified by

column chromatography, eluting with 10-100% EtOAc in cyclohexane. The appropriate fractions

were combined and concentrated in vacuo to give the title compound as a white solid (312 mg,

67%). ^{1}H NMR (400 MHz, MeOH-d_4) δ 7.76 (d, J = 1.5 Hz, 1H), 7.53 (dd, J = 1.8, 8.3 Hz, 1H),

7.31 (d, J = 8.1 Hz, 1H), 7.04 (s, 1H), 4.78–4.63 (m, 1H), 3.62 (d, J = 6.0 Hz, 2H), 3.40 (d, J = 7.1

Hz, 1H), 3.05 (s, 3H), 1.61 (d, J = 7.1 Hz, 3H); LCMS (high pH) $(M+H)^+$ = poor ionization, R_t =

0.74 min (100%).

(R)-7-((S)-1,2-Dihydroxyethyl)-1,3-dimethyl-5-(1H-pyrazol-4-yl)-1H-benzo[d]azepin-

2(3H)-one (38).   (R)-5-Bromo-7-((S)-1,2-dihydroxyethyl)-1,3-dimethyl-1H-benzo[d]azepin-

2(3H)-one (50 mg, 0.15 mmol), (1H-pyrazol-4-yl)boronic acid (52 mg, 0.46 mmol), Pd(PPh$_3$)$_4$ (9

mg, 0.008 mmol) and K_2CO_3 (53 mg, 0.38 mmol) in H_2O (0.5 mL) and i-PrOH (1.5 mL) were

added to a microwave vial. The vial was sealed, purged with N_2 and heated in a microwave at 100

°C for 3 h. The vial was resealed and the reaction mixture was heated in the microwave at 100 °C

for a further 2 h. The reaction was concentrated in vacuo to give a white solid. The solid was

dissolved in 1:1 MeOH:DMSO (1.8 mL) and purified by MDAP (high pH). The appropriate

fractions were combined and evaporated to give **38** as a white solid (3.4 mg, 7%). ^{1}H NMR (400 MHz, MeOH-d_4) δ 7.72 (s, 2H), 7.51 (dd, J = 1.7, 8.1 Hz, 1H), 7.46–7.31 (m, 2H), 6.87 (s, 1H), 4.80–4.56 (m, 1H), 3.60 (d, J = 5.9 Hz, 2H), 3.46 (q, J = 6.8 Hz, 1H), 3.11 (s, 3H), 1.65 (d, J = 7.3 Hz, 3H); LCMS (high pH) (M+H)$^+$ = 314.1, R_t = 0.59 min (100%).

(*R*)-7-((*S*)-1,2-Dihydroxyethyl)-1,3-dimethyl-5-(1-methyl-1H-pyrazol-4-yl)-1H-benzo[d]azepin-2(3H)-one (40). 1-Methyl-4-(4,4,5,5-tetramethyl-1,3,2-dioxaborolan-2-yl)-1H-pyrazole (110 mg, 0.53 mmol), (*R*)-5-bromo-7-((*S*)-1,2-dihydroxyethyl)-1,3-dimethyl-1H-benzo[d]azepin-2(3H)-one (115 mg, 0.35 mmol), tripotassium phosphate (225 mg, 1.06 mmol) and 2'-(dimethylamino)-2-biphenylyl-palladium(II) chloride dinorbornylphosphine complex (20 mg, 0.04 mmol) were added to a microwave vial. EtOH (3 mL) and H_2O (1 mL) were then added and the reaction was heated to 130 °C for 30 min in a microwave. The reaction was filtered through cotton wool and then concentrated under reduced pressure. The residue was dissolved in 1:1 MeOH:DMSO (1 mL) and purified by MDAP (high pH). The appropriate fractions were combined, and the solvent was evaporated in vacuo to give **40** as a yellow solid (51 mg, 44%). ^{1}H NMR (400 MHz, DMSO-d_6) δ 7.73 (s, 1H), 7.56 (s, 1H), 7.42 (dd, J = 1.5, 8.1 Hz, 1H), 7.35 (d, J = 1.5 Hz, 1H), 7.26 (d, J = 8.1 Hz, 1H), 6.87 (s, 1H), 5.18 (d, J = 4.0 Hz, 1H), 4.65 (br t, J = 5.5 Hz, 1H), 4.58–4.42 (m, 1H), 3.46–3.35 (m, 2H), 3.35–3.25 (m, 4H), 3.01 (s, 3H), 1.52 (d, J = 7.1 Hz, 3H); LCMS (high pH) (M+H)$^+$ = 328.1, R_t = 0.65 min (100%).

(*R*)-7-((*R*)-1,2-Dihydroxyethyl)-1,3-dimethyl-1H-benzo[d]azepin-2(3H)-one (61). AD-mix-β (13.84 g, 12.10 mmol) was added to a stirred solution of **55** (2.58 g, 12.10 mmol) in t-butanol (30 mL) and H_2O (30 mL). The resulting reaction mixture was stirred at rt for 18 h under N_2. The reaction was quenched by addition of sodium metabisulfite (14.1 g), and the mixture left stirring at rt for 4.5 h under N_2 to give a dark green solution. The mixture was filtered, and the filtrate was

diluted with H_2O (50 mL) and EtOAc (50 mL). The organic layer was collected, and the aqueous layer extracted with EtOAc (2 × 50 mL). The organic layers were combined, passed through a hydrophobic frit and then concentrated in vacuo to give an oil. The oil was purified by column chromatography by loading onto a 120 g silica cartridge with CH_2Cl_2 and eluting with EtOAc in cyclohexane (10-100%). The appropriate fractions were combined and concentrated in vacuo to give **61** as a white solid (2.27 g, 76%). ^{1}H NMR (400 MHz, MeOH-d_4) δ 7.44 (dd, J = 1.5, 7.8 Hz, 1H), 7.36 (d, J = 2.0 Hz, 1H), 7.31 (d, J = 8.3 Hz, 1H), 6.58 (br d, J = 9.3 Hz, 1H), 6.48 (br d, J = 9.3 Hz, 1H), 4.81–4.70 (m, 1H), 3.71–3.55 (m, 2H), 3.30–3.21 (m, 1H), 3.11 (s, 3H), 1.62 (br s, 3H); LCMS (high pH) $(M+H)^+$ = 248.2, R_t = 0.61 min (99%).

(*R*)-5-Bromo-7-((*R*)-1,2-dihydroxyethyl)-1,3-dimethyl-1H-benzo[d]azepin-2(3H)-one. A solution of phenyltrimethylaminotribromide (3.45 g, 9.18 mmol) in MeCN (15 mL) was added to a solution of **61** (2.27 g, 9.18 mmol) in MeCN (20 mL) at rt under N_2. The reaction was stirred at rt for 1 h. The resulting orange solution was diluted with H_2O (30 mL) and EtOAc (30 mL). The organic layer was separated and the aqueous washed with EtOAc (2 × 30 mL). The combined organic layers were passed through a hydrophobic frit and concentrated in vacuo to give the title compound as an orange oil (1.60 g, 53%). ^{1}H NMR (400 MHz, MeOH-d_4) δ 7.80 (s, 1H), 7.57–7.43 (m, 1H), 7.30 (br d, J = 8.1 Hz, 1H), 7.04 (s, 1H), 4.79–4.68 (m, 1H), 3.67–3.57 (m, 2H), 3.45–3.35 (m, 1H), 3.04 (s, 3H), 1.61 (d, J = 6.5 Hz, 3H); LCMS (high pH) $(M+H)^+$ = 326.0, 328.0, R_t = 0.74 min (100%).

(*R*)-7-((*R*)-1,2-Dihydroxyethyl)-1,3-dimethyl-5-(1H-pyrazol-4-yl)-1H-benzo[d]azepin-2(3H)-one (39). (*R*)-5-Bromo-7-((*R*)-1,2-dihydroxyethyl)-1,3-dimethyl-1H-benzo[d]azepin-2(3H)-one (100 mg, 0.31 mmol), (1H-pyrazol-4-yl)boronic acid (34 mg, 0.31 mmol) and K_2CO_3 (106 mg, 0.77 mmol) were added to a microwave vial, which was then purged with N_2 × 3. *i*-PrOH

(1.8 mL) and H_2O (0.6 mL) were added to the vial and the reaction mixture heated in a microwave at 100 °C for 1.5 h. The reaction mixture was resealed, purged with $N_2 \times 3$, and heated in a microwave at 100 °C for a further 1.5 h. Additional (1H-pyrazol-4-yl)boronic acid (34 mg, 0.31 mmol) was added and the vial re-sealed and purged with $N_2 \times 3$. The reaction mixture was heated in a microwave for a further 1.5 h. Again, additional (1H-pyrazol-4-yl)boronic acid (34 mg, 0.31 mmol) was added and the vial re-sealed and purged with $N_2 \times 3$. The reaction mixture was heated in a microwave for a further 1.5 hours. The reaction mixture was transferred to a vial, washing with EtOAc then dried under a stream of N_2. The residue was dissolved in 1:1 MeOH:DMSO (2 mL) and purified by MDAP (high pH). The appropriate fractions were combined, and the solvent removed under a stream of N_2 to give a white solid. The solid was repurified by MDAP (high pH), the appropriate fractions were combined, and the solvent removed under a stream of N_2 to give an off-white solid. The solid was again repurified by MDAP (high pH), the appropriate fractions were combined, and the solvent removed under a stream of N_2 to give **39** as a white solid (9 mg, 9%). ^{1}H NMR (400 MHz, MeOH-d_4) δ 7.71 (s, 2H), 7.51–7.40 (m, 2H), 7.36 (d, J = 8.1 Hz, 1H), 6.86 (s, 1H), 4.71–4.61 (m, 1H), 3.61–3.53 (m, 2H), 3.44 (q, J = 7.1 Hz, 1H), 3.09 (s, 3H), 1.63 (d, J = 7.1 Hz, 3H); LCMS (high pH) $(M+H)^+$ = 314.1, R_t = 0.58 min (99%).

(R)-7-((R)-1,2-Dihydroxyethyl)-1,3-dimethyl-5-(1-methyl-1H-pyrazol-4-yl)-1H-benzo[d]azepin-2(3H)-one (41). A mixture of (R)-5-bromo-7-((R)-1,2-dihydroxyethyl)-1,3-dimethyl-1H-benzo[d]azepin-2(3H)-one (700 mg, 2.15 mmol), 1-methyl-4-(4,4,5,5-tetramethyl-1,3,2- dioxaborolan-2-yl)-1H-pyrazole (670 mg, 3.22 mmol), tert-butyldiphenylphosphane (26 mg, 0.11 mmol), tripotassium phosphate (1.37 g, 6.44 mmol) and $Pd(OAc)_2$ (12 mg, 0.05 mmol) in H_2O (3 mL) and i-PrOH (9 mL) was sealed in a microwave vial. The mixture was evacuated and backfilled with N_2 (× 3) then heated at 100 °C in a microwave reactor for 1 h. The reaction

mixture was allowed to cool to rt then filtered through Celite, washing with EtOAc. The resulting orange solution was concentrated in vacuo to give an oil. The compound was loaded onto a silica cartridge (80 g) by dissolving in CH_2Cl_2, then purified by chromatography eluting with MeOH in EtOAc (0-15%). The appropriate fractions were combined, and solvent evaporated in vacuo to give an off white solid, which was dissolved in MeOH then evaporated under a stream of N_2 to give a yellow oil. The residue was dissolved in 1:1 MeOH:DMSO and re-purified by MDAP (high pH). The resulting fractions were combined and concentrated in vacuo to give a white foam. The foam was dried under a stream of N_2 and then triturated with Et_2O. The suspension was dried under a stream of N_2 to give **41** as a white solid (376 mg, 54%). ^{1}H NMR (600 MHz, DMSO-d_6) δ 7.74 (s, 1H), 7.56 (s, 1H), 7.42 (dd, J = 1.5, 8.1 Hz, 1H), 7.36 (d, J = 1.5 Hz, 1H), 7.26 (d, J = 8.4 Hz, 1H), 6.88 (s, 1H), 5.18 (d, J = 4.0 Hz, 1H), 4.66 (t, J = 5.9 Hz, 1H), 4.58–4.46 (m, 1H), 3.84 (s, 3H), 3.46–3.36 (m, 2H), 3.34–3.25 (m, 1H), 3.01 (s, 3H), 1.52 (d, J = 6.6 Hz, 3H); ^{13}C NMR (151 MHz, DMSO-d_6) δ 169.4, 141.4, 137.2, 135.8, 134.3, 129.3, 126.9, 126.4, 125.2, 122.9, 121.1, 120.5, 73.4, 67.3, 40.1, 38.5, 34.5, 12.7; HRMS (M+H)$^+$ calculated for $C_{18}H_{22}N_3O_3$ 328.1661; found 328.1660; LCMS (high pH) (M+H)$^+$ = 328.2, R_t = 0.62 min (100%). The enantiomeric and diastereomeric excess was confirmed by chiral HPLC analysis, Regis Whelk-O 1 [R,R] (250 × 4.6 mm, 5 μM), 15% EtOH:heptane (+0.2% isopropylamine), flow rate: 1 mL/min, wavelength: 215 nm, temperature: rt. R_t = 39.11 min, >99% ee.

(*R*)-7-(2-((*tert*-Butyldimethylsilyl)oxy)ethoxy)-1,3-dimethyl-1,3-dihydro-2H-benzo[d]azepin-2-one. To a microwave vial was added **57** (815 mg, 4.01 mmol) and acetone (15 mL). The reaction mixture was stirred for 2 min upon which K_2CO_3 (1.80 g, 13.02 mmol) was added and stirred for a further 5 min at rt. (2-Bromoethoxy)(*tert*-butyl)dimethylsilane (1.85 mL, 8.62 mmol) was then added, the vial sealed and heated to 70 °C for 16 h and then heated to 80 °C

for 8 h. The reaction mixture was allowed to cool, and the solvent evaporated via a stream of N_2. The residue was dissolved in CH_2Cl_2 (10 mL) and filtered. The organic solvent was then washed with H_2O (10 mL) and the organic layer separated, dried through a hydrophobic frit and concentrated in vacuo to yield an orange oil. The oil was purified using silica chromatography eluting with 0-40% *t*-BuOMe / cyclohexane. The relevant fractions were combined and concentrated in vacuo to give the title compound as a colorless solid (868 mg, 60%). ^{1}H NMR (400 MHz, CDCl$_3$) δ 7.27–7.18 (m, 1H), 6.98 (dd, *J* = 2.7, 8.6 Hz, 1H), 6.80 (d, *J* = 2.9 Hz, 1H), 6.47–6.34 (m, *J* = 9.3 Hz, 1H), 6.34–6.22 (m, *J* = 9.3 Hz, 1H), 4.11–3.94 (m, 4H), 3.40–3.19 (m, 1H), 3.14 (s, 3H), 1.57–1.50 (m, 3H), 0.93 (s, 9H), 0.12 (s, 6H); LCMS (high pH) $(M+H)^+$ = 362.2, R_t = 1.51 min (85%).

(*R*)-5-Bromo-7-(2-hydroxyethoxy)-1,3-dimethyl-1,3-dihydro-2H-benzo[d]azepin-2-one (62). To a microwave vial was added (*R*)-7-(2-((*tert*-butyldimethylsilyl)oxy)ethoxy)-1,3-dimethyl-1,3-dihydro-2H-benzo[d]azepin-2-one (868 mg, 2.40 mmol) and MeCN (7 mL) under N_2. To the solution was added trimethylphenylammonium tribromide (948 mg, 2.52 mmol) and the reaction mixture was left to stir for at rt for 5 h. The reaction mixture was concentrated in vacuo and then dissolved in CH_2Cl_2 (10 mL). The organic layer was washed with H_2O (2 × 10 mL). The aqueous layer was then extracted with CH_2Cl_2 (5 × 20 mL), The organic layers were combined, dried through a hydrophobic frit, and concentrated in vacuo to yield a waxy solid. The solid was purified using a 80 g silica column (0-100% cyclohexane/EtOAc). The relevant fractions were combined and concentrated in vacuo to give **62** as a white powder (585 mg, 75%). ^{1}H NMR (400 MHz, DMSO-d_6) δ 7.25–7.06 (m, 4H), 4.86 (t, *J* = 5.6 Hz, 1H), 4.13–3.91 (m, 2H), 3.72 (q, *J* = 4.9 Hz, 2H), 3.29–3.17 (m, 1H), 3.00 (s, 3H), 1.50 (d, *J* = 6.8 Hz, 3H); LCMS (high pH) $(M+H)^+$ = 326.0, 328.0, R_t = 0.88 min (100%).

(*R*)-7-(2-Hydroxyethoxy)-1,3-dimethyl-5-(4,4,5,5-tetramethyl-1,3,2-dioxaborolan-2-yl)-1,3-dihydro-2H-benzo[d]azepin-2-one. **62** (408 mg, 1.25 mmol), 4,4,4',4',5,5,5',5'-octamethyl-2,2'-bi(1,3,2-dioxaborolane) (476 mg, 1.88 mmol), *tert*-butyldiphenylphosphine (30 mg, 0.13 mmol), KOAc (491 mg, 5.00 mmol) and Pd(OAc)$_2$ (14 mg, 0.06 mmol) were sealed in a microwave vial which was evacuated and backfilled with N$_2$ × 3. 1,4-Dioxane (9 mL) was then added and the reaction mixture heated at 80 °C for 2 h. The reaction mixture was concentrated under vacuo to yield a green solid. The solid was dissolved in CH$_2$Cl$_2$ and passed through a syringe filter. The filtrate was concentrated in vacuo to yield a green oil. The oil was purified using a 120 g silica column (0-100% cyclohexane / *t*-BuOMe). The relevant fractions were combined and concentrated in vacuo to give the title compound as a yellow solid (380 mg, 81%). ^{1}H NMR (400 MHz, CDCl$_3$) δ 7.22 (d, *J* = 9.1 Hz, 1H), 7.19 (d, *J* = 2.5 Hz, 1H), 7.04 (s, 1H), 6.97 (dd, *J* = 2.5, 8.6 Hz, 1H), 4.15–4.09 (m, 2H), 4.04–3.91 (m, 2H), 3.22–3.12 (m, 4H), 2.05 (t, *J* = 6.5 Hz, 1H), 1.63 (d, *J* = 7.1 Hz, 3H), 1.38–1.36 (m, 12H); LCMS (high pH) (M+H)$^+$ = 374.3, R$_t$ = 1.03 min (92%).

(*R*)-7-(2-Hydroxyethoxy)-1,3-dimethyl-5-(2-methyl-1H-imidazol-4-yl)-1,3-dihydro-2H-benzo[d]azepin-2-one (42). To a microwave vial was added (*R*)-7-(2-hydroxyethoxy)-1,3-dimethyl-5-(4,4,5,5-tetramethyl-1,3,2-dioxaborolan-2-yl)-1,3-dihydro-2H-benzo[d]azepin-2-one (49 mg, 0.17 mmol), **63** (75 mg, 0.20 mmol), XPhos G2 precat (7 mg, 0.01 mmol), XPhos (4 mg, 0.01 mmol) and tripotassium phosphate (62 mg, 0.29 mmol) in 1,4-dioxane (1 mL) and H$_2$O (0.25 mL). The vial was sealed, degassed, and purged with N$_2$ × 3. The vial was heated in a microwave at 85 °C for 105 min. The reaction mixture was blown down to yield a yellow oil which was then dissolved with CH$_2$Cl$_2$ (10 mL) and H$_2$O (10 mL). The separated aqueous layer was washed with CH$_2$Cl$_2$ (3 × 10 mL). The combined organic phase was dried through a hydrophobic frit and

concentrated in vacuo to give a yellow oil. The oil was dissolved with CH_2Cl_2 (3 mL) under N_2 and TFA (0.30 mL, 3.89 mmol) was added and the reaction mixture stirred for 24 h. The reaction mixture was quenched with sat. aq. sodium bicarbonate and the layers were separated. The aqueous layer was washed with CH_2Cl_2 (6 × 10 mL). The organic layers were combined, dried through a hydrophobic frit and concentrated in vacuo to yield an orange oil. The oil was dissolved in 1:1 MeOH:DMSO and purified via MDAP (high pH). The relevant fraction was concentrated in vacuo to give **42** as a solid (6 mg, 11%). ^{1}H NMR (400 MHz, MeOH-d_4) δ 7.29 (d, J = 8.8 Hz, 1H), 7.11 (dd, J = 2.9, 8.8 Hz, 1H), 7.01 (d, J = 2.4 Hz, 1H), 6.94 (s, 1H), 6.88 (s, 1H), 4.09–3.94 (m, 2H), 3.92–3.77 (m, 2H), 3.50–3.34 (m, 1H), 3.12 (s, 3H), 2.41 (s, 3H), 1.61 (d, J = 7.3 Hz, 3H); LCMS (high pH) $(M+H)^+$ = 328.1, R_t = 0.67 min (99%).

4-Bromo-2-methyl-1-((2-(trimethylsilyl)ethoxy)methyl)-1H-imidazole (63). SEM-Cl (3.42 mL, 19.29 mmol) was added dropwise to a solution of 4-bromo-2-methyl-1H-imidazole (2.07 g, 12.86 mmol) in DMF (25 mL) over 20 min. The reaction mixture was then stirred at rt for 18 h. Additional SEM-Cl (1.14 mL, 6.43 mmol) was added dropwise over 10 min and then the reaction was stirred for 7 h. Additional SEM-Cl (3.42 mL, 19.29 mmol) added dropwise over 20 min and the reaction was stirred for 16 h. The resulting mixture was diluted with EtOAc (50 mL) and washed with 5% aq. LiCl solution (30 mL) and then saturated sodium hydrogen carbonate solution (50 mL). The organic phase was passed through a hydrophobic frit and the solvent removed under in vacuo. To remove residual DMF the mixture was washed with H_2O (50 mL), brine (50 mL) and aq. 5% LiCl solution (3 × 50 mL). The combined aqueous phase was extracted with EtOAc (50 mL), the combined organic phase was passed through a hydrophobic frit and evaporated under reduced pressure to give an oil. The oil was purified by silica gel chromatography, eluting with EtOAc in cyclohexane (0-100%). The appropriate fractions were combined and solvent removed

in vacuo to give **63** as a white solid (1.60 g, 43%). ^{1}H NMR (400 MHz, CDCl$_3$) δ 7.24 (s, 1H), 5.51 (s, 2H), 3.90–3.84 (m, 2H), 2.75 (s, 3H), 1.29–1.23 (m, 2H), 0.35 (s, 9H); LCMS (high pH) (M+H)$^+$ = 291.0, 293.0, R$_t$ = 1.18 min (98%).

(*R*)-Diethyl 2-(1,3-dimethyl-5-(1-methyl-1*H*-pyrazol-4-yl)-2-oxo-2,3-dihydro-1*H*-benzo[d]azepin-7-yl)malonate (64). To a stirred solution of **56** (500 mg, 1.45 mmol) in CCl$_4$ (5 mL), was added NBS (93 mg, 0.52 mmol) at 60 °C. The reaction mixture was stirred at 60 °C for 2 h and then poured into H$_2$O (20 mL). The mixture was extracted with EtOAc (2 × 50 mL) and the combined organic layer was washed with brine (50 mL), dried with Na$_2$SO$_4$, filtered and concentrated. The residue was purified by silica gel column chromatography eluting with 15% EtOAc in hexane. The collected fractions were concentrated to give an oil which was used without further purification. The oil was dissolved in 1,4-dioxane (8 mL) and H$_2$O (2 mL). To this stirred solution was added K$_3$PO$_4$ (749 mg, 3.54 mmol) and 1-methyl-4-(4,4,5,5-tetramethyl-1,3,2-dioxaborolan-2-yl)-1*H*-pyrazole (368 mg, 1.77 mmol). The reaction mixture was degassed under N$_2$ atmosphere for 15 min and then XPhos Pd G2 (93 mg, 0.12 mmol) was added. The reaction mixture was stirred at 100 °C for 18 h in a sealed tube. The reaction mixture was quenched with H$_2$O (20 mL) and extracted with EtOAc (2 × 50 mL), then the combined organic layer was washed with brine (30 mL). The organic layer was dried with anhydrous Na$_2$SO$_4$, filtered, and concentrated under vacuum. The residue was purified by silica gel column chromatography eluting with 50% EtOAC in hexane. The appropriate fractions were combined and concentrated to give **64** as an oil (300 mg, 37% over two steps). LCMS (formic method H) (M+H)$^+$ = 426.2, R$_t$ = 2.66 min (62%).

(*R*)-7-(1,3-dihydroxypropan-2-yl)-1,3-dimethyl-5-(1-methyl-1*H*-pyrazol-4-yl)-1*H*-benzo[d]azepin-2(3*H*)-one (43). To a stirred solution of **64** (300 mg, 0.71 mmol) in THF (20

mL) and MeOH (5 mL) was added NaBH₄ (213 mg, 5.64 mmol) portionwise at rt. Following stirring at rt for 4 h, the solvent was removed under vacuum. The resulting material was quenched with H_2O (30 mL) and extracted with EtOAc (2 × 50 mL). The combined organic phase was washed with brine (50 mL). The organic layer was dried with anhydrous Na_2SO_4, filtered, and concentrated under vacuum. The resultant residue was purified by silica gel column chromatography eluting with 80% EtOAC in hexane. The appropriate fractions were combined and concentrated to give **43** as an off-white solid (37 mg, 15%). ¹H NMR (400 MHz, DMSO-*d₆*) δ 7.74 (s, 1H), 7.56 (s, 1H), 7.32 (br dd, *J* = 1.5, 8.3 Hz, 1H), 7.26–7.18 (m, 2H), 6.87 (s, 1H), 4.51–4.46 (m, 2H), 3.83 (s, 3H), 3.68–3.49 (m, 4H), 3.28–3.22 (m, 1H), 3.01 (s, 3H), 2.81–2.72 (m, 1H), 1.50 (d, *J* = 6.8 Hz, 3H); LCMS (formic B) (M+H)⁺ = 342.2, R_t = 1.40 min (99%).

in vitro assays. All TR-FRET, hWB cytokine, hepatic clearance and in vitro pharmacokinetic assays have been described previously.[49]

in vivo studies statement. All animal studies were ethically reviewed and carried out in accordance with Animals (Scientific Procedures) Act 1986 and the GSK Policy on the Care, Welfare, and Treatment of Animals.

Supporting Information. The following files are available free of charge. All screening statistics, MetaSite metabolism prediction for (*R*)-**10**, representative LCMS traces of target compounds, full BROMO*scan* and selectivity data, and X-ray data collection and refinement statistics (PDF).

Molecular formula strings (CSV)

Accession Codes. Coordinates have been deposited with the Protein Data Bank under accession code XXXX (BRD2 BD2/**9** complex), XXXX (BRD2 BD2/(*R*)-**10** complex), XXXX (BRD2

BD2/(*R*)-**11** complex) and XXXX (BRD2 BD2/**41** complex),. Authors will release atomic coordinates and experimental data upon article publication.

Corresponding Author

*E-mail: philip.g.humphreys@gsk.com. Phone: +44 (0)7384 799695.

Present Addresses

D.J.H.: MSD, The Francis Crick Institute, 1 Midland Road, London, NW1 1AT, U.K.

K. L. J.: Charles River Laboratories, Chesterford Research Park, CB10 1XL, U.K.

N.H.T: The University of Manchester, Oxford Road, Manchester, M13 9PL, U.K.

Author Contributions

The manuscript was written through contributions of all authors. All authors have given approval to the final version of the manuscript.

Notes

ABBREVIATIONS

AMP, artificial membrane permeability; BD1, bromodomain 1 (N-terminal bromodomain); BD2, bromodomain 2 (C-terminal bromodomain); BRD2, bromodomain containing protein 2; BRD3, bromodomain containing protein 3; BRD4, bromodomain containing protein 4; BRDT, bromodomain containing protein, testis-specific; CAD, charged aerosol detection; CL_b, blood clearance; $CL_{b,u}$, unbound blood clearance; CL_{int}, intrinsic clearance; CLND, chemiluminescent nitrogen detection; FaSSIF, fasted state simulated intestinal fluid; Fu_b, fraction unbound in blood; LCMS, liquid chromatography mass spectrometry; LE, ligand efficiency; LipE, lipophilic efficiency; MCP-1, monocyte chemoattractant protein-1; MDAP, mass-directed auto preparation; MDI, metabolism dependent inhibition; pIC_{50}, $-\log_{10}(IC_{50})$; TR-FRET, time-resolved Förster resonance energy transfer; V_{ss}, volume of distribution at steady state; $V_{ss,u}$, unbound volume of distribution at steady state; WPF, tryptophan-proline-phenylalanine.

REFERENCES

(1) Padmanabhan, B.; Mathur, S.; Manjula, R.; Tripathi, S. Bromodomain and Extra-Terminal (BET) Family Proteins: New Therapeutic Targets in Major Diseases. *J. Biosci.* **2016**, *41*, 295–311.

(2) Muller, S.; Filippakopoulos, P.; Knapp, S. Bromodomains as Therapeutic Targets. *Expert Rev. Mol. Med.* **2011**, *13*, e29.

(3) Zaware, N.; Zhou, M.-M. Bromodomain Biology and Drug Discovery. *Nat. Struct. Mol. Biol.* **2019**, *26*, 870–879.

(4) Jain, A. K.; Barton, M. C. Bromodomain Histone Readers and Cancer. *J. Mol. Biol.* **2017**, *429*, 2003–2010.

(5) Filippakopoulos, P.; Knapp, S. Targeting Bromodomains: Epigenetic Readers of Lysine Acetylation. *Nat. Rev. Drug Discov.* **2014**, *13*, 337–356.

(6) Shi, J.; Vakoc, C. R. The Mechanisms Behind the Therapeutic Activity of BET Bromodomain Inhibition. *Mol. Cell* **2014**, *54*, 728–736.

(7) Shorstova, T.; Foulkes, W. D.; Witcher, M. Achieving Clinical Success with BET Inhibitors as Anti-Cancer Agents. *Brit. J. Cancer.* **2021**, *124*, 1478–1490.

(8) Clinicaltrials.gov. Accessed 13th May 2022.

(9) Waring, M. J.; Chen, H.; Rabow, A. A.; Walker, G.; Bobby, R.; Boiko, S.; Bradbury, R. H.; Callis, R.; Clark, E.; Dale, I.; Daniels, D. L.; Dulak, A.; Flavell, L.; Holdgate, G.; Jowitt, T. A.; Kikhney, A.; McAlister, M.; Méndez, J.; Ogg, D.; Patel, J.; Petteruti, P.; Robb, G. R.; Robers, M. B.; Saif, S.; Stratton, N.; Svergun, D. I.; Wang, W.; Whittaker, D.; Wilson, D. M.; Yao, Y. Potent and Selective Bivalent Inhibitors of BET Bromodomains. *Nature Chem. Biol.* **2016**, *12*, 1097–1104.

(10) Bradbury, R. H.; Callis, R.; Carr, G. R.; Chen, H.; Clark, E.; Feron, L.; Glossop, S.; Graham, M. A.; Hattersley, M.; Jones, C.; Lamont, S. G.; Ouvry, G.; Patel, A.; Patel, J.; Rabow, A. A.; Roberts, C. A.; Stokes, S.; Stratton, N.; Walker, G. E.; Wardm L.; Whalley, D.; Whittaker, D.; Wrigley, G.; Waring, M. J. Optimization of a Series of Bivalent Triazolopyridazine Based Bromodomain and Extraterminal Inhibitors: The Discovery of (3R)-4-[2-[4-[1-(3-Methoxy-

[1,2,4]triazolo[4,3-b]pyridazin-6-yl)-4-piperidyl]phenoxy]ethyl]-1,3-dimethyl-piperazin-2-one (AZD5153). *J. Med. Chem.* **2016**, *59*, 7801–7817.

(11) Rcsb.org. Accessed 13th May 2022.

(12) Filippakopoulos, P.; Picaud, S.; Mangos, M.; Keates, T.; Lambert, J. P.; Barsyte-Lovejoy, D.; Felletar, I.; Volkmer, R.; Muller, S.; Pawson, T.; Gingras, A. C.; Arrowsmith, C. H.; Knapp, S. Histone recognition and large-scale structural analysis of the human bromodomain family. *Cell* **2012**, *149*, 214–231.

(13) Mirguet, O.; Gosmini, R.; Toum, J.; Clement, C. A.; Barnathan, M.; Brusq, J. M.; Mordaunt, J. E.; Grimes, R. M.; Crowe, M.; Pineau, O.; Ajakane, M.; Daugan, A.; Jeffrey, P.; Cutler, L.; Haynes, A. C.; Smithers, N. N.; Chung, C. W.; Bamborough, P.; Uings, I. J.; Lewis, A.; Witherington, J.; Parr, N.; Prinjha, R. K.; Nicodeme, E., Discovery of epigenetic regulator I-BET762: lead optimization to afford a clinical candidate inhibitor of the BET bromodomains. *J. Med. Chem.* **2013**, *56*, 7501–7515.

(14) Jones, K. L.; Beaumont, D. M.; Bernard, S. G.; Bit, R. A.; Campbell, S. P.; Chung, C.-W.; Cutler, L.; Demont, E. H.; Dennis, K.; Gordon, L.; Gray, J. R.; Haase, M. V.; Lewis, A. J.; McCleary, S.; Mitchell, D. J.; Moore, S. M.; Parr, N.; Robb, O. J.; Smithers, N.; Soden, P. E.; Suckling, C. J.; Taylor, S.; Walker, A. L.; Watson, R. J.; Prinjha, R. K. The Discovery of a Novel Bromodomain and Extra Terminal Domain (BET) Protein Inhibitor, I-BET282E, Suitable for Clinical Progression. *J. Med. Chem.* **2021**, 64, 12200–12227.

(15) Humphreys, P. G.; Atkinson, S. J.; Bamborough, P.; Bit, R. A.; Chung, C.-W.; Craggs, P. D.; Cutler, L.; Davis, R.; Ferrie, A.; Gong, G.; Gordon, L. J.; Gray, M.; Harrison, L. A.; Hayhow, T. G.; Haynes, A.; Henley, N.; Hirst, D. J.; Holyer, I. D.; Lindon, M. J.; Lovatt, C.; Lugo, D.; McCleary, S.; Molnar, J.; Osmani, Q.; Patten, C.; Preston, A.; Rioja, I.; Seal, J. T.; Smithers, N.; Sun, F.; Tang, D.; Taylor, S.; Theodoulou, N. H.; Thomas, C.; Watson, R. J.; Wellaway, C. R.; Zhu, L.; Tomkinson, N. C. O.; Prinjha, R. K. 'Design, Synthesis and Characterization of I-BET567, a pan-Bromodomain and Extra Terminal (BET) Bromodomain Oral Candidate' *J. Med. Chem.* **2022**, *65*, 2262–2287.

(16) Wellaway, C.R.; Amans, D.; Bamborough, P.; Barnett, H.; Bit, R. A.; Brown, J. A.; Carlson, N. R.; Chung, C.-W.; Cooper, A. W. J.; Craggs, P. D.; Davis, R. P.; Dean, T. W.; Evans, J. P.; Gordon, L.; Harada, I. L.; Hirst, D. J.; Humphreys, P. G.; Jones, K. L.; Lewis, A. J.; Lindon, M. J.; Lugo, D.; Mahmood, M.; McCleary, S.; Mederiros, P.; Mitchell, D. J.; O'Sullivan, M.; Le Gall, A.; Patel, V. K.; Patten, C.; Poole, D. L.; Shah, R. R.; Smith, J. E.; Stafford, K. A. J.; Thomas, P. J.; Vimal, M.; Wall, I. D.; Watson, R. J.; Wellaway, N.; Yao, G.; Prinjha, R. K. Discovery of a Bromodomain and Extraterminal Inhibitor with a Low Predicted Human Dose through Synergistic Use of Encoded Library Technology and Fragment Screening. *J. Med. Chem.* **2020**, *63*, 714–746.

(17) Hopkins, A. L.; Groom, C. R.; Alex, A. Ligand Efficiency: A Useful Metric for Lead Selection. *Drug Disc. Today* **2004**, *9*, 430–431.

(18) Johnson, T. W.; Gallego, R. A.; Edwards, M. P. Lipophilic Efficiency as an Important Metric in Drug Design. *J. Med. Chem.* **2018**, *61*, 6401–6420.

(19) Freeman-Cook, K. D.; Hoffman, R. L.; Johnson, T. W. Lipophilic Efficiency: The Most Important Efficiency Metric in Medicinal Chemistry. *Future Med. Chem.* **2013**, *5*, 113–116.

(20) Stock, D. A.; Molinoff, P. B. The Value of Backup Compounds to Drug Development Programs. *Ther. Innov. Regul. Sci.* **2002**, *36*, 95–113.

(21) Bayliss, M. K.; Butler, J.; Feldman, P. L.; Green, D. V. S.; Leeson, P. D.; Palovich, M. R.; Taylor, A. J. Quality Guidelines for Oral Drug Candidates: Dose, Solubility and Lipophilicity. *Drug Disc. Today* **2016**, *21*, 1719–1727.

(22) Young, R. J.; Green, D. V. S.; Luscombe, C. N.; Hill, A. P. Getting Physical in Drug Discovery II; The Impact of Chromatographic Hydrophobicity Measruements and Aromaticity. *Drug Disc. Today* **2011**, *16*, 822–830.

(23) Maurer, T. S.; Smith, D.; Beaumont, K.; Di, L. Dose Prediction for Drug Design. *J. Med. Chem.* **2020**, *63*, 6423–6435.

(24) Young, R. J.; Leeson, P. D. Mapping the Efficiency and Physicochemical Trajectories of Successful Optimizations. *J. Med. Chem.* **2018**, *61*, 6421–6467.

(25) Leeson, P. D.; Bento, A. P.; Gaulton, A.; Hersey, A.; Manners, E. J.; Radoux, C. J.; Leach, A. R. Target-Based Evaluation of "Drug-Like" Properties and Ligand Efficiencies. *J. Med. Chem.* **2021**, *64*, 7210–7230.

(26) Vaidergorn, M. M.; Emery, F. D. S.; Ganesan, A. From Hit Seeking to Magic Bullets: The Successful Union of Epigenetic and Fragment Based Drug Discovery (EPIDD + FBDD). *J. Med. Chem.* **2021**, *24*, 13980–14010.

(27) Chung, C.-W.; Dean, A. W.; Woolven, J. M.; Bamborough, P. Fragment-Based Discovery of Bromodomain Inhibitors Part 1: Inhibitor Binding Modes and Implications for Lead Discovery. *J Med Chem.* **2012**, *55*, 576–586.

(28) Wang, L.; Pratt, J. K.; Soltwedel, T.; Sheppard, G. S.; Fidanze, S. D.; Liu, D.; Hasvold, L. A.; Mantei, R. A.; Holms, J. H.; McClellan, W. J.; Wendt, M. D.; Wada, C.; Frey, R.; Hansen, T. M.; Hubbard, R.; Park, C. H.; Li, L.; Magoc, T. J.; Albert, D. H.; Lin, X.; Warder, S. E.; Kovar, P.; Huang, X.; Wilcox, D.; Wang, R.; Rajaraman, G.; Petros, A. M.; Hutchins, C. W.; Panchal, S. C.; Sun, C.; Elmore, S. W.; Shen, Y.; Kati, W. M.; McDaniel, K. F. Fragment-Based, Structure-Enabled Discovery of Novel Pyridones and Pyridone Macrocycles as Potent Bromodomain and Extra-Terminal Domain (BET) Family Bromodomain Inhibitors. *J. Med. Chem.* **2017**, *60*, 3828–3850.

(29) Albrecht, B. K.; Gehling, V. S.; Hewitt, M. C.; Vaswani, R. G.; Côté, A.; Leblanc, Y.; Nasveschuk, C. G.; Bellon, S.; Bergeron, L.; Campbell, R.; Cantone, N.; Cooper, M. R.; Cummings, R. T.; Jayaram, H.; Joshi, S.; Mertz, J. A.; Neiss, A.; Normant, E.; O'Meara, M.; Pardo, E.; Poy, F.; Sandy, P.; Supko, J.; Sims, R. J.; Harmange, J.-C.; Taylor, A. M.; Audia, J. E. Identification of a Benzoisoxazoloazepine Inhibitor (CPI-0610) of the Bromodomain and Extra-Terminal (BET) Family as a Candidate for Human Clinical Trials. *J. Med. Chem.* **2016**, *59*, 1330–1339.

(30) Gosmini, R.; Nguyen, V. L.; Toum, J.; Simon, C.; Brusq, J.-M. G.; Krysa, G.; Mirguet, O.; Riou-Eymard, A. M.; Boursier, E. V.; Trottet, L.; Bamborough, P.; Clark, H.; Chung, C.-W.; Cutler, L.; Demont, E. H.; Kaur, R.; Lewis, A. J.; Schilling, M. B.; Soden, P. E.; Taylor, S.; Walker,

A. L.; Walker, M. D.; Prinjha, R. K.; Nicodème, E. The Discovery of I-BET726 (GSK1324726A), a Potent Tetrahydroquinoline ApoA1 Up-Regulator and Selective BET Bromodomain Inhibitor. *J. Med. Chem.* **2014**, *57*, 8111–8131.

(31) Leung, C. S.; Leung, S. S. F.; Tirado-Rives, J.; Jorgensen, W. L. Methyl Effects on Protein-Ligand Binding. *J. Med. Chem.* **2012**, *55*, 4489–4500.

(32) Piha-Paul, S. A.; Hann, C. L.; French, C. A.; Cousin, S.; Braña, I.; Cassier, P. A.; Moreno, V.; de Bono, J. S.; Duckworth Harward, S.; Ferron-Brady, G.; Barbash, O.; Wyce, A.; Wu, Y.; Horner, T.; Annan, M.; Parr, N. J.; Prinjha, R. K.; Carpenter, C. L.; Hilton, J.; Hong, D. S.; Haas, N. B.; Markowski, M. C.; Dhar, A.; O'Dwyer, P. J.; Shapiro, G. I. Phase 1 Study of Molibresib (GSK525762), a Bromodomain and Extra-Terminal Domain Protein Inhibitor, in NUT Carcinoma and Other Solid Tumors. *JNCI Cancer Spectrum* **2020**, *4*, pkz093.

(33) Trunzer, M.; Faller, B.; Zimmerlin, A. Metabolic Soft Spot Identification and Compound Optimization in Early Discovery Phases Using MetaSite and LC-MS/MS Validation. *J. Med. Chem.* **2009**, *52*, 329–335.

(34) Kirsch, P.; Hartman, A. M.; Hirsch, A. K. H.; Empting, M. Concepts and Core Principles of Fragment-Based Drug Design. *Molecules* **2019**, *24*, 4309.

(35) Garnier, J.-M.; Sharp, P. P.; Burns, C. J. BET Bromodomain Inhibitors: A Patent Review. *Expert Opin. Ther. Pat.* **2014**, *24*, 185–199.

(36) Chang, G.; Steyn, S. J.; Umland, J. P.; Scott, D. O. Strategic Use of Plasma and Microsome Binding to Exploit in Vitro Clearance in Early Drug Discovery. *ACS Med. Chem. Lett.* **2010**, *13*, 50–53.

(37) Free, S. M.; Wilson, J. W. A Mathematical Contribution to Structure-Activity Studies. *J. Med. Chem.* **1964**, *7*, 395–399.

(38) Segali, M. D. Multi-Paramter Optimization: Identifying High Quality Compounds with a Balance of Properties. *Curr. Pharm. Des.* **2012**, *18*, 1292–1310.

(39) Lazerwith, S. E.; Bahador, G.; Canales, E.; Cheng, G.; Chong, L.; Clarke, M. O.; Doerffler, E.; Eisenberg, E. J.; Hayes, J.; Lu, B.; Liu, Q.; Matles, M.; Mertzman, M.; Mitchell, M. L.; Morganelli, P.; Murray, B. P.; Robinson, M.; Strickley, R. G.; Tessler, M.; Tirunagari, N.; Wang, J.; Wang, Y.; Zhang, J. R.; Zheng, X.; Zhong, W.; Watkins, W. J. Optimization of Pharmacokinetics through Manipulation of Physicochemical Properties in a Series of HCV Inhibitors. *ACS Med. Chem. Lett.* **2011**, *2*, 715–719.

(40) Hughes J. D.; Blagg J.; Price D. A.; Bailey S.; Decrescenzo G. A.; Devraj R. V.; Ellsworth E.; Fobian Y. M.; Gibbs M. E.; Gilles R. W.; Greene N.; Huang E.; Krieger-Burke T.; Loesel J.; Wager T.; Whiteley L.; Zhang Y. Physiochemical Drug Properties Associated with in vivo Toxicological Outcomes. *Bioorg. Med. Chem. Lett.* **2008**, *18*, 4872–4875.

(41) Wu, C.; Decker, E. R.; Blok, N.; Li, J.; Bourgoyne, A. R.; Bui, H.; Keller, K. M.; Knowles, V.; Li, W.; Stavros, F. D.; Holland, G. W.; Brock, T. A.; Dixon, R. A. Acyl Substitution at the Ortho Position of Anilides Enhances Oral Bioavailability of Thiophene Sulfonamides: TBC3214, an ET$_A$ Selective Endothelin Antagonist. *J. Med. Chem.* **2001**, *44*, 1211–1216.

(42) BROMOscan recombinant protein binding assays were carried out at DiscoverX, http://www.discoverx.com.

(43) Caron, G.; Kihlberg, J.; Ermondi, G. Intramolecular Hydrogen Bonding: An Opportunity for Improved Design in Medicinal Chemistry. *Med. Res. Rev.* **2019**, *39*, 1707–1729.

(44) Meanwell, N. A. A Synopsis of the Properties and Applications of Heteroaromatic Rings in Medicinal Chemistry. *Adv. Heterocycl. Chem.* **2017**, *123*, 245–361.

(45) Hosea, N. A.; Collard, W. T.; Cole, S.; Maurer, T. S.; Fang, R. X.; Jones, H.; Kakar, S. M.; Nakai, Y.; Smith, B. J.; Webster, R.; Beaumont, K. Prediction of Human Pharmacokinetics from Preclinical Information: Comparative Accuracy of Quantitative Prediction Approaches. *Clin. Pharmacol.* **2009**, *49*, 513−533.

(46) Mahmood, I.; Balian, J. D. Interspecies Scaling: Predicting Clearance of Drugs in Humans. Three Different Approaches. *Xenobiotica* **1996**, *26*, 887−895.

(47) Evans, D. A.; Ennis, M. D.; Mathre, D. J. Asymmetric Alkylation Reactions of Chiral Imide Enolates. A Practical Approach to the Enantioselective Synthesis of α-Substituted Carboxylic Acid Derivatives. *J. Am. Chem. Soc.* **1982**, *104*, 1737−1739.

(48) Sharpless, K. B.; Amberg, W.; Bennani, Y. L.; Crispino, G. A.; Hartung, J.; Jeong, K. S.; Kwong, H. L.; Morikawa, K.; Wang, Z. M.; Xu, D.; Zhang, X. L. The Osmium-Catalyzed Asymmetric Dihydroxylation: A New Ligand Class and a Process Improvement. *J. Org. Chem.* **1992**, *57*, 2768–2771.

(49) Seal, J. T.; Atkinson, S. J.; Aylott, H.; Bamborough, P.; Chung, C.-W.; Copley, R. C. B.; Gordon, L.; Grandi, P.; Gray, J. R.; Harrison, L. A.; Hayhow, T. G.; Lindon, M.; Messenger, C.; Michon, A.-M.; Mitchell, D.; Preston, A.; Prinjha, R. K.; Rioja, I.; Taylor, S.; Wall, I. D.; Watson,

R. J.; Woolven, J. M.; Demont, E. H. The Optimization of a Novel, Weak Bromo and Extra Terminal Domain (BET) Bromodomain Fragment Ligand to a Potent and Selective Second Bromodomain (BD2) Inhibitor. *J. Med. Chem.* **2020**, *63*, 9093–9126.

For Table of Contents Only